



Technische Universität München

Fakultät für Medizin

Institut für Pharmakologie und Toxikologie

**Identification of hypertrophy-modulating Cullin-RING E3 ubiquitin ligases in  
primary cardiomyocytes**

**Maximilian Gustav Fischer**

Vollständiger Abdruck der von der Fakultät für Medizin der Technischen Universität München  
zur Erlangung des akademischen Grades eines

**Doktors der Medizin (Dr. med.)**

genehmigten Dissertation.

Vorsitzender: **Prof. Dr. Ernst J. Rummeny**

Prüfer der Dissertation:

**1. Prof. Dr. Dr. Stefan Engelhardt**

**2. Prof. Dr. Heribert Schunkert**

Die Dissertation wurde am 07.11.2017 bei der Technischen Universität München eingereicht  
und durch die Fakultät für Medizin am 10.10.2018 angenommen.

List of abbreviations:

Akt1 serin/threonine kinase 1

ANP atrial natriuretic peptide

AS aminoacid

ATP adenosintriphosphat

AU arbitrary units

BNP brain natriuretic peptide

bp basepair

Cand1 Cullin-associated NEDD8-dissociated protein 1

CM cardiomyocyte

CRL Cullin-RING ligase

ddH<sub>2</sub>O double distilled water

DMF N,N-Dimethylformamid

DNA deoxyribonucleic acid

dNTP deoxyribonucleotide

Erk1/2 extracellular regulated MAP kinase 1/2

FBS fetal bovine serum

IF immunofluorescence

IGF-1 Insulin-like growth factor 1

IGF-1R Insulin-like growth factor 1 receptor

IHC immunohistochemistry

kB kilobase

kDa kilodalton

MAPK1 mitogen-activated protein kinase 1

NO nitrogen monoxide

Nedd8 neural precursor cell expressed, developmentally down-regulated gene 8

Non-CM non-cardiomyocyte

NRCM neonatal rat cardiomyocyte

n.s. not significant

nt nukleotide

PI3K phosphoinositide-3-kinase

RNase ribonuclease

RT room temperature

RT- PCR real-time polymerase chain reaction

SD standard deviation

SDS-PAGE sodiumdodecylsulfate-polyacrylamide electrophoresis

SEM standard error of mean

SiRNA short interfering RNA

Skp1 (S-phase kinase associated protein 1)

Skp2 (S-phase kinase associated protein 2)

TAC transverse aortic constriction

TG transgenic

Vol volume

vs versus

WB western blot

Wt wildtype

## Directory:

<b>1</b>	<b>Abstract</b>	<b>5</b>
<b>2</b>	<b>Introduction</b>	<b>6</b>
<b>2.1</b>	<b>Ubiquitin-Proteasome System (UPS)</b>	<b>6</b>
2.1.1	Cascade of Ubiquitylation	6
2.1.2	Proteasome in the heart and growth control	7
2.1.3	Structure of the E3 ubiquitin ligases	9
2.1.4	Regulation of Cullin-RING ubiquitin ligase	12
2.1.5	F-box proteins	13
2.1.5.1	Structure of the F-box protein/F-box motif	13
2.1.5.2	Classification of the Fbox family	13
2.1.5.3	Function and Dysregulation of F-box proteins in different diseases	14
2.1.5.4	Homeostasis of F-box proteins	16
<b>2.2</b>	<b>Heart Hypertrophy</b>	<b>17</b>
2.2.1	Relevance	17
2.2.2	Pathophysiology	17
2.2.3	Signaling Pathways	18
<b>2.3</b>	<b>Role of E3 ligases in regulating heart hypertrophy</b>	<b>20</b>
2.3.1	Atrogin-1's role in skeletal and cardiac muscle hypertrophy	21
2.3.2	Murf1's role in heart disease	22
<b>3</b>	<b>Aim and objectives</b>	<b>23</b>
<b>4</b>	<b>Materials</b>	<b>24</b>
4.1	Antibodies	24
4.2	Oligonucleotides	24
4.3	Chemicals	34
4.4	Enzymes	35
4.5	Kits	35
4.6	Buffer, Solutions and Cell Culture media	35
<b>5</b>	<b>Methods</b>	<b>38</b>
5.1	Isolation and cell culture of primary neonatal rat cardiomyocytes	38
5.2	siRNA transfection	38

<b>5.3</b>	<b>SiGLO based transfection optimization .....</b>	<b>39</b>
<b>5.4</b>	<b>DNA Microarray.....</b>	<b>40</b>
<b>5.5</b>	<b>Cell size determination by hypertrophy assay .....</b>	<b>40</b>
5.5.1	Immunofluorescence Staining .....	40
5.5.2	Automated cell size acquisition of cardiomyocytes.....	40
<b>5.6</b>	<b>Isolation of RNA.....</b>	<b>41</b>
<b>5.7</b>	<b>Reverse Transcription of mRNA into cDNA.....</b>	<b>41</b>
<b>5.8</b>	<b>Quantitative real-time PCR .....</b>	<b>42</b>
<b>5.9</b>	<b>Nuclei count .....</b>	<b>43</b>
<b>5.10</b>	<b><sup>3</sup>H-Isoleucine incorporation .....</b>	<b>43</b>
<b>5.11</b>	<b>MTT assay.....</b>	<b>44</b>
<b>5.12</b>	<b>Statistical evaluation of data .....</b>	<b>44</b>
<b>6</b>	<b>Results.....</b>	<b>45</b>
<b>6.1</b>	<b>SiRNA transfection optimization of NRCM using siGLO method .....</b>	<b>45</b>
<b>6.2</b>	<b>DNA microarray for expression levels of Cullin and F-box proteins.....</b>	<b>47</b>
<b>6.3</b>	<b>Screening for hypertrophy-modulating Cullin-RING E3 ligases.....</b>	<b>51</b>
<b>6.4</b>	<b>Validation of candidate CRLs in NRCMs.....</b>	<b>57</b>
6.4.1	Quantification of siRNA-mediated knockdown by qPCR .....	57
6.4.2	Viability test in MTT assay .....	59
6.4.3	Analysis of nuclei count .....	61
6.4.4	<sup>3</sup> H-Isoleucine incorporation .....	63
<b>7</b>	<b>Discussion .....</b>	<b>66</b>
<b>7.1</b>	<b>Identification of hypertrophy modulating CRLs .....</b>	<b>67</b>
<b>7.2</b>	<b>Validation experiments for screening hits.....</b>	<b>72</b>
<b>8</b>	<b>Outlook .....</b>	<b>75</b>
<b>9</b>	<b>Supplement.....</b>	<b>76</b>
<b>10</b>	<b>References .....</b>	<b>83</b>
<b>11</b>	<b>Acknowledgement.....</b>	<b>98</b>

# 1 Abstract

**Background:** The Ubiquitin-Proteasome System (UPS) is a selective protein degradation pathway that is critically involved in the pathogenesis of several cardiac disorders. Cullin-RING ligases (CRLs) constitute the largest group of E3 ubiquitin ligases and utilize F-box proteins for substrate recognition. Two well-known players in the heart are Atrogin-1 and Murf-1. While Murf-1 is not a CRL by definition, publications demonstrate the importance of these E3 ligases for the hypertrophy-modulating role in the heart.

**Aim and Objectives:** The aim of the project was to identify other hypertrophy-modulating CRLs in primary cardiomyocytes.

**Methods:** A genomic approach using a rat siRNA library directed against 43 F-box proteins and other CRL components was combined with automated microscopy to assess the role of CRL depletion on neonatal rat cardiomyocyte (NRCM) cell size. Furthermore, the results were validated by cell count analysis and metabolic assays to ensure the effect of siRNA transfection on neonatal rat cardiomyocytes in vitro.

**Results:** We identified 13 CRL components (seven Fbxo-, two Fbxw-, one Fbxl- family members and several CRL subunits) that significantly affected NRCM cell size. Of these, Fbxo33, Fbxo25, Fbxo45, and Fbxw4 were identified as the most potent novel regulator of cardiac hypertrophy.

**Summary and Outlook:** This study identified several CRLs with effects stronger than Atrogin-1 that might play a yet unrecognized role in the regulation of cardiac hypertrophy. A deeper insight into the molecular basis of the hypertrophy-modulating role of the UPS could establish unknown paths to treat cardiac diseases by directly manipulating the turnover of essential proteins.

## 2 Introduction

### 2.1 Ubiquitin-Proteasome System (UPS)

#### 2.1.1 Cascade of Ubiquitylation

The turnover of intracellular protein is a precisely controlled process that is pivotal for a lot of fundamental cellular functions such as cell cycle progression, monitoring transcriptional and signal transduction. Several mechanisms ensure the proper regulation of proteolysis, including the lysosomes, the autophagy, the calpain system and the ubiquitin-proteasome system (UPS) (Kunkel et al., 2015; Sarikas et al., 2011).

It is assumed that the UPS degrades the majority of the intracellular protein (up to 80-90%). This system consists of a multi-step process involving E1 (ubiquitin activating enzyme), E2 (ubiquitin conjugating enzyme) and E3 (ubiquitin ligase) enzymes (Zolk et al., 2006).

Ubiquitin is one of the key proteins in this pathway and acts as a tag. Thus misfolded, old and dysfunctional proteins can be recognized by the UPS for degradation. It is an evolutionary high conserved 76 amino acid protein and contains seven lysine residues (Lys6, Lys11, Lys27, Lys29, Lys33, Lys48, and Lys63) (Sarikas et al., 2011). Polyubiquitin- chains are assembled by an isopeptide linkage between the lysine residues of the previous ubiquitin and the C-terminal glycine rest of the following ubiquitin (Zolk et al., 2006). Two major patterns in this process are called non-canonical and canonical. Since there are several lysine residues in a single ubiquitin molecule, different multiubiquitin chains can be formed. The fate of a protein tagged with monoubiquitination or polyubiquitination differs. While monoubiquitination often is a signal for receptor internalization and sorting of cell surface protein (McDowell & Philpott, 2013), the process of polyubiquitination of a lysine residue with a long chain of ubiquitin, also called canonical, leads mainly to proteolysis of the tagged protein in the proteasome.

The process of ubiquitination of a substrate involves three steps before the proteasome can solve the isopeptide bonds in the targeted protein.

In the first step, the E1 activates in an ATP depending reaction one ubiquitin-protein. By the second phase, the ubiquitin is transferred to the E2 and linked covalently. In the third and final step, the ubiquitin reaches its final destination by the E3 enzyme, which binds the ubiquitin to the substrate. Some E3 ligases act like a bridging factor and therefore a direct interaction with the E2 enzyme, while other E3 ligases form an ubiquitin-thiol-ester intermediate before transferring ubiquitin to the substrate (Sarikas et al., 2011) (**Fig.1**).

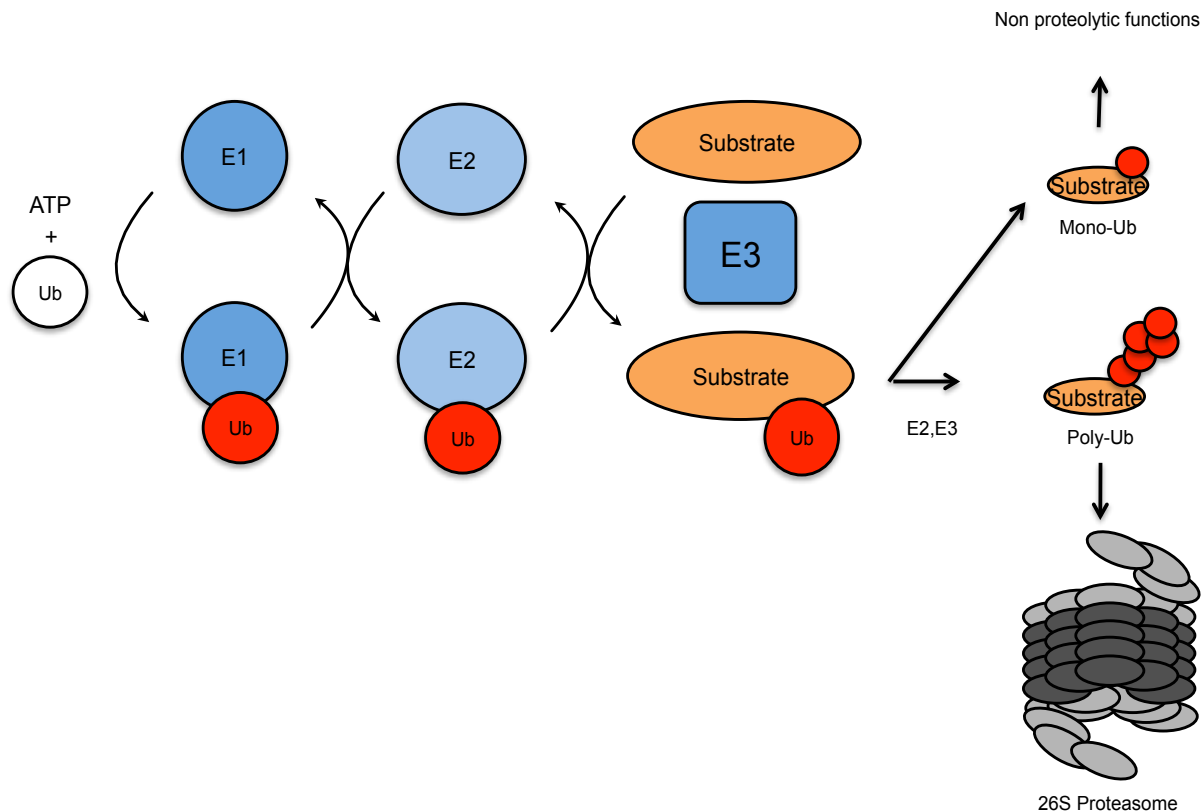


Figure 1: The process of ubiquitylation

The highly conserved ubiquitin (Ub) is activated by the ubiquitin activating enzyme (E1) in an ATP-dependent reaction. Then it is transferred to the ubiquitin conjugating enzyme (E2), which assists the ubiquitin ligase (E3) to precisely attach the ubiquitin tag onto a targeted substrate. The action of the E3 can result in mono- and polyubiquitination, for mainly nonproteolytic functions and the degradation of the substrate in the 26S proteasome, respectively.

### 2.1.2 Proteasome in the heart and growth control

The proteasome itself is an ATP- dependent complex that consists of a central 20S subunit that proteolysis the bonds between the amino acids. The two CAP structures, known as the 19S complexes are responsible for the recognition and the regulation of marked proteins (Schlossarek et al., 2014).

But not each protein that is ubiquitinated is automatically cleaved by the proteasome. Mono-ubiquitination, for example, acts as a signal for internalization and endosomal sorting of cell-surface proteins (Hicke & Dunn, 2003; Katzmann et al., 2001; Levkowitz et al., 1998).

Some proteins such as the nuclear factor kappa B (NF $\kappa$ B) precursor are processed by undergoing limited proteolysis to generate mature proteins (Cordero-Espinoza & Hagen, 2013). Furthermore, some proteins submit de-ubiquitination of targets (Eletr & Wilkinson, 2014).

Previous work has demonstrated a critical role of the UPS in the pathogenesis of hypertrophic cardiomyopathies (Carrier et al., 2010; Mearini et al., 2010; Sarikas et al., 2005; Schlossarek et al., 2012). CUL7 was identified as a novel regulator of the insulin and insulin-like growth factor (IGF-1) signaling pathway (Fan et al., 2013; Xu et al., 2008). Dysregulation of the CUL7 E3 ligase was found in patients with autosomal-recessive 3-M and Yakuts short stature syndromes (Sarikas et al., 2008). In vivo experiments with mice, in which CUL7 gene was ablated, resulted in intrauterine growth retardation and perinatal lethality. According to these results, it is assumed that the UPS has a significant role in growth regulation. Thus the CUL7 E3 ligase targets Cyclin D1 and Insulin Receptor Substrate 1 (IRS1) for ubiquitin-dependent degradation, this probably provides a molecular link between CUL7 E3 ligase and a growth regulatory pathway. Interestingly CUL7 needs an F-box protein named Fbw8 for its growth-regulatory function (Huber et al., 2005). The mRNA of CUL7 is expressed in many tissues, with high expression found in kidney and placenta, skeletal muscle, heart and pancreas.

Experiments of Li et al. (N. Li et al., 2015) showed that the cardiac proteasome activates during pressure overload promoted ventricular hypertrophy. Gene and protein expression of the proteasome and its subunits in heart tissue in a canine model of severe chronic left ventricular hypertrophy induced by aortic banding were compared with controls. Their results showed that gene and protein expression of proteasome subunits in left ventricular hypertrophy were increased versus control tissue. The proteasome inhibitor epoxomicin prevented left ventricular hypertrophy by blocking the proteasome. In total, they showed that a stable compensated hypertrophy is accompanied by an increase of the proteasome level. Moreover, they also showed in their mouse model, that this activation is required for the development of cardiac hypertrophy, so protein degradation pathways must be activated to promote an increase in cardiac muscle mass.

These data show that the proteasome system plays a major role in the process of cardiac hypertrophy.

Meiners et al. analyzed the effects of proteasome inhibition on hypertrophic growth of neonatal rat cardiomyocytes (Meiners et al., 2008). Their results show that partial inhibition of the proteasome effectively suppressed cardiomyocyte hypertrophy as determined by reduced cell size, inhibition of hypertrophy-mediated induction of RNA and protein synthesis, reduced expression of several hypertrophy marker genes and decreased transcriptional activation of the BNP promoter. The proteasome inhibition down-regulates multiple hypertrophic signaling pathways such as of Akt1 and Erk1/2. Interestingly the suppression of hypertrophic growth was independent of the hypertrophic agonist used. In hypertensive Dahl-salt-sensitive rats, inhibition with low-doses proteasome inhibitor Velcade significantly reduced also hypertrophic heart

growth. These data show that low-dose proteasome inhibition could be an approach to interfere with cardiac hypertrophy.

A lot of experiments and studies showed an effect that links the ubiquitin system to growth-regulation process in vitro and in vivo.

Razeghi et al. wanted to examine and characterize which transcriptional profile of regulators of the UPS during atrophy, hypertrophy, and hypoxemia-induced remodeling of the heart are important (Razeghi et al., 2006). The cardiac atrophy was induced by heterotopic transplantation of the rat heart, left ventricular hypertrophy was induced by banding of the aorta to create increased afterload and to induce the effects of hypoxemia. Then Razeghi et al. measured the transcriptional levels of six regulators of the UPS, ubiquitin B, the ubiquitin-conjugating enzymes UbcH2 and E2-14kDa, the ubiquitin ligases Mafbx/Atrogin-1 and MuRF-1 and the proteasomal subunit PSMB4 using quantitative RT-PCR (Razeghi et al., 2006). Their results show that induced-atrophy increases the mRNA levels of ubiquitin B and decreased levels of both ubiquitin ligases, while transcript levels of all UPS genes investigated heightened in the hypertrophic and hypoxic heart (except the E2-14 kDa). These data suggest that ubiquitin B is a transcriptional marker for load-induced and hypoxia-mediated cardiac remodeling.

### **2.1.3 Structure of the E3 ubiquitin ligases**

The E3 ubiquitin ligases can recognize both, the E2 conjugating enzyme and a substrate. There are two major classes of E3 ubiquitin ligases: the HECT-type and the RING-type E3 ligases (Pickart, 2001).

The HECT-type ligase is a single molecule, that is characterized by a homologous to the E6-AP carboxyl terminus (HECT) domain. The RING-type E3 ligase uses a RING (really interesting new gene) - zinc finger to bind and activate the corresponding E2-ligase for ubiquitin transfer to the substrate.

The largest family of the E3 ubiquitin ligases, with more than 600 alleged members (W. Li et al., 2008) is the RING-type E3 ligase family, which consists of multi-subunit proteins that contain a scaffold protein (CUL 1, 2, 3, 4A, 4B, 5, 7, PARC), one of various Adaptor (Skp1, EloC/EloB, BTB, etc.), a RING or called ROC/ Rbx protein for binding the E2 ligase and a substrate recognition subunit (i.e.: F-box protein, VHL, BTB) (**Fig. 2 and Fig.3**).

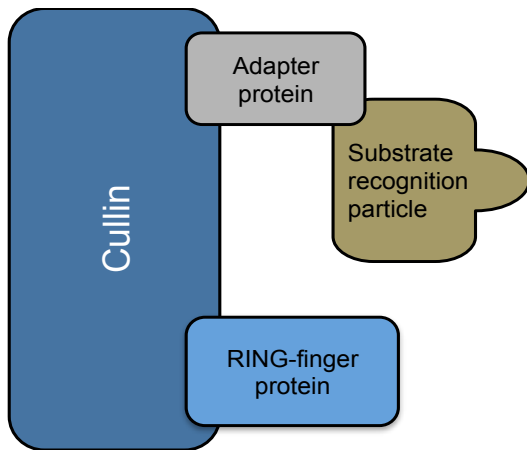


Figure 2: Common modular structure of Cullin-RING E3 ligases

The multisubunit complex of a Cullin-RING E3 ligase (CRL) consists of a Cullin, as a backbone, which is anchoring the RING-finger protein for delivery of the ubiquitin by the E2 and one of the various adaptors to link it to the substrate recognition particle for precisely targeting a substrate for attachment of the ubiquitin.

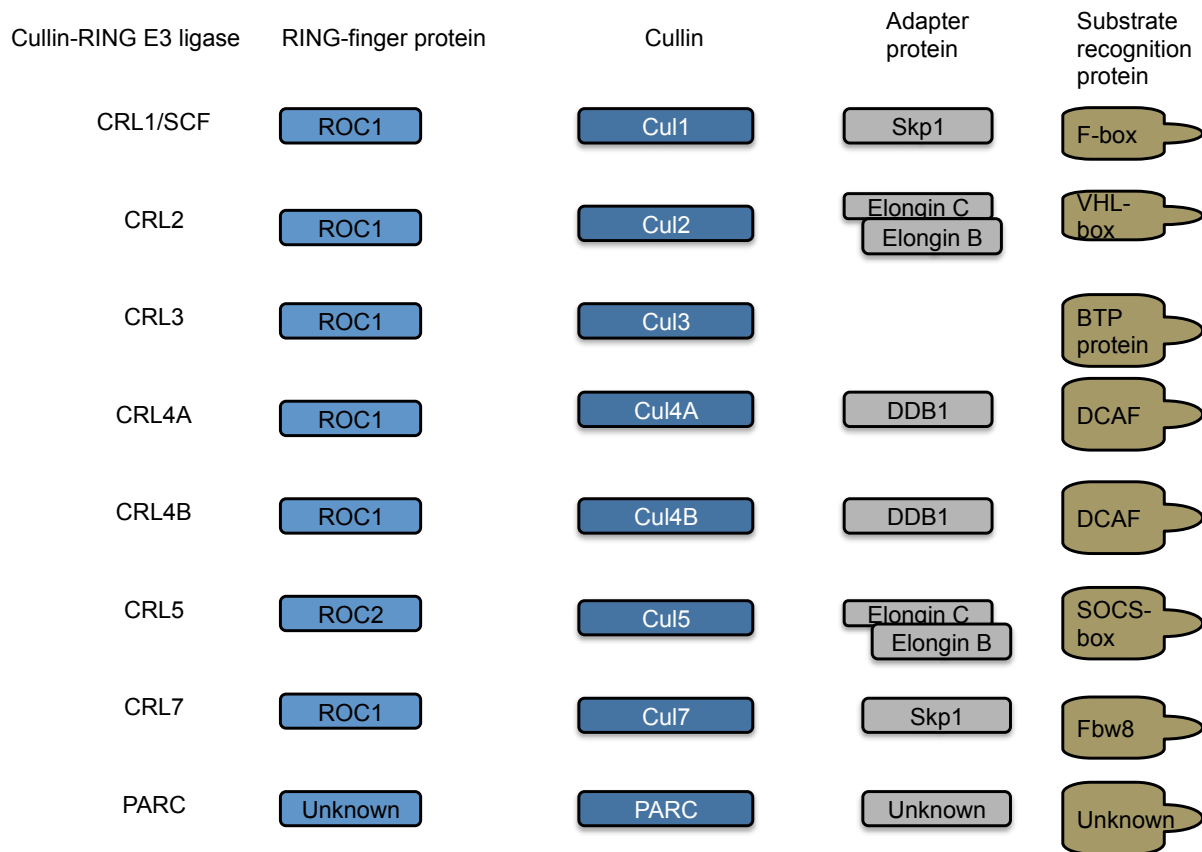


Figure 3: The specific structure of the various Cullin-RING E3 ligases with their different modular subunits

The various CRLs consist of one of the Cullin protein or the PARC protein as the backbone of the multisubunit complex, which combines with one of the different adaptors displayed and its associated substrate recognitions protein. The preliminary model of the CRL is the SCF, consisting of the Skp1, Cul1, F-box protein and the ROC1.

#### 2.1.4 Regulation of Cullin-RING ubiquitin ligase

According to their important role in cell function, CRLs are strictly regulated by several Cullin-associated proteins, for example Nedd8 (neural precursor cell expressed, developmentally downregulated gene) or CAND1 (cullin-associated and neddylation-disassociated protein 1).

Nedd8 is a small protein that is greater than 50% identical to ubiquitin and conjugates to cullin family members (Petroski & Deshaies, 2005). A study of Ohh et al. showed that a functioning Nedd8 pathway is essential for the degradation of SCF targets in the mammalian cell (Ohh et al., 2002). Thus, neddylation, the process of conjugating the Nedd8 molecule to a specific lysine residue in a cullin regulates the activity of E3 ubiquitin ligases. The binding of cullin to CAND1 inhibits neddylation, and Nedd8 is removed from cullins by the proteolytic activity of the COP9/ signalosome (CSN) complex.

Furthermore, Bornstein et al. showed that Skp2 (S-phase kinase associated protein 2), an F-box protein, promotes the dissociation of Cul1 from CAND1, whereas a substrate prevents de neddylation by CSN (Bornstein et al., 2006). Also findings of Kawakami et al. indicate that the neddylation of cullin accelerates the formation of the E2-E3 complex, which stimulates protein polyubiquitylation.

An essential regulator of the CRL activity is CAND1 as mentioned earlier (cullin-associated and neddylation-disassociated protein 1/TATA-binding-protein interacting protein 120A) (Petroski & Deshaies, 2005). This protein specifically binds to unneddylated Cullin1 to sequester them in an unassembled and inactive state and thus inhibits the assembly of the active multisubunit E3 ligase complex (Goldenberg et al., 2004; Zheng et al., 2002). However, CAND1 also acts as an exchange factor that accelerates the rate of which Cul1-Roc1 assemble with multiple F-box proteins adaptor modules (Pierce et al., 2013).

Another protein that is assumed to regulate the Cullin-RING ubiquitin ligase 1 is called Spliceosome-associated protein 130 (SAP 130) (Cordero-Espinoza & Hagen, 2013).

Cordero-Espinosa and Hagen reported that SAP130 overexpression reduces the binding of adaptor protein Skp1 and substrate receptor Skp2 to Cul1 but not affecting the CAND1 binding to Cul1. Furthermore, they showed the overexpression of SAP130 decreases the degradation rate of p27, a protein substrate of the SCF<sup>SKP2</sup> ligase. However, interestingly, high levels of SAP 130 is unable to affect the stability of the Cul2 and Cul3 substrates, HIF-1 (hypoxia induced factor 1) and NRF-2 (Nf-E2 related factor 2). So they prove a novel regulator of the Cullin-RING ubiquitin ligase 1, by the mechanism of competing with the adaptor protein/F-box protein for Cul1 binding and interfering the assembly of the SCF ligase.

## **2.1.5 F-box proteins**

### **2.1.5.1 Structure of the F-box protein/F-box motif**

Many F-box proteins contain specific interaction domains, such as WD40 repeats or leucine-rich repeats, which can link to their substrates. Up to now, there are 61 known human F-box proteins, which all can bind to Skp1 through their F-box motif. Thus they assemble into the SCF complex. The F-box proteins were first characterized as components of SCF ubiquitin-ligase complexes (named after their main containing subunits: Skp1, Cullin, and a F-box protein). The F-box motif is approximately 50 amino acids long and links the F-box protein to other components of the SCF and a phosphorylated substrate. It plays a major role in many cellular functions as reviewed elsewhere (Skaar et al., 2013).

The SCF complex is an E3 ligase composed by multi-subunits, which include Skp1, Rbx1, Cdc53 and the interchangeable F-box protein that submits the substrate specificity. These F-box proteins consist of an F-box motif, which enables them to link to Skp1 and the core complex of the E3 ligase on the one hand and on the other hand to bind specific substrates for ubiquitination.

### **2.1.5.2 Classification of the Fbox family**

The F-box motif was discovered as a homology region of the proteins Cdc4, b-TrCP, Met30, Scon2 and MD6 (Kipreos & Pagano, 2000). They all contain WD (Trp-Asp) repeats. In 1996 Bai et al. recognized that the F-box was a popular motif for protein-protein interaction and they gave the F-box its name, according to the presence of this specific motif in cyclin F.

The F-box protein family can be divided up into three subgroups, determined by the presence of different substrate recognition domains within the proteins. The FBXW subgroup contains the WD40 repeat domain. This group counts ten members including the well-known  $\beta$ -TRCP1, FBXW7 (also known as CDC4) and  $\beta$ -TRCP2 (known as FBXW11). The next biggest group is the F-box and leucine-rich-repeat protein (FBXL) family with 22 members, including SKP2 (known as FBXL1), that all contain leucine-rich repeat as a hallmark of their structure. The third and biggest group, consisting of 37 F-box proteins are called FBXO proteins. They contain various structural domains and therefore called F-box other proteins (Z. Wang et al., 2014; Jin, 2004). Some recent studies have begun to reveal the biological function of the F-box proteins, but there are still lots of uncharacterized domains in several of these proteins, likewise the RNI-like region in Fbxo33 (Jin, 2004). The F-box motif contains about 50 residues. Whereas there are only very few invariant positions (Kipreos & Pagano, 2000).

### 2.1.5.3 Function and Dysregulation of F-box proteins in different diseases

Some F-box proteins are located in both the cytoplasm and in the nucleus. Some in all tissues and others are tissue specific.

The F-box motif functions to link proteins. First described in the SCF, the F-box protein facilitates the binding and ubiquitination of target proteins and thus their turnover in the proteasome. The SCF can bind several F-box proteins, which enlarges, therefore, the substrate repertoire of these protein degradation units. F-box proteins use short defined motifs, known as degrons, to target the substrate. In Fbxw7, for example, this degron is the conserved sequence of (Leu-X-pThr (or pSer)-Pro-Pro-X-pSer (or pThr, Glu or Asp) (Nash et al., 2001; Ravid & Hochstrasser, 2008; Skaar et al., 2013). There are several mechanisms elucidated up to now, how degrons work. Some substrates show canonical phosphor- degrons, cofactor-dependent degrons, priming phosphorylation or even covalent modifications beyond phosphorylation which were recently reviewed by Skaar et al (Skaar et al., 2013).

There are plenty of different F-box proteins encoded in the genome. This high number of databases suggests that F-box proteins play a critical role in a variety of transcriptional regulation, ranging from glucose induction in *S. cerevisiae*, methionine repression in yeasts and the amino acid biosynthesis. Furthermore, the F-box proteins also play a critical role in various cell signaling pathways, which includes the LIN-12/Notch pathway, the hedgehog pathway, the wingless pathway, the NF $\kappa$ B pathway and the E2F-1 and cell cycle regulation (Craig & Tyers, 1999).

In the context of virology, the interaction of the F-box motif in the pathogenicity of human papillomavirus was elucidated, which uses its E6 protein to recruit an E3 ligase called E6-AP to degrade the tumor suppressor p53 (Scheffner et al., 1993). Furthermore, the HIV exploits a F-box pathway to destroy the CD4 membrane receptor in infected T cells, thus minimizing the exposure to the human immune system (Margottin et al., 1998).

New studies also showed that the F-box proteins play a major role in the turnover of cardiac proteins (Spaich et al., 2012). According to Spaich et al. F-box and leucine-rich repeat protein 22 is a cardiac- enriched F-box protein that seems to be essential for the regulation of sarcomeric protein turnover and the maintenance of contractile function in vivo. Their results showed that the in vitro overexpression of Fbxl22 mediates the degradation of  $\alpha$ -actinin and filamin c. The inhibition of the proteasome via MG-132 stops the degradation of both. The targeted knockdown of Fbxl22 in rat cardiomyocytes resulted in the accumulation of  $\alpha$ -actinin associated with an impaired contractile function and cardiomyopathy.

The nuclear factor kappa B (NF $\kappa$ B) signaling pathway controls important cellular functions such as proliferation, differentiation, apoptosis and immune response. Kuiken et al identified F-box only protein 7 (FBXO7) as a negative regulator of NF $\kappa$ B signaling. The pathway activation occurs rapidly upon TNF $\alpha$  stimulation and is highly dependent on ubiquitination events (Kuiken et al., 2012). They used synthetic siRNA library screening for targeting enzymes, which are involved in ubiquitin conjugation and de-conjugation for a modifier of regulatory ubiquitination events in the NF $\kappa$ B signaling pathway. Their results showed that F-box protein 7 (FBXO7) binds to and mediates ubiquitin conjugation to components of the TNF-R1 signaling complex, cIAP1 and TRAF2, which are also ubiquitin ligases, resulting in decreased RIP1 ubiquitination and lowered NF $\kappa$ B signaling activity.

While belonging to the F-box protein family, which in the context of the SCF ubiquitin ligase complex, confers substrate specificity in the process of ubiquitination, this F-box protein depending on the context, is able to stabilize and destabilize its interaction partners (Hsu et al., 2004; Winston et al., 1999).

There is evidence that the dysregulation of the F-box proteins contributes to many diseases, including cancer, diabetes, mood disorders, sleep disorders, bacterial and viral infections (Akari et al., 2001; Bour et al., 2001; Dupuis et al., 2010; Fonzo & Dekker, 2009; Price et al., 2009; Sandberg et al., 2012; Toh et al., 2001; C. Wang et al., 2005; E. E. Zhang et al., 2010; L. Zhang et al., 2009).

Most of the studies have been conducted in the context of cancer research, and the best characterized F-box proteins are SKP2, FBXW7, and  $\beta$ -TrCP (Skaar et al., 2013).

#### **2.1.5.4 Homeostasis of F-box proteins**

F-box proteins are regulated by several mechanisms and at different levels, for example, synthesis, degradation, and association with SCF components (Kipreos & Pagano, 2000). According to the literature, the turnover of the F-box proteins itself is achieved by different mechanisms.

Interestingly some of the F-box proteins are intrinsically unstable, meaning their levels of abundance do not change during the cell cycle. Meaning that they are degraded by an autocatalytic mechanism (Kipreos & Pagano, 2000). The degradation of Cdc4 and Grr1 is dependent on their ability to bind Skp1 through their F-boxes (Galan & Peter, 1999; Zhou & Howley, 1998).

Another example is the F-box protein Met 30, which seems to be ubiquitinated in a cullin-dependent manner but a F-box independent manner (Patton et al., 2000). The information provided by literature is sparse on this topic. However, the mechanisms of the regulation of the amount of F-box proteins contained in cells is an interesting issue, while it would reveal a great insight in the regulation of the regulator of protein turnover.

## **2.2 Heart Hypertrophy**

### **2.2.1 Relevance**

In the western world, the leading cause of death is not due to cancer, but cardiovascular diseases such as myocardial infarction, heart failure, and lethal arrhythmias. The heart itself incorporates the duty of supplying all organs with oxygen-saturated blood and an appropriate blood pressure to ensure their proper functioning. It can modulate the cardiac output when the conditions of the cardiovascular system change. Therefore in the setting of the transition of human from a newborn into adulthood, pregnancy, exercise, as examples of physiologic changes and hypertension, myocardial infarction from coronary artery disease, as examples of human diseases, the heart can compensate the altering demand. Since it is accepted that cardiomyocytes cannot divide anymore after birth, the mechanism is hypertrophy of existing heart muscle cells.

### **2.2.2 Pathophysiology**

The stimuli leading to heart hypertrophy can be split up into the two groups of physiologic and pathophysiologic. Adolescence, exercise, and pregnancy are considered as physiologic changes during life, whereas chronic hypertension, myocardial infarction are triggers of pathophysiologic hypertrophy.

A characteristic of physiological hypertrophy is the normal or enhanced contractile function in the setting of normal organization of cardiac cells (Weeks & McMullen, 2011). Whereas pathophysiological hypertrophy is associated with fibrosis, capillary rarefaction, increased production of inflammatory cytokines, increased death of on cellular level and reduction in systolic and diastolic function, that progresses into heart failure clinically (Shimizu & Minamino, 2016). There is growing evidence that the molecular mechanism leading to physiological and pathological hypertrophy of cardiomyocytes differ in their signaling pathways, what will be discussed in the next caption.

Hypertrophy of the heart can also be classified by the definitions of eccentric and concentric hypertrophy. Eccentric hypertrophy is characterized as normal growth response with a matched increase in ventricular walls, ventricular septum, and chambers. The cardiomyocytes grow in width and length, but the increase in length is more prominent. Concentric hypertrophy is defined by thickening of walls and septum, with no increase in chamber volume. The cardiomyocytes grow more in width than length (Heineke & Molkentin, 2006; Maillet et al., 2013). It is commonly accepted that concentric hypertrophy over a long time, leads to larger chambers

with the loss of wall and septal thickness resulting in a dilatative cardiomyopathy (Van Berlo et al., 2013).

### 2.2.3 Signaling Pathways

Recent reviews on this topic, share the opinion that specific triggers lead to either physiologic or pathophysiologic heart hypertrophy. Most pathways can be assigned to one of these categories of cardiac hypertrophy. Only the insulin triggered pathway seems to be in an intermediate position in this partitioning.

First, the physiologic hypertrophy pathways known will be shortly mentioned and explained. The physiologic signal includes growth hormones, such as thyroid hormone, insulin, insulin-like growth factor 1 and vascular endothelial growth factor and mechanical forces that merge downstream into a limited number of intracellular pathways such as PI3K, AKT, AMP-activated protein kinase and mTOR (Maillet et al., 2013).

Thyroid hormones act as a transcriptional activator in the postnatal growth by triiodothyronine (T<sub>3</sub>), which activates the two thyroid hormone receptors (TR $\alpha$  and TR $\beta$ ). T<sub>3</sub> activates the transcription of many channels and receptors, that play a major role in the heart, such as  $\beta$ 1 adrenergic receptor, sodium and potassium channels, cardiac troponin I, ANF and others.

Another pivotal player is insulin, what regulates protein synthesis and gene expression through shifting glucose intracellular via GLUT channels and by affecting glycolysis, glycogen synthesis, fatty acid oxidation (Maillet et al., 2013). Insulin attaches its associated insulin receptor (IR), what leads to the activation and phosphorylation of the adaptors insulin-like receptor substrate 1 (IRS1) and IRS2, triggering the PI3K-AKT signaling pathway. Belke et al. generated a cardiomyocyte-specific insulin receptor knockout that showed a decrease in cardiomyocyte size by 20-30% concomitant with a strong expression of  $\beta$ -MHC isoform. The fatty acid oxidation rate was decreased as result of the reduced expression of enzymes needed for  $\beta$ -oxidation (Belke et al., 2002).

Another important player in this pathway is the insulin-like growth factor 1 (IGF1) that binds the insulin receptor and the IGF1 receptor. The binding to this receptor also activates the PI3K-AKT-phosphoinositide-dependent protein kinase 1 (PDK1)- glycogen synthase kinase 3 $\beta$  (GSK3 $\beta$ ) pathway. Mice deficient of IGF1 or IGF1-receptor show growth retardation and perinatal death due to respiratory distress which illuminates the essential role of IGF1 in normal growth and development.

IGF1 overexpression experiments under the control of an  $\alpha$ -MHC promotor showed an increase in the count of cardiomyocytes in the heart and an increase in heart weight (Reiss et

al., 1996). These results underline the importance of the insulin and IGF1 signaling for the heart growth.

A furthermore critical system for the heart is mechanosensory, which permit the cells to evaluate the wall stress and contraction forces. Due to these receptors, the heart realizes if a change in its physiology is needed to maintain the demand of the blood supply. The mechanosensory are called transient receptor potential (TRP) channels (Maillet et al., 2013). They are stretch sensitive mediators that trigger downstream pathways. TRP channels activation lead to calcium influx and activation of signaling pathways. Another stretch sensors in the heart are muscle LIM protein (MLP), actinin-associated LIM protein (ALP), nebulin (NEB), cipler, telethonin (Tele), obscurin (Obs) and the titin protein. For more information, please be revised to the associated reviews on the proteins.

One of the most important intracellular signaling pathways in the context of physiological hypertrophy is the PI3K, which is the common receptor in response to insulin and IGF1 signaling. Already in 2000, a group in Boston could show that this kinase is pivotal for the heart size in mice (Shioi, 2000). They created transgenic mice with constitutively active or dominant-negative mutants of PI3K in the heart that resulted in increased heart size in the overexpression mice, while the knockout mice had smaller hearts and cardiomyocyte size.

Another main hypertrophic signaling pathway is serine/threonine protein kinase AKT, is modulating several signaling pathways. For example, it inhibits the activity of forkhead box protein O3 (FOXO3), which is involved in the function of ubiquitin ligase Atrogin-1 and the muscle-specific RING finger protein 1 (MURF1), which are involved in regulation of cardiac hypertrophy.

In contrast to physiological hypertrophy, that is mainly triggered by athletes exercise, pregnancy and growing up, the pathophysiological heart hypertrophy develops in the context of cardiac diseases. The main event in this type of hypertrophy is myocardial infarction, aortic stenosis, and long-term elevated blood pressure. Recent papers suggest that also the molecular basis is different in contrast to physiological hypertrophy. The main player of the pathophysiological heart hypertrophy are the pathways involved in calcineurin,  $\beta$ -adrenergic signaling, cGMP kinase G signaling, protein kinase C and mitogen-activated protein kinase and the insulin/AKT signaling in its intermediate position in this separation.

The intracellular increase in  $Ca^{2+}$  activates the calcineurin/NFAT signaling (Molkentin et al., 1998). Calcineurin is a  $Ca^{2+}$ -activated serine-threonine protein phosphatase that de-attaches NFAT and thereby enabling NFATs translocation into the nucleus, what is inducing heart hypertrophy (Shimizu & Minamino, 2016). Interestingly the calcineurin/NFAT induced hypertrophy seems to be unique for pathological hypertrophy and not be involved in physiological

hypertrophy (Wilkins et al., 2004). Some papers show that the ubiquitin ligase Atrogin-1 (Fbxo32) is engaged in this hypertrophy mediating pathway (H. Li et al., 2004).

Another major player is the  $\beta$ -adrenergic receptor signaling. The  $\beta$ -blockers are nowadays in the standard therapy regime for heart failure and show a significant reduction of mortality in patients. Catecholamine such as epinephrine and norepinephrine bind to adrenergic receptors, which are G-protein coupled receptors and activate the CaMKII pathway.  $\beta$ -receptor blockers are widely in clinical use and also permit their effect on the kidney and the renin-angiotensin-aldosterone system that increases the level of angiotensin II and induces cardiac hypertrophy (Ahles & Engelhardt, 2014). Activation of the G-protein coupled receptors by catecholamines induce growth in neonatal rat ventricular myocytes as well increases the level of ANP, BNP, and MHC-2, which are strong markers of cardiac hypertrophy.

The role of cGMP was elucidated by the work of Takimoto et al (Takimoto et al., 2005). They blocked the intrinsic catabolism of cGMP by using PDE-5 inhibitor sildenafil, what suppressed heart hypertrophy in vivo in a transaortic constriction (TAC) model. Sildenafil even reversed the previous hypertrophy. Many hypertrophy inducing pathways were diminished.

The protein kinase C and mitogen-activated protein kinase (MAPK) signaling induces heart hypertrophy, while its suppression inhibits hypertrophy (Takeishi et al., 2000). There are three main sub-signaling pathways, which are p38MAPK, c-Jun N-terminal kinases (JNK) and the extracellular signal-regulated kinase (ERK1/2). Most of the MAPK signaling proteins are increased in heart failure as well in humans and in animal models (Gutkind & Offermanns, 2009; Haq et al., 2015; Toischer et al., 2010).

Finally, the insulin/AKT signaling plays a role in physiological heart hypertrophy as well as in pathological conditions. Chronic hyperinsulinemia, for example, was found to promote pathological hypertrophy by fostering angiotensin II signaling (Samuelsson et al., 2006). Another paper from Shimizu et al. shows that excessive cardiac insulin signaling worsens cardiac function by developing myocardial hypoxia in a pressure overload stress model (Shimizu, Ippei, Komuro, 2010). Inhibition of these high levels of insulin improved the cardiac dysfunction significantly. All leading to the conclusion that longterm hyperinsulinemia worsens cardiac function and leads to cardiac hypertrophy.

### **2.3 Role of E3 ligases in regulating heart hypertrophy**

The field of E3 ligases as regulators of cardiac hypertrophy is not yet that well established in the literature. The two largest players in the ubiquitin-proteasome system that have extensively focused on are Atrogin-1 and Murf1. First discovered at the beginning of the new millennium,

Atrogin-1 and Murf1's importance role have been proven by in vitro and in vivo data by several research groups.

### **2.3.1 Atrogin-1's role in skeletal and cardiac muscle hypertrophy**

One of the major atrophy related E3 ubiquitin ligase that was discovered first in striated muscle is the Atrogin-1/MAFbx (Gomes et al., 2001). This F-box protein contained in an E3 ligase is upregulated in skeletal muscle by stimuli that lead to the loss of muscle mass (Bodine et al., 2001; Lecker et al., 2004).

Zeng et al performed experiments with neonatal rat cardiomyocytes (Zeng et al., 2013). These cells were infected by adenovirus Atrogin-1 or GFP-control and incubated for 24 hours. As a result, they found upregulated and down-regulated genes with the main function in categories as cell death proliferation, inflammation, metabolism, structure, and function.

Moreover, they showed that overexpression of Atrogin-1/MAFbx inhibits cardiomyocytes survival, hypertrophy, and inflammation even in response to endotoxin lipopolysaccharide LPS, whereas the knockdown of Atrogin-1 by siRNA had opposite effects. The molecular mechanisms of these effects were associated with the inhibition of MAPK and NFkB signaling pathways.

Furthermore, data show that Atrogin-1 overexpression inhibits cardiac hypertrophy through calcineurin/NFAT (nucleus factor of activated T cells) and phosphatidylinositol 3-kinase/Akt/Foxo signaling pathways (H. H. Li et al., 2007; H. Li et al., 2004; Skurk et al., 2005).

Castillero et al. showed that suppression of Atrogin-1 in vitro resulted in increased expression of MURF1 and vice versa (Castillero et al., 2013). Suppression of both resulted in myotube hypertrophy and even prevented dexamethasone-induced myotube atrophy. They concluded that these results create a link between increased levels of Atrogin-1 and MURF1 and glucocorticoid-induced muscle atrophy, what is a frequent clinical feature in longterm treatment of patients receiving steroids for i.e. immunosuppression.

Summarizing the data concerning Atrogin-1, it is the most important F-box protein in muscle hypertrophy and atrophy in the recent decades and a paramount player in the regulation of cells. Further publication will be described in the discussion part of this thesis.

### 2.3.2 Murf1's role in heart disease

Another major player in the process of regulation the muscle mass under various pathological and physiological conditions is Murf1.

The leading experts of Murf1's role in various cardiac disease modell are Monte S. Willis and Cam Patterson. Their work lead to the identification of muscle RING finger 1 (Murf1) as a cardiac-specific protein that regulates cardiomyocytes mass by degradation of sarcomeric proteins and inhibition of transcription factors involved in hypertrophy signaling pathways (Patterson et al., 2011).

To determine the role of Murf1 in cardiac ischemia/reperfusion (I/R) injury in vitro, experiments on H9C2 cardiomyocytes with an adenovirus were conducted. With increasing Murf1 expression the cardiomyocytes were protected against the I/R challenge (H.-H. Li et al., 2011). Increased levels of Murf1 also reduced TUNEL positive cells and cleaved caspase-3, thus inhibiting apoptotic cell death. This effect was conducted by the proteasome-dependent degradation of phosphor-c-jun.

The muscle RING finger protein 1 (Murf1) plays a pivotal role in preventing cardiomyocyte hypertrophy by inhibiting the PKC-mediated signal response in neonatal rat ventricular myocytes. Murf1 blocks the PKCepsilon translocation, which normally initiates a hypertrophic signaling cascade. The overexpression of Murf1 leads to a decrease in the activity of downstream effector ERK1/2 and also inhibits the phenylephrine-induced increase in cell size (Arya et al., 2004). In vivo experiment with mice lacking Murf1 and Murf2 develop cardiac and skeletal muscle hypertrophy at baseline. Transgenic (Tg+) mice overexpressing cardiac Murf1 showed a thinning of the left ventricular wall and a decrease in cardiac function. In TAC (transaortic constriction) experiments the MURF1 Tg+ animals showed rapid heart failure (M. S. Willis et al., 2009). Willis et al could also exhibit in this work, that pivotal changes in metabolic functions occurred, i.e. alterations in CK activity, that lead to increased heart susceptibility following TAC. Furthermore, Murf1 is a necessary protein to regulate cardiac atrophy after the placement of a left ventricular assist device (M. S. Willis et al., 2009). After the release of TAC in Murf1<sup>-/-</sup> and wild-type mice, the Murf1 knockout animals cardiac mass and cardiomyocytes cross-sectional areas decreased approximately 70% less compared to their wildtype littermates in the four weeks after release of TAC. The wild-type mice returned to baseline values after four days after TAC release. A second model in these MURF1<sup>-/-</sup> KO mice showed resistance to dexamethasone-induced cardiac atrophy.

To summarize the role of Murf1 in the heart, it can be concluded that Murf1 expression leads to a reduction of hypertrophy and atrophy while its depletion causes hypertrophy. These findings are similar to the role of Atrogin-1.

### 3 Aim and objectives

The aim of the project was to identify hypertrophy-modulating CRLs in primary cardiomyocytes by using a genomic approach using a rat siRNA library directed against 43 F-box proteins and other CLR components, combined with automated microscopy to assess the role of the CRL depletion in neonatal rat cardiomyocyte cell size.

The first objective the transfection of neonatal rat cardiomyocytes in vitro by specially designed siRNA oligonucleotides to knock down the mRNA of the F-box protein. After a few days of cell culture in medium, the dishes were fixated and stained with DAPI and  $\alpha$ -actinin for accurate evaluation of cardiomyocytes by microscopy. An automated program took the immunofluorescence picture and measured the cell size.

The second objective aimed for further validation of candidate CRLs in an NRCM culture that significantly changed the cell size after transfection with the target siRNA. Nuclei count analysis of cardiomyocytes and MTT assays were performed to exclude cell damage and death.

To evaluate the efficiency of the knockdown of the mRNA, we used a quantitative real-time polymerase chain reaction. After transcription of mRNA into cDNA, we measured the efficiency of the knockdown of the target mRNA.

In a third validation experiment, we determined the change of incorporation of isotope-labeled  $^3\text{H}$ -isoleucine into the cells, as performed in the Jentzsch paper (Jentzsch et al., 2012), that first published the screening protocol carried out at the Institute of Pharmacology and Toxicology at the TU Munich.

These experiments should help to get a deeper insight in the emerging field of the CRLs in the heart, beside of the known E3 ligases, such as Atrogin-1 and Murf1, which are already evaluated in vitro and in vivo. These results could provide critical knowledge about the role of CRLs in protein turnover in the heart and its effect in heart diseases by unveiling new target for potential enzyme inhibitors or enhancer comparable to Protac-1 (Sakamoto et al., 2001).

## 4 Materials

### 4.1 Antibodies

Antibody for microscopy	Clone (if monoclonal)	Produced in/isotype	Dilutions or final concentration	Company
Anti- $\alpha$ -actinin	EA-53	Mouse IgG1	1:1000	Sigma-Aldrich Deisenhofen, D
Alexa 488 anti-Mouse IgG H+L	-	Goat	1:200	Life Technologies, Carlsbad, USA (Invitrogen A11029)

### 4.2 Oligonucleotides

Application or target gene	Designation	Sequence (5' -> 3')	Amplicon size
cDNA-synthesis	Oligo(dt)	TTTTTTTTTTTTTTTT	-
Rat Primers			
<i>Fbxo45</i>	<i>Fbxo45</i> fwd	TGGCAGTGATAGGGATTGCT	239 bp
	<i>Fbxo45</i> rev	TACCCACGCTCAAAGGCTAA	
<i>Fbxo25</i>	<i>Fbxo25</i> fwd	ACCAACCCTGTACATGCTCA	171 bp
	<i>Fbxo25</i> rev	ACTGCTCTTTGGTCGGGTAA	

<i>Fbxw4</i>	Fbxw4 fwd	AGGAACGAGTGAAGCTGTCT	103 bp
	Fbxw4 rev	CTTCTAGCTGCATCCAAGGC	
<i>Fbxo6</i>	Fbxo6 fwd	CTTCGAGAGGGCTTTGTCAC	172 bp
	Fbxo6 rev	GCTCTCCACCTTCCACTCAT	
<i>Fbxo33</i>	Fbxo33 fwd	GGTTTTATTGGCATGGCGGT	173 bp
	Fbxo33 rev	ATCCTGGTCGGCTAGTTCAC	
<i>Roc1</i>	Roc1 fwd	CGGCGATGGATGTGGATAC	107 bp
	Roc1 rev	ACAATATCCCAGGCCAGAG	
<i>Fbxo9</i>	Fbxo9 fwd	TCTGCTGGGTCATTATCGCT	160 bp
	Fbxo9 rev	CAGCCCCACATGAAAGTTGT	
<i>Fbxo30</i>	Fbxo30 fwd	TGAGGGACATTTGTGGCAGT	227 bp
	Fbxo30 rev	GCTTCCTCCCGCTTCTCTAT	
<i>Fbxo32</i>	Fbxo32 fwd	TTGGATGAGAAAAGCGGCAC	100 bp
	Fbxo32 rev	CTTCTTGGCTGCAACATCGT	

<i>Cul1</i>	Cul1 fwd	GGATGACCTCAGAGCTGGAA	200 bp
	Cul1 rev	CTCCAAGCCGACAAACTGAG	
<i>Ddb1</i>	Ddb1 fwd	GGTGCCATCATCATTGGACA	198 bp
	Ddb1 rev	CCATCCATCTGCTCCTCCTT	
<i>Fbxl14</i>	Fbxl14 fwd	GTCCCTCTCCCTTTGCTCTT	183 bp
	Fbxl14 rev	ATCCTAGTGCAGCCGTACAG	
<i>Fbxw5</i>	Fbxw5 fwd	ATGGCTATATCTGGGACCGC	211 bp
	Fbxw5 rev	GCAAACCAGGAGAAGAAGGG	
<i>Gapdh</i>	Gapdh fwd	TGACAACTCCCTCAA- GATTGTCA	121bp
	Gapdh rev	GGCATGGACTGTGGTCATGA	

ON-TARGETplus Rat siRNA- SMART pool	
Target gene	Sequence (5' -> 3') of oligonucleotides
<i>Cul3</i>	UUCAAGAAAUCCAGCGUAA GAGAUCAAGUUGUACGGUA UGACAGAAAACACGAGUA ACAGGAAGUAGAAACGAUA
<i>Cul4b</i>	UAACAGUAGUAACGAGAGA CCAAUUGAUGCUGCGAUC UGAUUGAGAGAGAGCGGAA AGACUUAGCCAAACGCCUA
<i>Cul5</i>	CUGCAAGAGAUAAAGGCGUA AAGGCAUGAUCAAGCGAAA GGAAGACAGUAUUGUUCGA UUAGAAACAAGACGAGAAU
<i>Fbxl3</i>	GCUUAGAACAUUUGCGCAU ACAUGAUGCCUACGUGGUA AUGCCUGACUUGUGGCGAU AGACACACUCCACACGAU
<i>Fbxl17</i>	UGAUAGCCAUUGGGCGAUA GUUACAAGAUCUCGGACGA GAAUAUACAUGCAGGAGAA GUGUGGAGGUUAUCGCAA
<i>Fbxl20</i>	CGGAUAGACCGUUCGAUU GUUCUCAACAGUGACGAA UCGUGGGUGUCUCGGAGUA CAGAACUGCCCUCGGCUUA

<i>Fbxo3</i>	GCAGGAAACUAGCACGGAA ACUCAGAUGUAGGAAGUA UGAAAGAGGGUGCGGUGA AGUUAGAGUUCUCACGCUA
<i>Fbxo4</i>	GAUACUUUCUGUUUCGAGA UGUUCAGCCUACAGAGCGA GCUCAUGAACUUCGUCUCA AGAAUCUAAGCAUGCGAAA
<i>Fbxo9</i>	GUGAGAAGCUACACGGCGU UGGCCGAUCUCCUGUCGUA GGCACCAAGUGGAAUAUUA AGGCGUAGGUUCCAGUAAU
<i>Fbxo21</i>	GAAUAUAAGUUCGGCAGA AGCACAAGAGGUACGGCUA CCUGGAAGUACUACGCUAA GGGCACGAGUGGAUCCGAA
<i>Fbxo22</i>	CGUGGUAGCUGAAGCGCUU GGAGAGAGUGUGUGCGUAG CAGAUGAAGGACAGCGUUA GAAUUÜAACUCUCGAAAGA
<i>Fbxo28</i>	AAUCCAAACGACUGCGGAA CCAGAUCAUAGGCGAGCAA GCACAUUACAUGCGGAUUU GCUUUAUGUCCUACGACGA
<i>Fbxo30</i>	CAGCCUAAGCAGCGUUCAA AGACAAAGCAGUCGAUACU AAGAAAAGGUGUGGCGAUU UGAAAUUGUUGGAACGUGA

<i>Fbxo32</i>	GGCAGAUCCGCAAGCGAUU ACAUGUGGGUGUAUCGAAU CAUAAGACUCAUACGGGAA ACUUUAAGCUUGUGCGAUG
<i>Fbxo45</i>	GAUAGGGAUUGCUACGAAA GACUUUAGCCUUUGAGCGU GGAGAGAGAAUCCGAGUCA CAACAUGCCUUCAGCACGA
<i>Fbxw7</i>	GGUCAGCGGUCACGGGUAA CGGGUGAAUUUAUCCGAAA CGUUACAGUUUGACGGCAU GCUCAGACGUGUCGAUACU
<i>Fbxw11</i>	GAUAAGUAAUGGAACGUCA AGAUAAUACCAUCCGGUUA AUUAAAGUGUGGAGCACGA CAUCUUAUCUCACGAAUGU
<i>Cul1</i>	GAACAGUGCGAGUGACGAU GAGCUCAGUUUGUCGGCUU GCAAAGGGCCCUACGUUAA AAGAAUAAUUUGGAGCGAGU
<i>Cul4a</i>	CCAUGUGAGUAAACGUCUA GACAGUGAGUUGCGAAGAA CAAAAUGGCCACCGGCAUA GCUGAUUGGGCGUGAACGA
<i>Cul7</i>	CUACAUGGUUCGUGCACAA CCGCAUGCUAGCCGAGUAA UCAAGAAGUAAAACGCAGA AGAUGAGGCUGGCGCUGAA

<i>Fbxl5</i>	GGGACGAAGAUGCCGAUUAU CCAAGAGACUGGACGAGUA GCUGAAGAUUUGGCCGAUA CAAAAUGAGUCUUCGGCAU
<i>Fbxl12</i>	CUGCCUAGUUAUCGUCAGA GCUGGAAUGCAUCGUGCUA GCUGCGAAAUCUCGAUGAU CCGAGAUGUGCGCAAGAUU
<i>Fbxl14</i>	UGGCCAUGAUCUUCGGCUA GCAUAGACCUAGUACGGCUG GUAGAAAGCMGCCCGACU CGACMCAUCAGCGACACU
<i>Fbxl19</i>	GGGAGMGCUGGAGCGUUU GCAUGMGCAGUCGUGCCU UGCCAUUUCUGCCGAGACA GCUGAGGGUGUUAUCMUU
<i>Fbxo6</i>	CCUGAGAUCAUGGCGGAUA GGCCGGACAUUGUGGUUAA UCUUAUGGGAUGUGCCUCA GAGGAAGAUACUCAGCUUU
<i>Fbxo8</i>	CCAAAUGCAUUGCGAGAAU AAGCACAAUUGUUCGAACU GAGAGAGUUUAUUCGAAAU UCACACCAGUCACCGGAAA
<i>Fbxo10</i>	GGACAGUACCCGUUGGCGA CAAGGAAGCCAUGGCGCUA AGGAAGAAGGAGCGACGUA GAAUUUGUGGGCAGCGAAA

<i>Fbxo11</i>	UCCAAUUUUUAGACGGAAU AGAAAAGGCUGUUAGUAGA ACUAAGAAGAAAUCGGUAU AGGUAAAAGCCUACGCUAA
<i>Fbxo18</i>	AGAAUCGCCUGCACGGUAU GGUUAGAGUUUGACACGGU GGUACUUGAUCAACGAAGA CAGCAAAGUGGACGGCAUU
<i>Fbxo25</i>	GCUGAACGCCACACGUAGA GACUUGAGCUCGACCCUUU GGGAAAUCAGUGUUAGUUG UGGAUAAAAUCGUGCAAAA
<i>Fbxo33</i>	CAGUCGAACUAGAGCGCUU CAAAGAACGUAGUCGGGUA UCGAGUUUCUCAUGCGCAA GCGAGAGUCCUGACCGACA
<i>Fbxw2</i>	GUGCAGACAAGUACGAGAU AGGUUUACUUGAAGGCUAU UCUCUAAGCAGUGGAAUAA GGCAGUGUGUUUACGGCAU
<i>Fbxw4</i>	CCAGUAAAGGAACGAGUGA CUUACAACCUCCACGUCUU CACAAGAGCAGGAGCGUCA GAAGAAGGGCCGAGACGCU
<i>Fbxw5</i>	UUUAGCAGUAAACGCCUUA GGGAGCAGUUCUACCGCUA CAAGGAAGGUUUACGGCGU CCUUUCAUACUCAGCCAAA

<i>Fbxw8</i>	GCAAAGGUGCCGUGAGCGA CUUAUGAACUGGCGAUCAA CAUGGAAGGUGAUUGCCGA ACGAGAAGGUGCUGCGAAA
<i>Roc1</i>	CCCAUUUGUUACUCGUUUA GGAUCUUUGUAUCGAGUGU AAUCUUGGCUGGCAAUAGA GGUACUUGGGAAUUAGGUA
<i>Roc2</i>	GCUGGGACGUUGAGUGCGA CAAGAAGUGGAACGCGGUA GGUUAACUUGUACUGAGU GGAAGGUUGUAUUGUAUGU
<i>Skp2</i>	GGCCUAAGCUCAAUCGAGA GGUAUCAA AUGCCGACUGA UGUCAAAACCUCCACGGGAU CAGCCGGUGCUACGAUAUA
<i>Ddb1</i>	CCACUGAUGAGGAGCGGCA ACACUUUACUUCAGCGGAA CCUCAGGAGCUCCGGCAA AGAU AUGGAAGGACGGCUU
<i>Elongin-B</i>	CCUUUGAAGCGCUGCGUAU GCACGGUGUUCGAACUGAA UGAACAAGCUGUGCAGUGA CCACAGGAUUCUGGAGGCA
<i>Elongin-C</i>	CAGGUCAGUUUGCGGAGAA GCCAUGUAUGUGAAAUUAA GCAUUAACAUCAGGAACAA UCGAAAGUGUGCAUGUAUU

<i>BTRC/Fbxw1</i>	CCAGAUAAAUAACGCGACA CGGUCAAUGUUGUCGACUU GGACAUAGAGUGCGGUGCA UCAGAGUGUGGGACGUAAA
<i>Cul9</i>	ACAUGAGGGCAUCGAGCAA GAACAGAGUUUUACGCCAU GCACAAAGACUAUGCGGUA GGACAGGAAGCCAGCGCAU

### 4.3 Chemicals

Chemical	Producer
4, 6-Diamidin-2-phenylindol (DAPI)	Sigma-Aldrich, Deisenhofen, D
Bromodeoxyuridine (BrdU)	Sigma-Aldrich, Deisenhofen, D
Bromophenol blue	Merck Chemicals, Darmstadt, D
Deoxynucleoside triphosphate (dNTPs)	Life Technologies, Carlsbad, USA
Dulbecco's Modified Eagle Medium (DMEM)	Gibco, Karlsruhe, D Sigma-Aldrich, Deisenhofen, D
Ethanol	AppliChem, Darmstadt, D
Fetale bovine serum (FBS)	PAN Biotech, Aidenbach, D
Glucose	Merck Chemicals, Darmstadt, D
Glycerol	Merck Chemicals, Darmstadt, D
Isopropyl alcohol	Carl Roth, Karlsruhe, D
Lipofectamine 2000	Invitrogen, Karlsruhe, D
Dharmafect 1	GE Healthcare Dharmacon Inc., Denver (USA)
Dharmafect 3	GE Healthcare Dharmacon Inc., Denver (USA)
MEM	Sigma-Aldrich, Deisenhofen, D
Methanol	AppliChem, Darmstadt, D
MTT dye	Sigma-Aldrich, Deisenhofen, D
OptiMEM I	Gibco, Karlsruhe, D
Paraformaldehyde (PFA)	Sigma-Aldrich, Deisenhofen, D
Penicillin/Streptomycin	Pan Biotech, Aidenbach, D
Phenylephrine (PE)	Sigma-Aldrich, Deisenhofen, D
Phosphate-buffered saline (PBS) (sterile)	Gibco, Karlsruhe, D
RNAse Out Recombinant Ribonuclease Inhibitor	Invitrogen, Karlsruhe, D
Hydrochloric acid (37%)	Merck Chemicals, Darmstadt, D
Rotiszint eco plus	Carl Roth, Karlsruhe, D

SiGLO Red Transfection Indicator	GE Healthcare Dharmacon Inc., Denver (USA)
TriFast	Peqlab, Erlangen, D
Trichloroacetic acid (TCA)	AppliChem (Darmstadt, D)
Triton X-100	Sigma-Aldrich, Deisenhofen, D
Vectashield-DAPI	Vector Laboratories, Burlingame, USA
Vitamin B12	Sigma-Aldrich, Deisenhofen, D

#### 4.4 Enzymes

Collagenase Typ II (280 U/mg)	Roche, Basel, CH
Protoscript II Reverse Transcriptase	New England BioLabs, Ipswich, USA
Trypsin	Promega, Mannheim, D
DNase	Sigma-Aldrich, Deisenhofen, D

#### 4.5 Kits

Fast Start Universal SYBR Green Mastermix (ROX)	Roche, Basel, CH
---	------------------

#### 4.6 Buffer, Solutions and Cell Culture media

##### **Triton-X Buffer**

Triton X-100	0.5 ml
ddH <sub>2</sub> O	ad 100 ml

##### **Paraformaldehydsolution (4%)**

Paraformaldehyde	20 g
PBS (1x)	480 ml
Heat solution at 60°C	
NaOH (1 M) to pH 7.2	
PBS (1x)	ad 500 ml
Store at -20°C	

### **Buffer and solutions for cell culture**

The following buffer and solutions were produced under sterile conditions

#### **BrdU**

BrdU	230 mg
ddH <sub>2</sub> O	74.8 ml
Store at -20°C	

#### **Vitamin B12**

Vitamin B12	100 mg
ddH <sub>2</sub> O	50 ml
Store at -20°C	

### **Cell culture medium**

Enclosed medium were prepared under sterile conditions and stored at -4°C.

#### **NRCM basic medium**

MEM	10.8 g
Vitamin B12	1 ml
NaHCO <sub>3</sub>	350 mg
ddH <sub>2</sub> O	ad 1 l

pH 7.3

**NRCM culture medium**

FS – 0.1%, 1% oder 5% (PAN)	0.5 ml, 5 ml or 25 ml
Penicillin/Streptomycin	5 ml
BrdU	5 ml
NRCM basic medium	ad 500 ml

**Pre-plating Medium**

FBS (PAN)	25 ml
Penicillin/Streptomycin	5 ml
NRCM basic medium	ad 500 ml

**Calcium and bicarbonate-free Hanks with HEPES (CBFHH)**

add

1.75 mg/ml trypsin

10 µg/ml DNase II

## 5 Methods

### 5.1 Isolation and cell culture of primary neonatal rat cardiomyocytes

Neonatal rat cardiomyocytes were isolated and digested from 1-2 day old Sprague-Dawley rat as described previously in Jentzsch et al (Jentzsch et al., 2012). All steps were performed under sterile conditions. The hearts were excorparated and transferred into a 10cm dish filled with calcium and bicarbonate-free Hanks with HEPES (CBFHH) buffer and placed on ice. After separating the atriums, the hearts were cut into small pieces and digested with 15 ml Trypsin for 20 min at room temperature (RT) on a magnetic mixer. The trypsin solution was discarded, and the tissue was digested in new trypsin (10 ml) for 10 min on the magnetic mixer. The suspension was carefully pipetted up and down, and the supernatant was transferred into a 50 ml tube, filled with 7.5 ml FBS and incubated in a 37°C water bath until the next step. This procedure was repeated until most of the heart was digested. The isolated cells were centrifuged (800x g, 10 min, RT) and resuspended in 10 ml NRCM pre-plating medium. This suspension was filtered (40 µm pore size; BD, Heidelberg D) and 10 ml each transferred into a 10 cm dish and put into an incubator for 1 hour at 1% CO<sup>2</sup>, 37°C). In this pre-plating step, the fibroblasts grow on the dish soil faster, while the cardiomyocytes stay in the supernatant, allowing the separation of these two different cell populations. The cardiomyocytes enriched supernatant was transferred into a new 50 ml tube, and the cells were counted (Countess Cell Counter, Invitrogen, Karlsruhe, D). In the last step, NRCM suspension was diluted with 5% FBS NRCM medium to the desired concentrations on cells and thawed into the dishes followed by incubation at 37°C and 1% CO<sup>2</sup> in the incubator. The medium in the dishes was changed every two or three days, according to the indicator pH color and number of cells thawed per well.

### 5.2 siRNA transfection

Each ordered ON-TARGETplus Rat siRNA- SMART pool was first diluted to 20 µM concentration. In the first step, the provided tube with the 3 nmol siRNA was spined down and then diluted by adding 120 µl RNase free water to the tube. After pipetting three to four times up and down, it was put on an orbital shaker for 30 min at 23°C and 600 rpm. The concentration was measured at a Nanodrop (absorbance at 260 nm, RNA-40). Then 30 µl of provided 5x siRNA Buffer was added and mixed by pipetting up and down. 10 µl aliquots for each siRNA were stored at -20°C.

Transfection of NRCM with 50 nM final concentration of siRNA in 96 well plate dish. The following amounts are used for one single well.

A falcon tube with the necessary amount of Opti-MEM I was prewarmed in the water bath and 5% FBS NRCM medium without antibiotics (PenStrep) was always prepared fresh before every transfection. In the first step, the transfection samples are prepared by mixing and diluting volume for 20  $\mu$ M siRNA with (25  $\mu$ l – " equivalent volume")  $\mu$ l OptiMEM I. The next step the transfection reagent (TR) was prepared by adding 0.25  $\mu$ l of TR into 24.75  $\mu$ l OptiMEM I. After mixing it gently, it is incubated for 5 min at room temperature. Don't incubate longer than 25 min. In the third step, the diluted siRNA is combined with the diluted TR and incubated for 20 min at room temperature. For each well, there is a 50  $\mu$ l mix consisting of 25  $\mu$ l diluted siRNA and 25  $\mu$ l diluted TR. While incubation the medium is changed to 50  $\mu$ l of 5% FBS NRCM medium without antibiotics (PenStrep) in each well. It is recommended to wash the well twice with this medium, to secure no antibiotic rests in the dish. After that, the 50  $\mu$ l siRNA-TR complex is added to each well. Gently rocking back and forth helps to distribute the solution properly. The NRCMs were incubated at 37°C and 1% CO<sup>2</sup> for 4-6 hours. After this incubation time, the medium is changed to 200  $\mu$ l 0.1% FBS NRCM medium with antibiotics, and the dish is put in the incubator (37°C and 1% CO<sup>2</sup>) for 48 hours. For the transfection in 48-, 24- and 12-well plates all the amounts used, are up-scaled by 2-fold, 3.5-fold and 10-fold in comparison to the provided procedure for 96 well plate dish.

### **5.3 SiGLO based transfection optimization**

The SiGLO Red transfection indicator was purchased from GE Healthcare Dharmacon Inc. It is a fluorescent oligonucleotide duplex that localizes to the nucleus of cells and thereby enabling a microscopic assessment of the optimal siRNA transfection conditions and monitoring the qualitative efficiency of delivering siRNA into cells. The SiGLO red transfection indicator (DY-547) is a Cy3 analog with an Absorbance/Emission Maximum of 557/570nm. In our microscope settings, we used a Cy3 filter. Further information can be found on the homepage of the company with supporting data.

Following microscope systems were used at the Institute of Pharmacology and Toxicology of the TU Munich for picture acquisition: 10x objective used: AxioObserver.Z1 (Zeiss, Jena, D), motorised Scan Table (130x85; Märzhäuser, Wetzlar, D), Lumen200 fluorescence illumination (Prior, Cambridge, UK) and Retiga-4000DC CCD-Kamera (QImaging, Surrey, Kanada). The picture acquisition and analysis is based on MetaMorph Basic imaging software packets (molecular devices, Downington, USA). The same microscope was used for the determination of the assessment of hypertrophic response after the siRNA transfection in the hypertrophy assay.

An electronic microscopy journal counted the siGLO red positive cells and the DAPI stained nuclei and calculated the number of the cells merging both signals. The data were exported as in an Excel sheet for further evaluating.

## **5.4 DNA Microarray**

MRNA expression analysis was carried out on RNA samples isolated from adult cardiomyocytes (500 ng input) by using the Affymetrix GeneChip® Mouse Expression Set 430.

## **5.5 Cell size determination by hypertrophy assay**

The hypertrophy assay was established and published by Claudia Jentzsch at the Institute of Pharmacology and Toxicology at the Technical University of Munich (Jentzsch et al., 2012).

### **5.5.1 Immunofluorescence Staining**

NRCMs were thawed in a 96 well dish, with 50000 cells each well to determine cell size microscopically. On day six of the experiment, the cells were fixed with 100 µl 4% paraformaldehyde (PFA) per well for 5 min at room temperature and then washed three times with 1x PBS. To permeabilize 100 µl of 0.2% Triton-x was added to each well and incubated for 5 min at room temperature followed by three times washing step with 1x PBS. Then the NRCMs were stained in a two-step incubation with a cardiomyocyte-specific anti- $\alpha$ -actinin antibody (Sigma 1:1000 in 1x PBS). Then washed three times with 1x PBS and in a second step incubated with a solution containing DAPI (20 mg/ml, 1:200 in 1x PBS) and the Alexa 488-conjugated anti-mouse IgG (Invitrogen, 1:200 in 1x PBS) with each 45 min incubation time at 37°C. 100 µl of 50% Glycerol was added to each well of the 96 well plate, and the dish was stored at 4°C until cell size determination at the microscope.

### **5.5.2 Automated cell size acquisition of cardiomyocytes**

The microscopical analysis of NRCM size was established by Claudia Jentzsch et al. as an entirely automated procedure to determine cell size and cell count in a 96well plate dish. The following microscope systems were used for picture acquisition: 10x objective used: AxioObserver.Z1 (Zeiss, Jena, D), motorized Scan Table (130x85; Märzhäuser, Wetzlar, D), Lumen200 fluorescence illumination (Prior, Cambridge, UK) and Retiga-4000DC CCD-Kamera (QImaging, Surrey, Kanada). The picture acquisition and analysis is based on MetaMorph Basic imaging software packets (molecular devices, Downington, USA). A major journal,

consisting of three minor journals were generated. The first sub-journal regulates the standardized moves of the 96 well plate dish, the focusing, and acquisition of four photos per well in two different fluorescence absorbances. The second sub-journal combines the 384 pictures taken per 96 well plate into a stack of images and combines the different fluorescence into one picture. The last journal determines the cell size and count, transforming the immunofluorescence pictures into image segmentations according to the MetaMorph plug-ins cell scoring, which is working on the previously generated stacks of pictures produced.

## 5.6 Isolation of RNA

First, the NRCMs were washed once with 1x PBS, and then 0.5 ml of TriFast was added to each well of the plate under a fume hood, and the cells were lysed by pipetting vigorously. The solution incubated for 5 min. 0.2 ml chloroform was added per ml TriFast and then continued with vortexing for 50 s. Incubate at room temperature for 10 min and centrifuge after that at 4°C for 5 min at 12000 x g. Carefully transfer the upper RNA-containing aqueous phase to a new tube without touching the interphase or the lower organic phase. By adding 0.5 ml isopropanol per 1ml TriFast, the RNA should precipitate. This solution is mixed and incubated at 4°C for 10 min and then centrifuged at 4°C for 10 min at 12000 x g. The supernatant is discarded without disturbing the pellet. Then wash the pellet with 1 ml of 75% Ethanol. Vortex and centrifuge at 4°C for 10 min at 12000 x g. The pellet is dried at room temperature by keeping the tube inverted on a tissue. After that, the pellet is suspended in 20 µl of RNase-free water, and the concentration is measured at the Nanodrop. The RNA can be stored at -80°C.

## 5.7 Reverse Transcription of mRNA into cDNA

The mRNA of a cell consists of a sequence of oligonucleotides with a cap structure at the 5' end and a poly-A tail at the 3' end. After binding of an Oligo (dT) primer (MWG Biotech, Ebersberg, Germany) to the tail of the mRNA, the reverse transcriptase can synthesize the complementary cDNA of each mRNA gained from the RNA isolation. The cDNA is then used in a quantitative real-time polymerase chain reaction (qRT-PCR) to determine the level of mRNA in the lysed cells after for example the treatment of knocking down mRNA by siRNA transfection.

Components for each tube:

substance	mass/volume
-----------	-------------

RNA	Up to 750 µg
Oligo (dT) Primer (10mM)	1 µl
dNTPs (10mM)	1 µl
RNAse free water	Up to 12 µl of total volume
Incubation for 5 min at 65°C and then 2 min at 4°C	
5x Buffer	4 µl
DTT	2 µl
RNAse inhibitor	1 µl
Protoscript enzyme	1 µl

This reaction mix is incubated for 1 hour at 42°C for reverse transcription and then heat-inactivated for 5 min at 80°C. The tubes containing cDNA can be stored at -20°C.

## 5.8 Quantitative real-time PCR

The qRT-PCR is based on a common polymerase chain reaction with the special ability to quantify its amplification by detecting the fluorescence signal produced, which are proportional to the amount of PCR product. Made possible by the intercalation of the SYBR Green fluorophore into the double-stranded DNA. With each PCR cycle, the signal intensity rises in contrast to the reference fluorophore. The cycle, first emerging to be significant to the reference signal is called cycle-threshold (Ct) – value. According to this value, it is possible to quantify through a mathematical intervention of the  $\Delta\Delta Ct$ - method ( $=2^{-(\Delta Ct(\text{group X})-\Delta Ct(\text{control group}))}$ ).

Components for one reaction in a well:

substance	volume
SYBR Green Master Mix	6.25 µl
Primer fwd (1:50, 20 pmol/µl)	0.25 µl
Primer rev (1:50, 20 pmol/µl)	0.25 µl
ddH2O	3.75 µl
cDNA (11 ng/µl)	2 µl

Cycle program (StepOne Plus, Applied Biosystems New Jersey, USA):

	Step	Temperature	Time	Cycles
Step 1	Pre-denaturing	95 °C	600 s	1x
Step 2	Denaturation	95°C	15 s	40x
Step 3	Hybridisation/Elongation	60°C	60 s	

## 5.9 Nuclei count

The analysis for the nuclei count was performed simultaneously in the electronic journal of the hypertrophy assay. After the cells had been stained with  $\alpha$ -actinin and DAPI, the neonatal cardiomyocytes were counted in the course of the hypertrophy assay journal and the data were exported into an Excel Sheet. Please look in the methodic explanation of the hypertrophy for further information of microscopic settings.

## 5.10 $^3\text{H}$ -Isoleucine incorporation

NRCMs were thawed into 48 well plates with 100000 cells in each well and incubated overnight in the incubator (37°C and 1% CO<sup>2</sup>). The next day the NRCMs were transfected with scramble siRNA control and target-siRNA as described above. After the transfection, the NRCMs were incubated in 0.1% FBS NRCM medium at 37°C and 1% CO<sup>2</sup> for 48 hours. After these two days, the medium was changed to 0.1% FBS NRCM medium containing  $^3\text{H}$ -isoleucine (1  $\mu\text{Ci}$  per 1 ml medium) and put back in the incubator for another 48 hours. In the last step the NRCMs were washed twice with 1x PBS, and then 400  $\mu\text{l}$  of ice-cold 5% TCA was added to each well, and the plate was incubated for 1 hour at 4°C. After that, the plate was washed with 400 ml ice-cold ddH<sub>2</sub>O. Then 250  $\mu\text{l}$  of 0.2 M NaOH was added, and the plate was incubated for 30 min at 37°C by shaking one or two times the dish in the incubator. As the last step, the 200  $\mu\text{l}$  of each lysate was transferred into a scintillation tube, filled with 4 ml scintillation fluid, which was measured automatically to determine the incorporation of isotope-labeled isoleucine into the NRCMs.

## 5.11 MTT assay

NRCMs were thawed into a 24 well plate, 200000 cells each well and incubated overnight at 37°C and 1% CO<sup>2</sup> in the incubator. The next day the cells were transfected as described above. 48h after transfection the medium was renewed by new 0.1% FBS NRCM medium. Again 48 hours later 8 mg MTT was weighed and resuspended in 500 µl of 1x PBS. 400 µl from the dissolved MTT was added into 12 ml of 0% FBS NRCM medium, mixed and prewarmed in the water bath at 37°C. The medium of the 24 well plate containing the NRCMs was removed, and 400 µl of the 0% FBS NRCM medium with MTT was added and incubated in the incubator (37°C and 1% CO<sup>2</sup>) for 1 hour. After the hour the medium was removed, and the NRCMs were washed once with 1xPBS. Then 200 µl of acidified isopropanol (10 ml isopropanol with 90 µl concentrated HCL) was added to each well. The solution gets purple and is pipetted up and down several times to lyse all NRCMs. The content of each well is transferred into a transparent 96well plate, and the absorbance is measured in a plate reader at 570 nm minus the background absorbance at 650 nm.

## 5.12 Statistical evaluation of data

The mean values were illustrated as Mean +/- standard error mean (SEM). The statistical analysis was done in Prism Software Packet (Graphpad, San Diego, USA). Statistical significance was evaluated by ANOVA testing followed by Bonferroni Test or Student's T-test, if \*\*\* P < 0,001, \*\* P < 0,01 und \* P < 0,05 the data were considered statistically significant.

## 6 Results

### 6.1 SiRNA transfection optimization of NRCM using siGLO method

A step crucial in this screening for hypertrophy-modulating CRLs was working with a system that allows high efficacy in transfection of siRNA and concomitant avoidance of toxic effects on the treated neonatal rat cardiomyocytes.

We thereby transfected siGLO red transfection indicator and compared different transfection reagents, such as Lipofectamine 2000, Dharmafect 1 and Dharmafect 3, each in different concentrations. The DAPI stained NRCMs were counted per picture to ensure equal numbers of cells and thereby eliminating possible toxic effects of the transfection reagent itself. In a second step, an automated cell count program registered the siGLO fluorescent oligonucleotide duplex that localizes to the nucleus, thus permitting the visual assessment of uptake in the NRCMs.

Neither a statistically significant difference in the nuclei count analyses (control vs. Lipofectamin 2000: 1way ANOVA with Bonferroni Mean Difference 68.28 and  $t=0.6916$ ,  $p>0.05$ , mean  $769.1 \pm 43.93$  SEM), nor a significant difference in the transfection efficiency (Lipofectamine 2000 mean  $80.86 \pm 3.303$  SEM,  $p>0.05$  vs. Dharmafect 1 mean  $79.05 \pm 1.458$  SEM in 1way ANOVA with Bonferroni Mean Difference 1.814 with  $t=0.4940$ ,  $p>0.05$ ) could be measured.

**(Fig.4 A and B)**

Whereas the percentage of siGLO positive cell transfected with Dharmafect 3 transfection reagent was reduced (mean  $60.93 \pm 1.796$  SEM with Mean Difference 19.94 with  $t=5.431$ ,  $p<0.0001$  between Lipofectamine 2000 vs. Dharmafect 3). Using half the amount of Dharmafect resulted in a lower efficiency (mean  $37.09 \pm 10.66$  SEM in 1way ANOVA with Bonferroni Mean Difference 43.78 with  $t=11.66$  and  $p<0.0001$ ).

According to these preliminary experiments resulting in efficient transfection of the siGLO oligonucleotides, we decided to work with Dharmafect 1 reagent as transfection reagent for the screening.

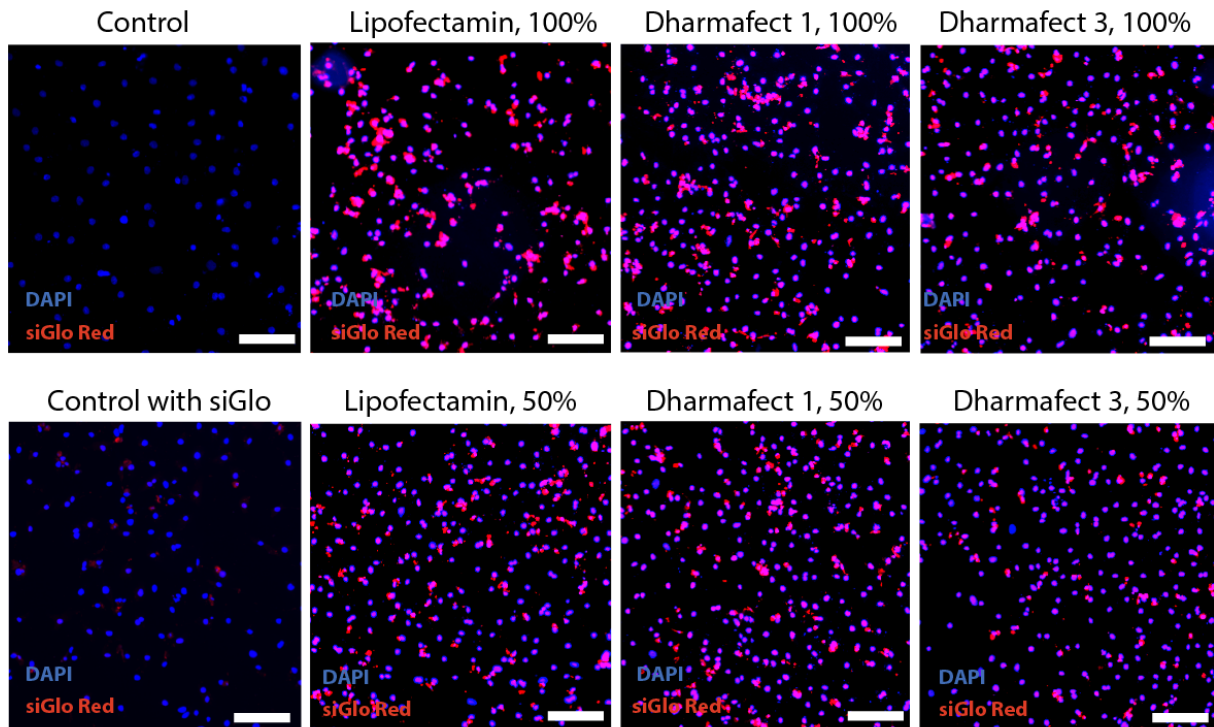
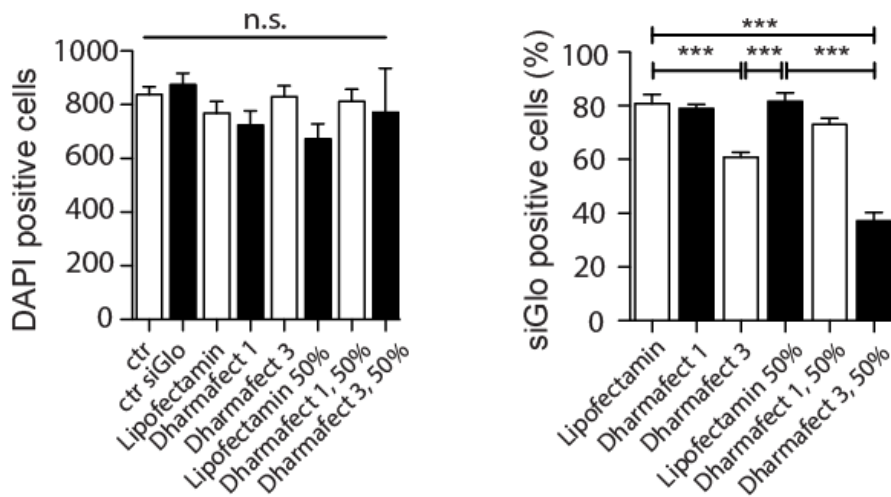
**A****B**

Figure 4: SiGlo Red transfection of NRCMs under different conditions

Representative immunofluorescent stainings of NRCM cultures after transfection (A). Nuclei stained with DAPI in blue and siGlo in red. Scale bars represent 100  $\mu$ m. DAPI stained cells and siGlo Red cells were counted and compared using different products and amounts of transfection reagents to determine cell count and efficiency of transfection procedure (B). N=3, 1way ANOVA, Bonferroni \*\*\* P < 0.001.

## 6.2 DNA microarray for expression levels of Cullin and F-box proteins

The aim of the DNA microarray was to determine the expression level of the members of the Cullin and F-box family in the heart for preselection of targets, which should be analyzed in a hypertrophy assay after siRNA-mediated knockdown of mRNA in neonatal rat cardiomyocytes (NRCMs).

The acquisition of the samples was performed before the start of work for the MD thesis and performed mainly by Simon Leierseder, who did the mouse work and Antonio Sarikas, who evaluated the results and consequently picked the targets for the siRNA-mediated hypertrophy screening.

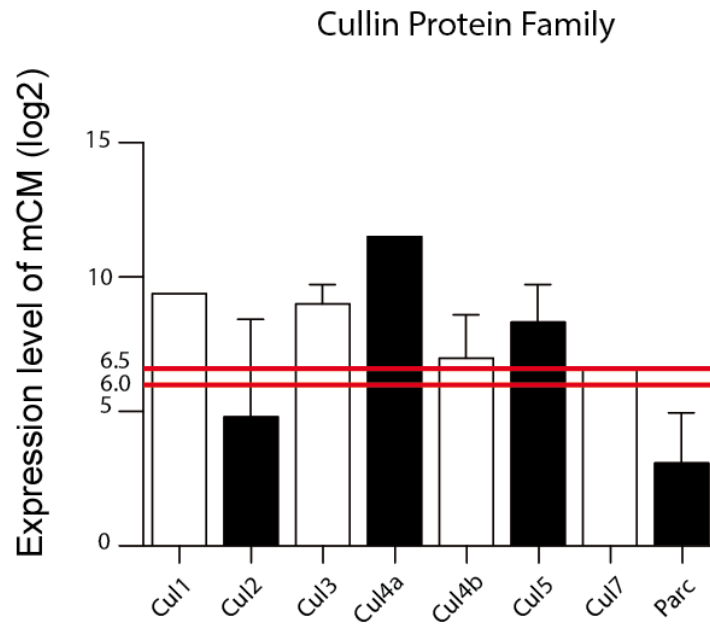
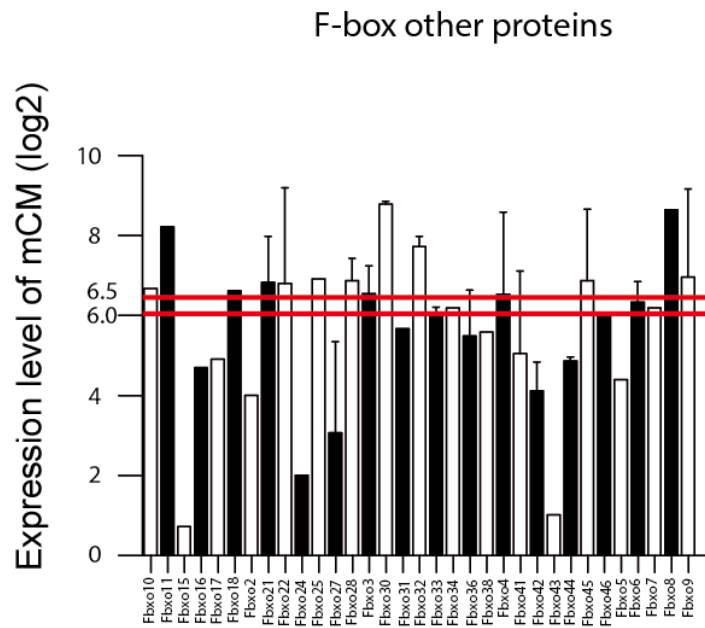
Six months old wild type (WT) and  $\beta$ 1-transgenic mice were sacrificed for RNA isolation of cardiomyocytes (CM) and cardiofibroblasts (CF). Criteria for the selection of targets were expression higher than 6.5 on a  $\log_2$  scale provided by Netaffx and a higher expression in CM than CF to work with mainly heart-specific targets in the following experiments. According to Netaffx, this threshold secures a translation of the mRNA into proteins and thereby the expression of targets in the heart.

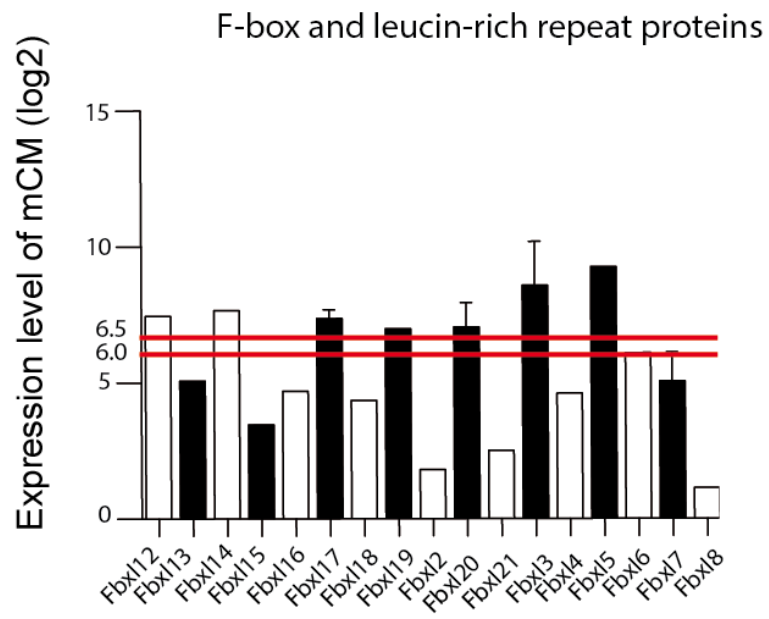
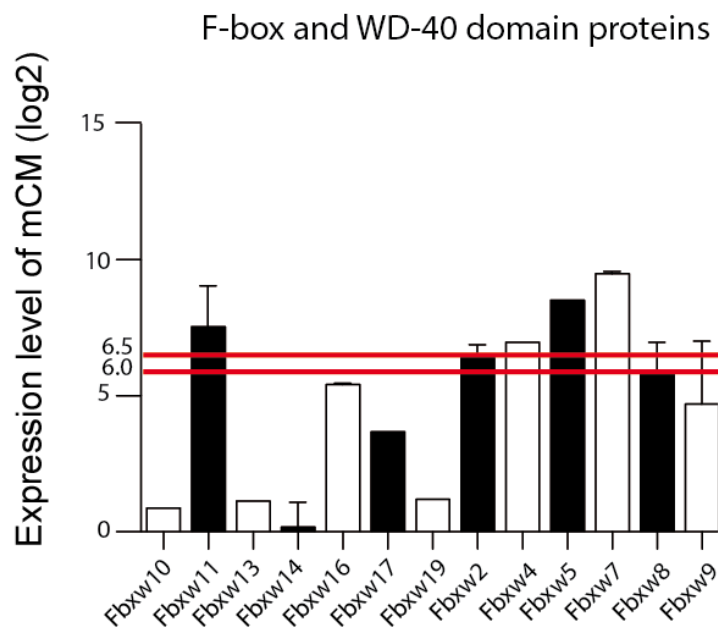
**Fig. 5 A to D** show the microarray data for the cullin protein family and the three F-box protein families. They are separated through protein specific domains such as WD-40 repeats (Fbxw) or leucine-rich repeats (Fbxl), while the third group the F-box other protein family contains the rest of F-box proteins which can't be added to the other two families with their specific domains.

Analysis of the provided Netaffx data resulted thereby in three groups of targets according to their expression level, which is illustrated in **Fig. 5 E**. Group 1 included the highest expressed targets with a value greater than 6.5 in multiple measurements and mean values, which should result in a secured expression of the translated protein. The second group with values in multiple measurements and mean values between 6 – 6.49 in  $\log_2$  scale.

Moreover, the third group includes special targets such as components of the Cullin-RING E3 ligases (e.g. backbone proteins and adaptors) for control reactions by knocking down essential subunits of the multisubunit Cullin-RING E3 ligase complex.

Using the microarray for the subunits of the CRLs in cardiomyocytes, enhanced the specificity of the search for new hypertrophy-modulating E3-ligases by eliminating only weakly expressed members of the screening.

**A****B**

**C****D**

# E

Group 1 (multiple measurements > 6.5 in CM)	Group 2 (multiple measurements 6.0-6.49 in CM)	Group 3
Cullin 3	Cullin 1	Rbx1 (Roc1)
Cullin 4b	Cullin 4a	Rnf7 (Roc2)
Cullin 5	Cullin 7	Skp2
Fbxl3	Fbxl5	DDB1
Fbxl17	Fbxl12	Tceb2 (Elongin B)
Fbxl20	Fbxl14	Tceb1 (Elongin C)
Fbxo3	Fbxl19	BTRC (Fbxw1)
Fbxo4	Fbxo6	Cul9 (PARC)
Fbxo9	Fbxo8	
Fbxo21	Fbxo10	
Fbxo22	Fbxo11	
Fbxo28	Fbxo18	
Fbxo30	Fbxo25	
Fbxo32	Fbxo33	
Fbxo45	Fbxw2	
Fbxw7	Fbxw4	
Fbxw11	Fbxw5	
	Fbxw8	

Figure 5: DNA microarray

DNA microarray for determination of the expression level in a  $\log_2$  scale of the members of the Cullin and F-box family in cardiomyocytes. Redline at 6.0 and 6.5 marks according to Netaffx the level for secure protein expression. (A) Members of the Cullin Protein Family. (B) Members of the F-box other protein family. (C) F-box and leucine-rich repeats proteins family. (D) Members of F-box and WD-40 domain proteins family. (E) shows the three targets groups sorted by their expression level in cardiomyocytes.

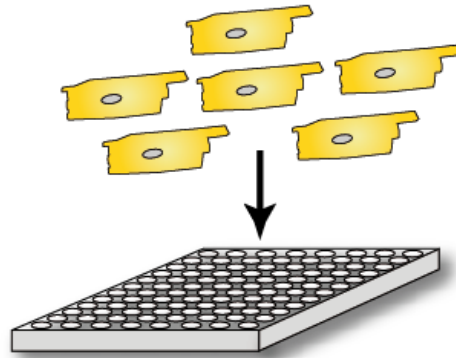
### 6.3 Screening for hypertrophy-modulating Cullin-RING E3 ligases

To screen for hypertrophy after the siRNA-mediated knockdown in NRCMs, we used a system established by Jentzsch et al. at the Institut of Pharmacology and Toxicology (IPT) at the Technical University of Munich. In this procedure, neonatal rat cardiomyocytes were isolated from 2-3 days old pups and plated the cells into 96-well plates for the hypertrophy assay. The procedure and timeline of this assay are shown in **Fig 6 A**. Two conditions were used in this screening for exploring the effects of basal treatment and stimulation of NRCMs with Phenylephrine (PE), which is a potent inducer of hypertrophy by activating the  $\alpha$ 1-adrenergic receptor in cardiomyocytes. The treatment with PE (concentration 50  $\mu$ M, 1:1000) results in a cardiomyocytes cell size change of 2-fold increase in contrast to the basal condition without PE (Students paired t-test mean 2.02 +/- 0.062 SEM,  $p < 0.001$ ). We could also show that this effect is dose-dependent (**Fig. 6 D**). We continued to work with the maximal induction of hypertrophy for the screening.

# A

Day 1

**Isolation and plating of NRCMs  
onto 96-well plate**



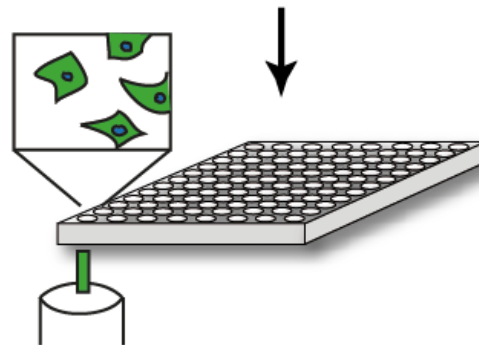
Day 2

**Transfection with siRNA  
Starvation at 0.1% FBS for 48 h**



Day 4

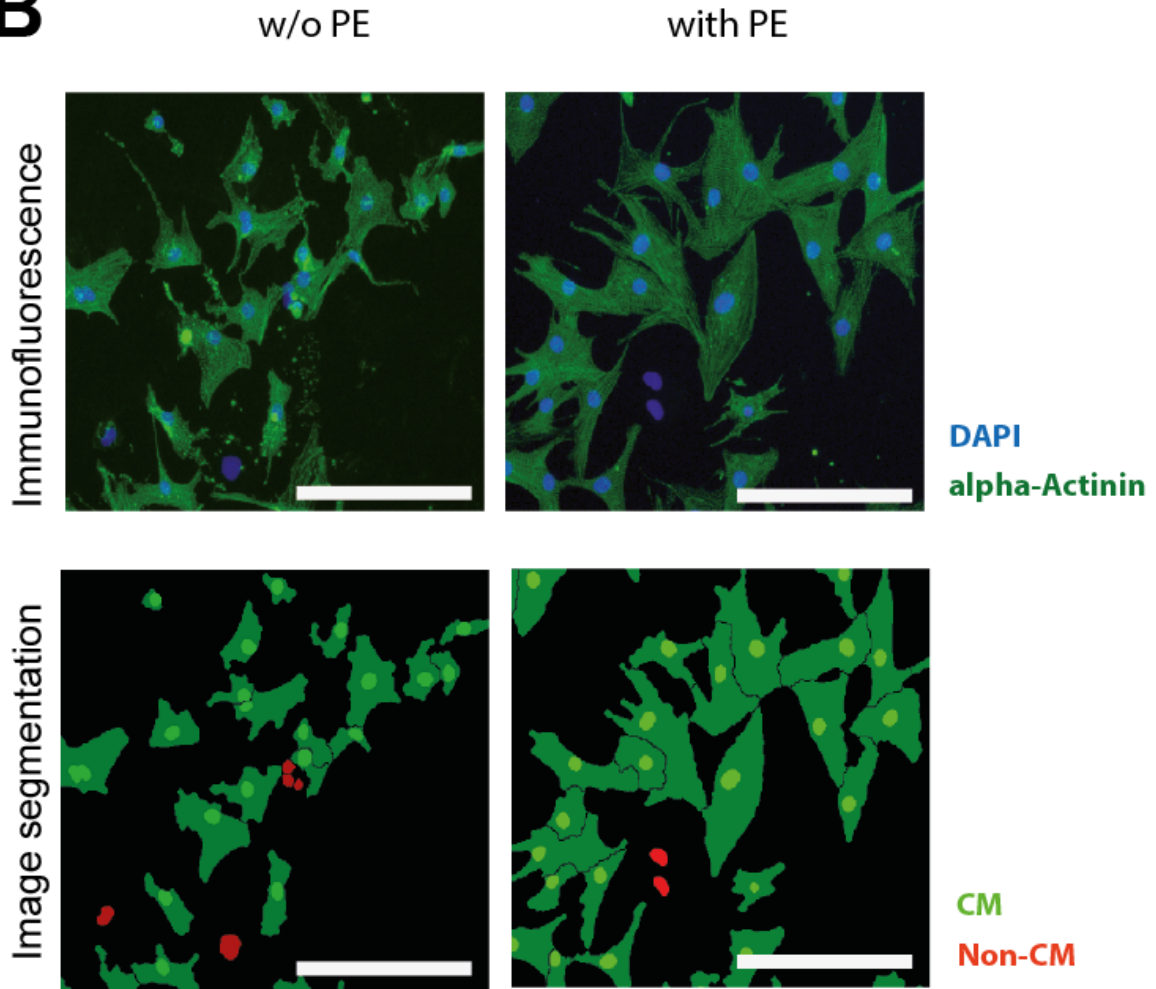
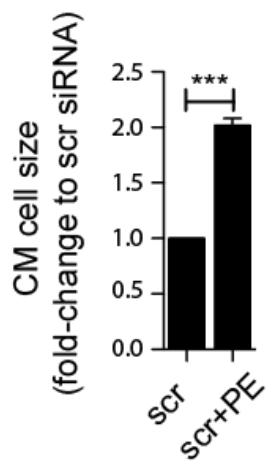
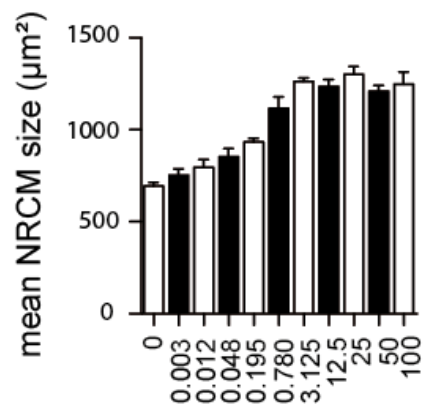
**Stimulation of NRCM culture  
under basal and 50  $\mu$ M PE  
condition for 48 h**



Day 6

**Fixation and Staining**

**Segmentation Analysis of cell size**

**B****C****D**

## Figure 6: Hypertrophy Assay

An assay to determine cardiomyocyte cell size by automated microscopy and image segmentation.

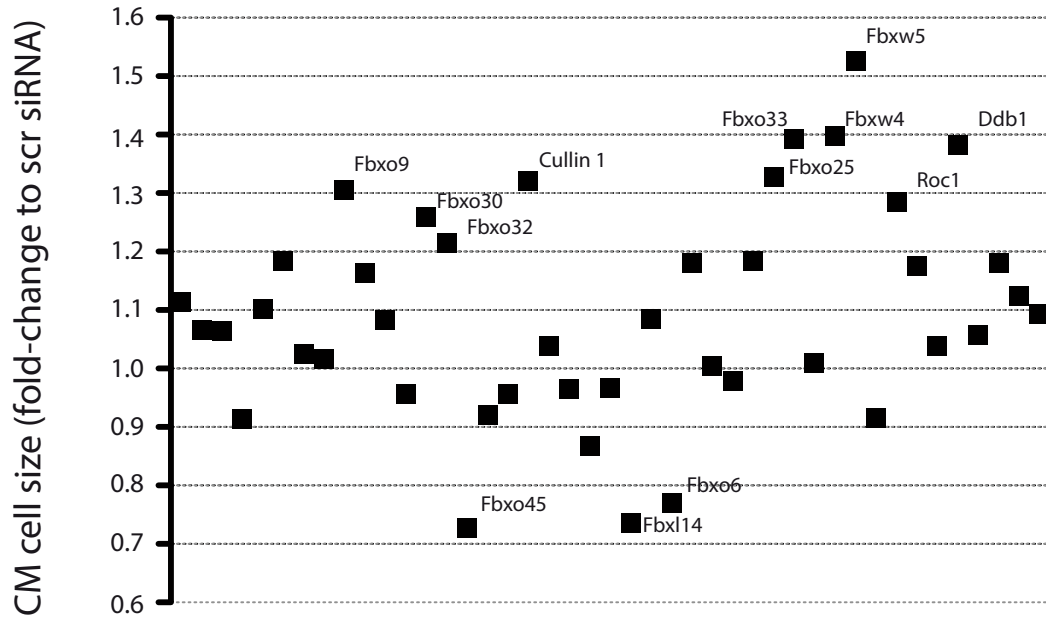
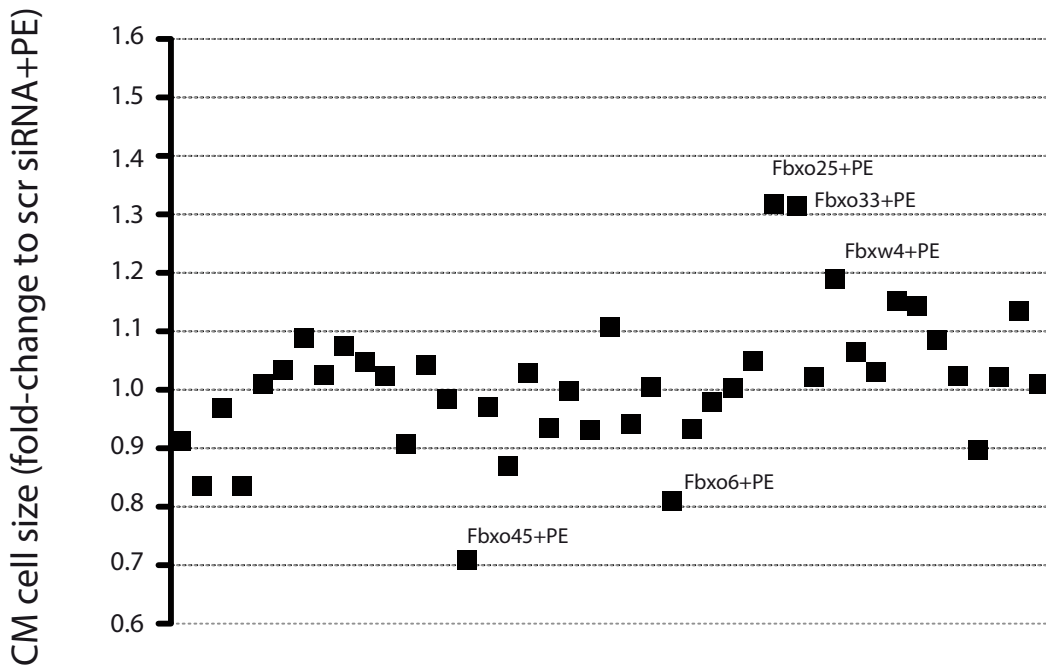
(A) Schematic workflow: Cells were isolated from neonatal rat hearts, pre-plated to enrich for cardiomyocytes, and seeded onto 96 well plates. After transfection with siRNA against the most highly expressed targets of the UPS in the heart, cell size, and cell identity were determined by immunostaining and image segmentation.

(B) Representative immunostaining and image segmentation of NRCMs in culture; cardiomyocytes ( $\alpha$ -actinin) were stained for the marker protein. Nuclei stained with DAPI in blue. Scale bar represents 250  $\mu$ m. CM=cardiomyocyte, Non-CM=Non-cardiomyocyte.

(C) Effect of transfected siRNA scramble control on cardiomyocyte size under basal conditions or stimulation with phenylephrine (PE) 50 $\mu$ M. Fold change of NRCMs size after transfection with siRNAs. Data are normalized to scrambled siRNA control. N=3, Students paired t-test, \*\*\*P < 0.001.

(D) Dose-dependent effect of the pro-hypertrophic stimuli PE (in  $\mu$ M) added to the medium to induce hypertrophy in NRCMs. The effect was measured by cell size change in the established system. N=3, 1way ANOVA, Bonferroni, \*\*\* P < 0.001.

We thereby identified 13 CRL components (seven Fbxo-, two Fbxw-, one Fbxl- family members and several CRL subunits) that significantly affected NRCM cell size under basal condition (**Fig 7**). Seven out of them (e.g.: Fbxo9 (mean 1.305 +/- 0.049 SEM, p<0.001), Cullin1 (mean 1.321 +/- 0.047 SEM, p<0.001), Fbxo25 (mean 1.327 +/- 0.033 SEM, p<0.001), Fbxo33 (mean 1.391 +/- 0.064 SEM, p<0.001), Fbxw4 (mean 1.398 +/- 0.017 SEM, p<0.001), Fbxw5 mean (1.526 +/- 0.049 SEM, p<0.001) and Ddb1 (mean 1.382 +/- 0.049 SEM, p<0.001) showed after the siRNA transfection an increased cell size by more than 30%. We could also detect targets that showed a significant decrease in cell size such as Fbxo45 (mean 0.727 +/- 0.034 SEM, p<0.01), Fbxl14 (mean 0.735 +/- 0.021 SEM, p<0.01), Fbxo6 mean (0.769 +/- 0.028 SEM, p<0.05) over 20% compared to the scramble control siRNA. Furthermore, five out of these still showed this effect under stimulated conditions with phenylephrin (PE). The strongest effect could be shown for the F-box proteins: Fbxo33 (mean 1.315 +/- 0.026 SEM, p<0.001) and Fbxo25 (mean 1.317 +/- 0.035 SEM, p<0.001) with more than 30% increase in cell size compared with the scramble siRNA control stimulated with PE. Also Fbxw4 (mean 1.190 +/- 0.026 SEM, p<0.001) showed an increase in cell size change by appr. 20%. The knockdown of Fbxo45 (mean 0.708 +/- 0.0235 SEM, p<0.001) and Fbxo6 (mean 0.809 +/- 0.0145 SEM, p<0.001) resulted in a decrease in cell size after PE stimulation of 20-30%.

**A****B**

C

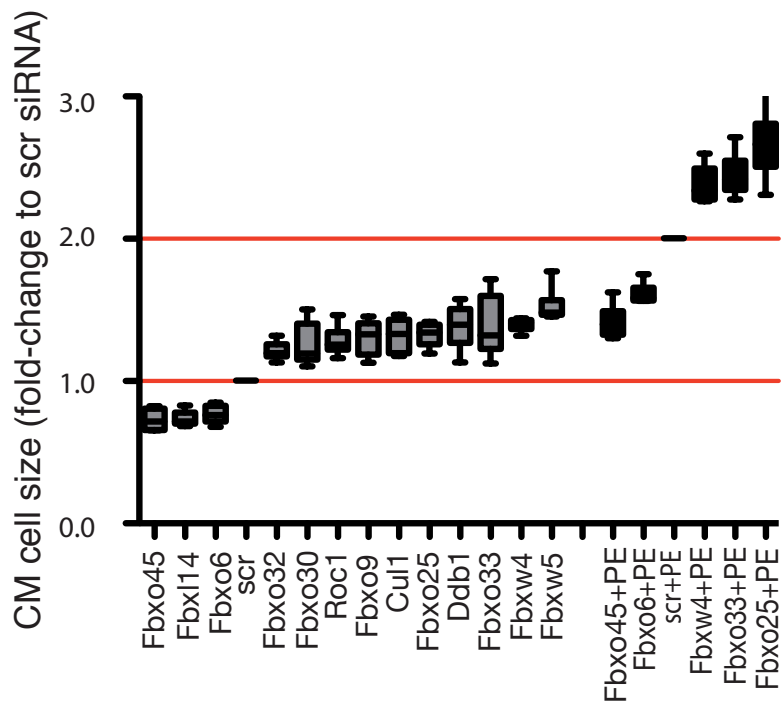


Figure 7: Effect of target siRNA Transfection

Effect of siRNA transfection on cardiomyocyte size. Fold change of cell size after transfection of siRNA. Data are normalized to scramble siRNA control. Relative change of cardiomyocyte size plotted against annotated target name. All annotated target are highly significant in N=3 independent experiments in 1way ANOVA Bonferroni, \*\*\* P <0.001. Mean value is shown. Cardiomyocyte size change under basal (A) and PE stimulated conditions (B). (C) Overview of the statistically significant targets revealed in the hypertrophy assay in cell size fold-change to scramble control under basal and PE stimulated conditions.

## 6.4 Validation of candidate CRLs in NRCMs

### 6.4.1 Quantification of siRNA-mediated knockdown by qPCR

A step pivotal to validate the findings was to assess the efficiency of the siRNA-mediated knockdown of the targeted mRNA. After the transfection of the neonatal rat cardiomyocytes in a dish as performed for the hypertrophy assay, we collected the mRNA according to the Peggold Protocol in the time frame of 36-48 hours after transfection. We measured the levels of each siRNA target in a quantitative real-time polymerase chain reaction (qRT-PCR) compared with the scramble siRNA control for the evaluation of the knockdown. We achieved for each of our F-box proteins and the essential subunits of the CRLs a significant knockdown of 80 to 90% on mRNA level as seen in **Fig. 8**. For example the knockdown of Cul1 mRNA resulted in normalized mean value of 0.102 +/- 0.035 SEM,  $p=0.0084$  and Fbxo33 mRNA led to a normalized mean value of 0.168 +/- 0.049 SEM,  $p=0.0002$ .

As a result, we concluded that the methodical knockdown approach was working and the target mRNA was drastically reduced in the neonatal rat cardiomyocytes.

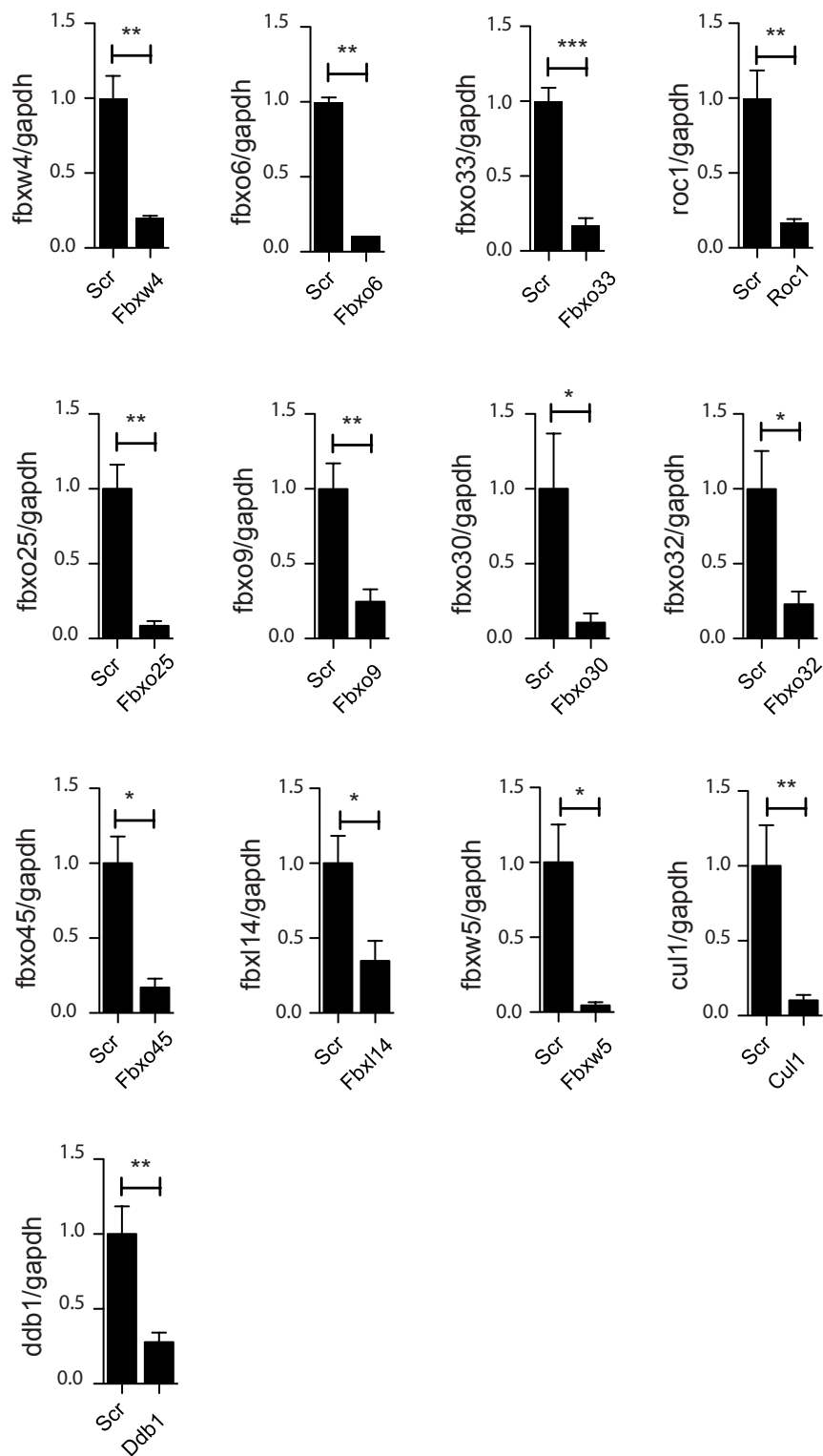


Figure 8: qPCR validation of target mRNA knockdown

Validation of each siRNA-mediated knockdown of mRNA by qPCR in NRCMs after transfection. Scramble siRNA served as control. Data was normalized to gapdh as housekeeping mRNA. N=3 independent experiments. Data are mean +/- SEM. Student's T-test. \* P< 0.05, \*\* P< 0.01, \*\*\* P<0.001.

#### 6.4.2 Viability test in MTT assay

To test the viability and evaluation of possible toxic effect in the neonatal rat cardiomyocytes after siRNA transfection, we used the MTT assay to assess toxic or beneficial effects on the NRCMs. In this NAD(P)H-dependent cellular oxidoreduction, the MTT dye reflects viable cells and is thereby a tool to evaluate cells after a treatment such as toxic reagent or growth inducing stimuli such as IGF-1 or PE. In our assays, we used the same timeline for thawing, transfection, and change of medium in the dishes as in the hypertrophy assay. Just the endpoint of the experiment has been modified from microscopic analysis after staining to the addition of MTT into the dish. Thus at day 6 of the experiment, we added the MTT dye to the medium, and after an incubation time, the NRCMs were lysed, and the turnover of the dye performed by the cells was evaluated by photometric analysis. Here we could detect a significant increase in the turnover of the tetrazolium dye MTT for Fbxo25 (mean 1.623 +/- 0.038 SEM,  $p < 0.01$ ), Fbxw4 (mean 1.801 +/- 0.147 SEM,  $p < 0.001$ ), Fxl14 (mean 1.812 +/- 0.159 SEM,  $p < 0.001$ ) and Fbxw5 (mean 2.105 +/- 0.212 SEM,  $p < 0.001$ ) (**Fig. 9**). The other targets of our screen did not show a statistically significant change in comparison to the scramble siRNA control.

To summarize, these results show that the experiments using siRNA is not affecting the cell viability or causes an induction of cell death.

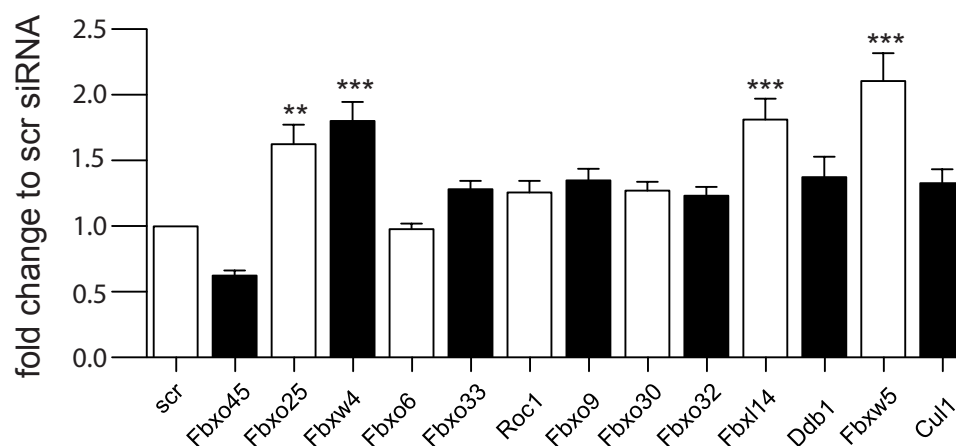


### Figure 9: MTT assay

Cell viability after siRNA transfection was evaluated in an MTT assay. Uptake and metabolism of MTT reaction was assessed to determine a toxic or beneficial effect on NRCMs. Data was normalized to scramble siRNA control. N=3 independent experiments Data are mean +/- SEM and statistically analysed by 1way ANOVA Bonferroni \* P< 0.05, \*\* P< 0.01, \*\*\* P< 0.001.

### 6.4.3 Analysis of nuclei count

Another way to determine toxic effects after treatment is counting of cardiomyocytes that are identified by DAPI and  $\alpha$ -actinin stainings. These data were simultaneously gathered in the hypertrophy assay. The mean cardiomyocyte count was by approximately 400 cells, while each point represents the cell count of a picture taken by electronic microscopy after thawing 50.000 NRCMs in each well of the 96 well plate at the beginning of the procedure for the hypertrophy assay. Only for the F-box proteins Fbxo45 (mean 164.1 +/- 18.21 SEM,  $p < 0.0001$ ) and Fbxw5 (mean 297.5 +/- 20.54 SEM,  $p = 0.0003$ ) and the CRLs multisubunit components Roc1 (mean 446.7 +/- 20.11 SEM,  $p = 0.0064$ ) and Ddb1 (mean 227.9 +/- 21.03 SEM,  $p < 0.0001$ ) there were changes in the cardiomyocyte count after siRNA-mediated knockdown of the target mRNA (**Fig. 10**). To sum up, we could detect no significant statistical change in cardiomyocyte count for most of our targets.

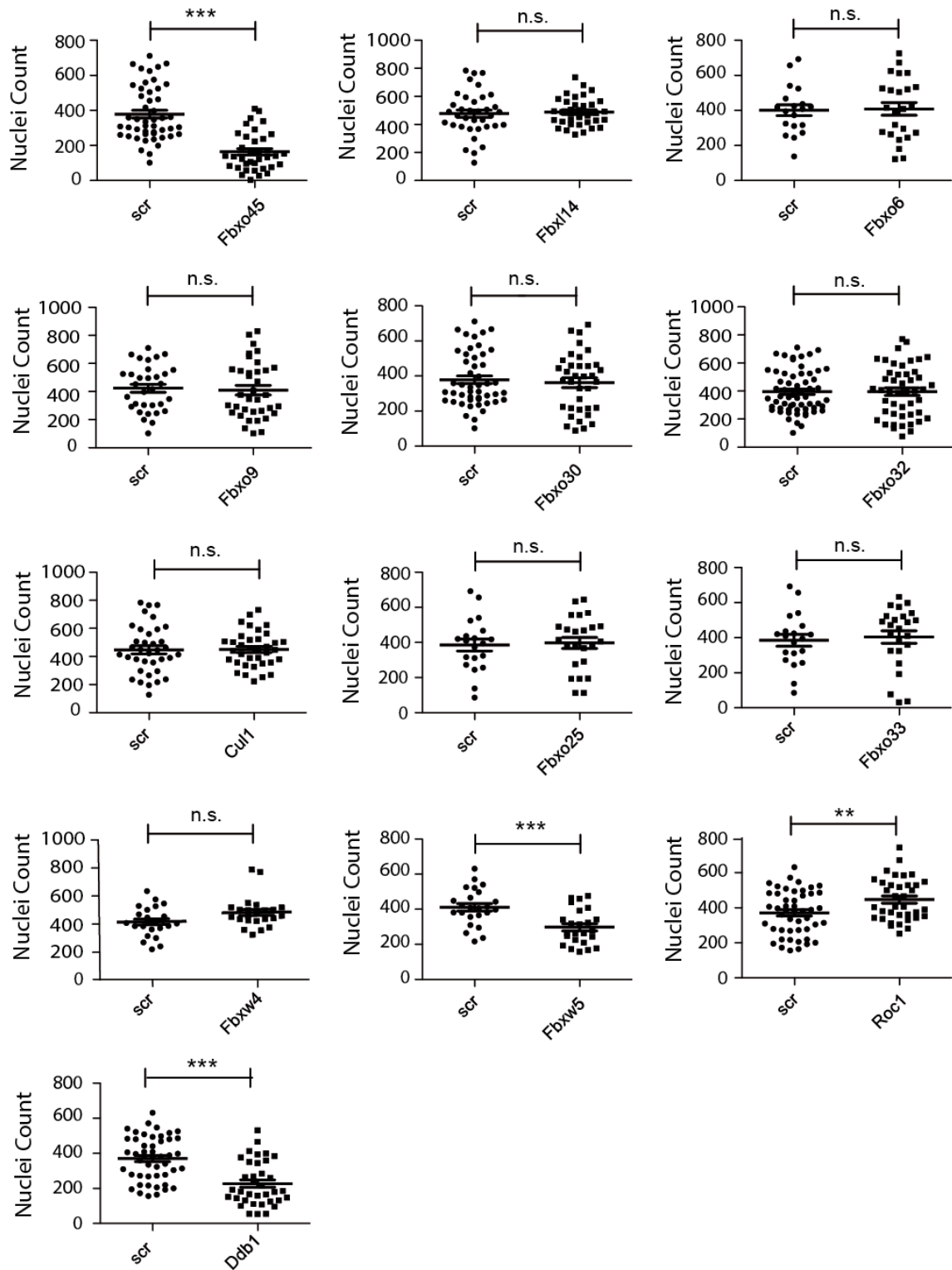


Figure 10: Nuclei Count Analysis

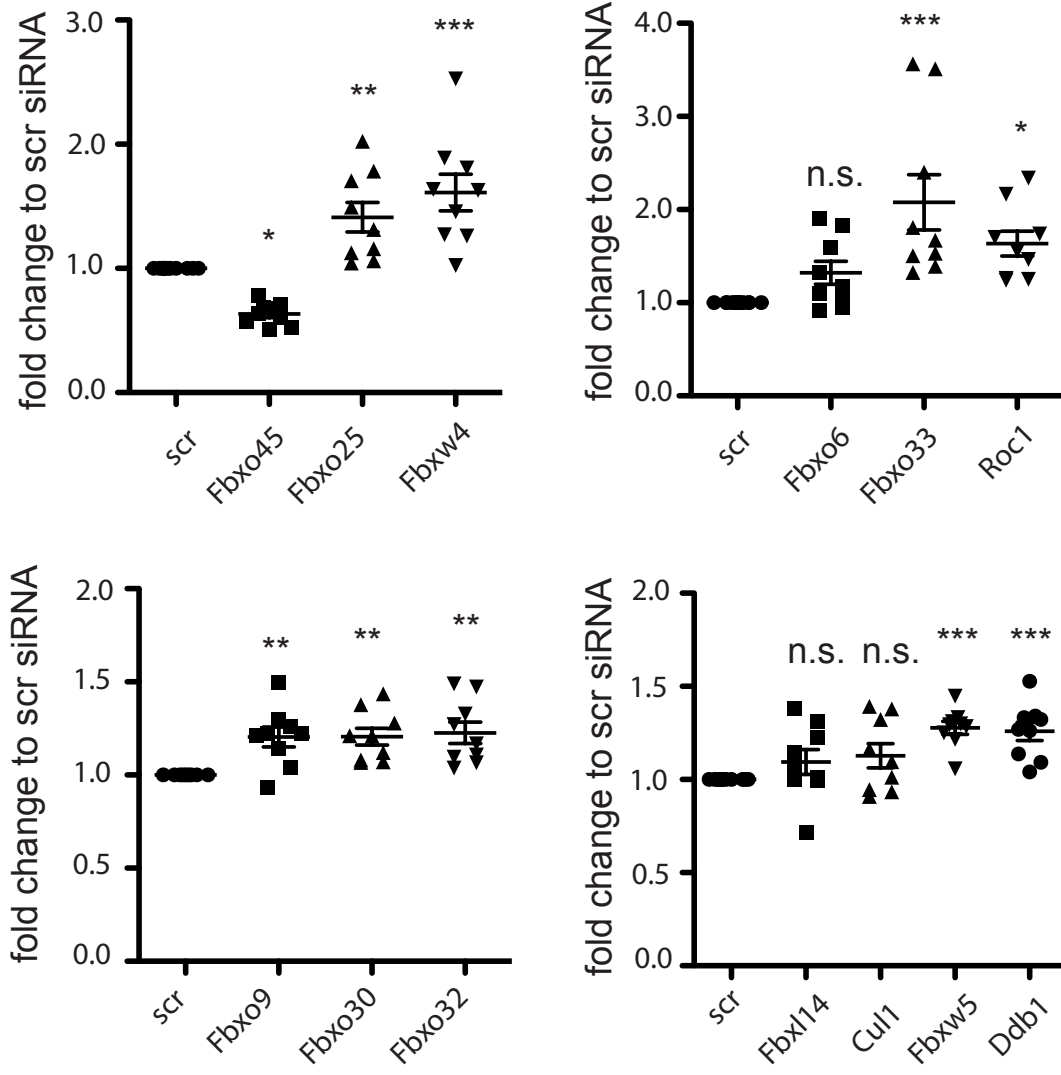
DAPI and  $\alpha$ -actinin positive cells of the hypertrophy screening data were counted and compared to scramble siRNA transfected cells. Each point represents the count of NRCMs in one picture taken by electronic microscopy during the hypertrophy assay. N=3. Data are mean  $\pm$  SEM and Student's T-test. \*  $P < 0.05$ , \*\*  $P < 0.01$ , \*\*\*  $P < 0.001$ .

#### 6.4.4 <sup>3</sup>H-Isoleucine incorporation

To validate the hypertrophy and atrophy induced by knockdown of the target mRNA, we used a functional assay to measure cell growth or proliferation by a radioactive readout of proteins translated with isotope labeled amino acid added to the standard cell culture medium after siRNA transfection. We investigated both conditions, the basal without phenylephrine stimulation and the hypertrophy induction due to PE treatment of the cardiomyocytes for the exact experiment procedure as used in the hypertrophy assay and in the MTT assay to have the same schedule. Scramble siRNA served as control. In this test, we could repeat the method published by Jentzsch et al., which show a strong correlation between cardiomyocyte cell size and uptake of isotope labeled <sup>3</sup>H-isoleucine incorporation into the proteins of the cell. Fbxo32 (Atrogin-1) for example showed 1.22 fold-increase in <sup>3</sup>H-isoleucine incorporation and 1.21 fold-increase of cell size in the hypertrophy assay under basal conditions without the stimulation with PE. The most potent F-box proteins under basal conditions are Fbxo45 (mean 0.6339 +/- 0.030 SEM, p<0.05), Fbxo33 (mean 2.079 +/- 0.295 SEM, p<0.001), Fbxw4 (mean 1.611 +/- 0.147 SEM, p<0.001) and Fbxo25 (mean 1.412 +/- 0.119 SEM, p<0.01). After the hypertrophy stimulation with PE, Fbxo45 (mean 0,741 +/- 0.066 SEM, p<0.01) shows a decrease in the uptake of <sup>3</sup>H-isoleucine. Whereas Fbxw4 (mean 1.271 +/- 0.082 SEM, p<0.01), Fbxo33 (mean 1.582 +/- 0.058 SEM, p<0.001) and Fbxo25 (mean 1.398 +/- 0.053 SEM, p<0.001) show an increased uptake after PE Stimulation in comparison to the PE stimulated scramble control (**Fig 11**).

Concluding that Fbxo45, Fbw4, Fbxo33, and Fbxo25 are the most potent F-box proteins that can change the <sup>3</sup>H-isoleucine uptake after siRNA transfection.

**A**



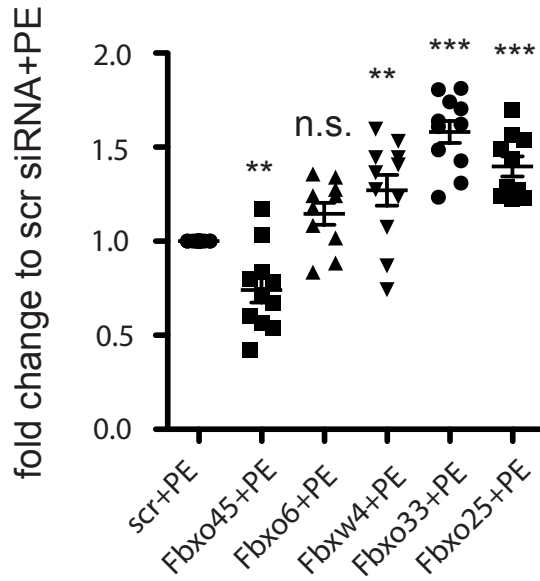
**B**

Figure 11: <sup>3</sup>H-isoleucine incorporation

Validation of the effect of cell size changing siRNA-mediated knockdown on NRCMs by <sup>3</sup>H-isoleucine incorporation. Data was normalized to scramble siRNA control. N=3-4 independent experiments. (A) shows data under basal conditions and (B) with stimulation with Phenylephrine (PE) 50  $\mu$ M. Data are mean +/- SEM. 1way ANOVA Bonferroni \* P< 0.05, \*\* P< 0.01, \*\*\* P<0.001.

## 7 Discussion

In the last decade, there is growing evidence on the UPS in the context of cardiac diseases. Proteasomal dysfunction seems to be linked to ischemia, reperfusion, hypertrophy, atherosclerosis, heart failure, hypertrophic and dilated cardiomyopathies (Day, 2013).

Several studies investigated the role of the UPS in human cardiomyopathies and heart failure. Tissue samples were mainly acquired from dilated cardiomyopathies (DCM), valvular heart diseases such as aortic stenosis, left ventricular assistant devices (LVAD), coronary artery diseases and hypertrophic cardiomyopathies (Birks et al., 2008; Predmore et al., 2010; Tsukamoto et al., 2006; Wohlschlaeger et al., 2010).

In the year 2003, Weekes et al published that there are increased ubiquitinated proteins and increases in the E1 and E2 abundance in western blot analysis in DCM hearts (Weekes et al., 2003). Another study by Hein et al in valvular heart disease patients suffering from aortic stenosis with ejection fractions range from 50 to 30, as well resulted in increased proteasomal activity in human hearts (Hein et al., 2003). Kostin could show similar results in heart transplants and DCM hearts with increased ubiquitinated proteins in western blots and immunofluorescence assays. Atrogin-1 was found to be increased on mRNA and protein level in biopsies of coronary arteries undergoing coronary artery bypass graft (CABG) operation with ejection fractions below 40 (Galasso et al., 2010).

Thus indicating the involvement of the ubiquitin-proteasome system in different heart diseases in human heart tissue.

In 2011 Jie Li published a paper on the enhancement of proteasomal function protecting against cardiomyopathy and ischemia-reperfusion injury in mice (Jie Li, Horak, et al., 2011). They created transgenic mice with cardiomyocyte-restricted overexpression of proteasome 28 subunit  $\alpha$  (CR-PA28  $\alpha$  OE) to increase the proteasomal protein turnover. These mice had an increased life span, and cardiac hypertrophy was decreased. In the ischemia-reperfusion experiment, they observed a reduction in infarct size and better cardiac function. Therefore, enhancing of the proteasomes proteolytic functions seems to show a benefit in the event of a cardiac infarct. This group as well published data in vitro, by using the proteasomal enhancement on cultured neonatal rat cardiomyocytes (Jie Li, Powell, et al., 2011). PA28  $\alpha$  overexpression protected the cardiomyocytes against oxidative stress induced by  $H_2O_2$ .

Since the growing data on the role and impact of the ubiquitin-proteasome system in the heart, our aim was to screen for further E3-ligases, containing F-box proteins and components of the multisubunit complex, which play a major role in heart hypertrophy. By using a siRNA-mediated knockdown in neonatal rat cardiomyocytes, we wanted to assess changes in cell size and amino acid incorporation, such as described for Atrogin-1 in many publications.

## 7.1 Identification of hypertrophy modulating CRLs

The assay of screening for hypertrophy first established and published by Claudia Jentsch for the search of micro RNAs that regulate cardiomyocytes contains a set of benefits in gathering information and data. A significant advantage of this assay is that only  $\alpha$ -actinin stained cells are counted as cardiomyocytes determined by the clear fluorescence signal of this staining and thereby excluding all other cell types such as fibroblasts, vascular smooth muscle cells or epithelial cells that might be a remnant after the isolation of the neonatal rat cardiomyocytes.

We included Atrogin-1 (Fbxo32) in our screening according to the result of the DNA microarray as one of the highly expressed CRLs in cardiomyocytes, despite being already published and well studied in this context. Thus providing us the opportunity of an internal control for experiments. Likewise in the experiments of Li et al. the usage of siRNA to knock down the mRNA of Atrogin-1 resulted in an increase in cardiomyocyte cell size (H. H. Li et al., 2007). This effect was also shown by Zeng et al. in a similar setting (Zeng et al., 2013).

In 2004 Li et al. demonstrated that the SCF complex containing Atrogin-1 decreases the calcineurin level by promoting its proteolysis as a target of ubiquitination. Calcineurin is a well-known inductor of cardiac hypertrophy that localizes to the Z-disc in cardiomyocytes via  $\alpha$ -actinin, but till then the molecular basis of its regulation remained unknown (H. Li et al., 2004). Their work exhibits that Atrogin-1 attenuates agonist-induced calcineurin level and represses calcineurin-dependent transactivation and NFATc4 translocation to the nucleus leading to hypertrophy. This effect could be reversed by the downregulation of Atrogin-1 expression and thus leading to an increase in calcineurin levels and cardiomyocyte hypertrophy. In vivo experiments with transgenic mice overexpressing Atrogin-1 in the heart, lead to a reduction of calcineurin levels and obtunded the pathophysiological cardiac hypertrophy in a TAC model.

Li et al. could also show that Atrogin-1 is involved in the disruption of Akt-dependent pathway, which are responsible for physiologic hypertrophy (H. H. Li et al., 2007). They demonstrate that Atrogin-1 acts as a coactivator for members of the Forkhead family of transcriptions factors, which are downstream of Akt. Biochemically Atrogin-1 is polyubiquitinating the lysine 63 of Foxo1 and Foxo3a. Transgenic mice overexpressing Atrogin-1 show increased Foxo1 ubiquitylation and Forkhead target genes accompanied by suppression of hypertrophy. Furthermore, they could demonstrate Atrogin-1's role in voluntary running exercise as a model of induction of physiologic hypertrophy. In this exercise experiment their knockout mice lacking Atrogin-1 resulted in marked cardiac hypertrophy in response to the running exercise in contrast to wild-type mice with a mild increase in cardiac hypertrophy.

The molecular mechanism that regulates the stability of Atrogin-1 remained unclear until Li et al. showed that Atrogin-1 underwent ubiquitin-mediated degradation by the proteasome (Jun-jie Li et al., 2011). Their results show that the F-box motif of Atrogin-1 and Skp1-CUL1-Roc1-F-box (SCF) complex are required for the ubiquitination and degradation of Atrogin-1. Furthermore, their results demonstrated that the p38 MAPK pathway plays a major role in the turnover of Atrogin-1 as well as serum starvation-induced expression of Atrogin-1 and reduction of H9c2 cell size.

Another clinical scenario is the usage of a left ventricular assistant device to decrease the workload of the heart. Baskin et al. stimulated this setting in a mechanical unloading model, achieved by heterotopic transplantation of either wild-type vs. MAFbx/Atrogin-1  $-/-$  knockout hearts (Baskin et al., 2014). Wild-type mouse hearts showed a decrease in heart weight and cardiomyocytes cross-sectional area. Surprisingly the knockout hearts hypertrophied after transplantation accompanied by an upregulation of calcineurin that is a regulator of cardiac hypertrophy. They could show that mechanical unloading of failing human hearts with a left ventricular device also had increased Atrogin-1 protein levels and higher levels of genes regulated by NFAT expression. Thus Atrogin-1 is essential for atrophic remodeling in hearts.

Recently Al-Yacoub et al. could identify a missense mutation in Atrogin-1 (Fbxo32) as a novel cause of dilatative cardiomyopathy (DCM) (Al-Yacoub et al., 2016). They showed that this mutation leads to a disrupted binding of the F-box protein into SCF complex, thus leading to inactive multi-subunit complex and impaired autophagy of target proteins.

In line with the published literature that shows that depletion of Atrogin-1 results in hypertrophy, we could also see this effect after the siRNA-mediated knockdown in our assays. We could confirm the change in cardiomyocyte size by the concomitant increase of  $^3\text{H}$ -isoleucine uptake.

In our screening, we could detect more members of the F-box protein family that have a stronger effect than Atrogin-1.

Our screening showed a statistically significant effect on cardiomyocyte cell size increase in Fbxo9, Fbxo30, Fbxo32, Cullin1, Roc1, Fbxo25, Fbxo33, Fbxw4, Fbxw5 and Ddb1 and decrease in cell size in Fbxo45, Fbxl14 and Fbxo6 in basal conditions without PE stimulation. After phenylephrine induction of hypertrophy in NRCMs, Fbxo25, Fbxo33, Fbxw4, Fbxo6 and Fbxo45 resulted in statistically significant changes of cell size.

Despite Atrogin-1 (Fbxo32), up to now, data published about the role of F-box proteins in the context of heart diseases or growth signaling pathways is rare, what offers huge opportunities for further research.

The F-box protein often described in the cardiac context is Fbxo25. Jang et al. showed that Fbxo25 acts as an E3 ligase for the turnover of cardiac specific transcription factors (Jang et al., 2011). Thus the knockdown of mRNA should lead to accumulation of the pro-stimulating signals affecting cardiomyocyte hypertrophy.

This F-box protein was shown to be nuclei-specific in vitro and cardiomyocytes. Also, the expression level was higher in fetal than in adult heart cells. The expression of Fbxo25 facilitates the degradation of the cardiac-specific transcription factors Nkx2-5, Isl1, Hand1, and Mef2C. To sum it up, their results showed that Fbxo25 acts as an ubiquitin E3 ligase that targets cardiac transcription factors, which indicates a pivotal role for protein homeostasis through this F-box protein in the course of heart development. The rise in cardiomyocyte size after knockdown of the Fbxo25 mRNA in the hypertrophy assay underlines its potential role in cardiac hypertrophy. Therefore these results show the importance of the F-box protein for maintenance of proper function in cardiac cells.

Another publication of Teixeira et al. shows that Fbxo25 promotes the degradation of ELK-1, what is known as the regulator of c-fos (Teixeira et al., 2013). The HAX-1 protein is a well-known player in the heart (Zhao et al., 2009). Recently Baumann et al. showed that this protein is targeted by Fbxo25 (Baumann et al., 2014). In this context, the ubiquitin ligase containing Fbxo25 could play a critical role in cardiomyocyte hypertrophy and biology.

The CRLs are multisubunit complexes, which can only function when all components are linked and active. The cullin protein acts as a scaffold, anchoring the RING finger protein and the adaptor for the attachment of the F-box protein. As a consequence, the knockdown of each of the subunits should prevent the CRLs to maintain their function. That is what we see as a result in the hypertrophy assay. The knockdown of the backbone Cul1 and the Roc1, both essential for the ubiquitination of substrates, resulting in similar hypertrophy measured by the increase in cell size by approximately 30% in basal condition. Concluding the Cul1 family ubiquitin ligases act collectively in the same direction. Whereas the various F-box proteins can lead to atrophic and hypertrophic effects.

Phenylephrine (PE), an  $\alpha$ 1-adrenergic agonist, is often used to induce hypertrophy in cultured cardiomyocytes (Usui et al., 2011). The induction of hypertrophy by PE doubles the cell size, which can be measured by the staining of the sarcomeres. This induced hypertrophy was consistent with previously published work (Jentsch et al., 2012). Since Fbxo25, Fbxo33, and Fbxw4 still showing a hypertrophic effect on top of the PE-induced hypertrophy, these findings indicate a strong phenotype after the knockdown of mRNA. However, it is up to now unclear if these F-box proteins are involved in the pathway, that PE uses to induce hypertrophy or regulate pathways independent of PE.

Fbxo45 and Fbxo6 still show reduced cell size despite being treated by PE, what might underline an essential role in cell size regulation. However, little is known about Fbxo45 in the context of heart diseases. The existing publications on Fbxo45 are mainly in the field of neuronal differentiation and regulation of p73, a mediator of cell cycle arrest and apoptosis, and mTOR signaling (Chung et al., 2014; Han et al., 2012; Peschiaroli et al., 2009; Saiga et al., 2009).

Whereas data about the function and biology of Fbxo6 on cell size regulation is rare. The published data involve the field of ER stress, interaction with glycoproteins (B. Liu et al., 2012) and cell cycle replication stress (Y. W. Zhang et al., 2009). In 2014 an article was published that Fbxo6 inhibits ER stress and JNK activation (Du et al., 2014). They state that Fbxo6 is responsible for the degradation of ER proteins. They induced cell stress by cadmium, thus resulting in increased expression of ER stress proteins and inhibition of Fbxo6. They concluded that Fbxo6 could reduce ER stress due to its function as an ubiquitin ligase. Transferring this publication to our results, which show that siRNA-mediated knockdown results in decreased cell size, could be interpreted, that a lack of this protein reduces the cell ability to counteract stress, such as induced by the low level of FBS starvation time till the end of the hypertrophy. Ultimately leading to decreased cell size.

After knockdown of Fbxo9 in our assays, we could see a significant increase in cardiomyocyte cell size and uptake of <sup>3</sup>H-isoleucine. However, there are no other published data on Fbxo9 in the heart. NFκB seems to be an important transcription factor in atrophy. Data on wild-type mice and mice lacking *Nfkb1* gene (nuclear factor κB) used in a hindlimb unloading model, showed upregulation of Fbxo9 in skeletal muscle on mRNA level (Wu et al., 2011). They checked the mRNA level of different genes in skeletal muscle atrophy and could confirm that Atrogin-1 (Fbxo32) as well is upregulated in their unloading model. Thus these findings are coherent to our results since the knockdown seems to lead to hypertrophy and the mRNA is increased in atrophy.

Another publication (Fernández-Sáiz et al., 2013) in cancer cells shows that Fbxo9 adjusts the mTOR signaling for growth factor abundance. They found a high level of Fbxo9 in multiple myelomas cells, which seems to be necessary for the PI(3)K/TORC2/Akt signaling. Interestingly using shRNA for reducing the level of Fbxo9, resulted in an increase in cell size in T89G cancer cells. Other publications on the Fbxo9 show, its role in adipocyte differentiation and innate immunity (Lee et al., 2013). To summarize Fbxo9 could be a novel regulator of cell size, but further research is needed, especially in muscle cells, since most of the publications concentrate on other tissues and cancer.

Data provided on Fbxo30 elucidates its role in the bone morphogenic protein (BMP) signaling, which is an important signal for muscle hypertrophy in mice (Sartori et al., 2013). BMP acts through proteins of the Smad family. Muscle atrophy can be induced by inhibition of the BMP

signaling in myostatin-deficient mice, that normally show a strong hypertrophy phenotype. Fbxo30 seems to be the ubiquitin ligase required for muscle loss. The signaling of the BMP decreases the level of Fbxo30. These data sets are consistent with the result that the knock-down of Fbxo30 mRNA in heart muscle cells causes a hypertrophic response.

Another publication in skeletal muscle shows that Fbxo30 seems to play a pivotal role in muscle hypotrophy in Nebulin knockout mice (F. Li et al., 2015). Nebulin is a filamentous protein associated with actin in the skeletal muscle. Deficiency of Nebulin leads to nemaline myopathy. Their research shows a switch of fiber towards the oxidative types and reduction in the muscle force. The abundance level of Murf1 and Fbxo30 seem to be upregulated, while the muscle cells undergo hypotrophy determined by a decrease in the cross-sectional area.

Other data published show the role of Fbxo30 silenced by shRNA disrupting mitosis in mam-mopoiesis (Y. Liu et al., 2016). Accordingly, to the published data on Fbxo30 in muscle cells, our findings are consistent. Fbxo30 seems to be a major player in the regulation of muscle hypertrophy and atrophy regulation.

One of the most potent regulators of heart hypertrophy according to our results is the ubiquitin ligase containing Fbxw4. Nevertheless, there is no published data available in the context of heart or muscle cell size regulation. Fbxw4 was shown to interact in the SCF, and its malfunction is associated with human cancers (Lockwood et al., 2013). It also seems to play a role in dactyl aplasia, which is limb malformation and in split hand syndrome (Filho et al., 2011; C. Li et al., 2015). Another major player according to our data is Fbxo33. The knockdown of the mRNA resulted in a statistically increase in cardiomyocyte cell size under basal and phenylephrine-stimulated conditions in the hypertrophy assay as well in the <sup>3</sup>H-isoleucine incorporation assay.

A study from 2006 identified the SCF E3-ligase containing Fbxo33 being responsible for the degradation of the multifunctional regulator Y-box-binding protein 1 (YB-1) (Lutz et al., 2006). YB-1 is involved in many functions such as cell proliferation and differentiation, stress response and malignant cell transformation (Lyabin et al., 2014). A possible explanation for the results of the screening is that YB-1 seem to be able to control the abundance of growth factors, cyclins and oxidative phosphorylation proteins as explained in the review of Lyabin in 2014. However, still, the data on Fbxo33 in the heart as in the other tissues and its function is still nebulously.

Similarly, little data is published on Fbxl14 in the context of cardiac diseases. This ubiquitin ligase was shown to play a role in controlling the epithelial-to-mesenchymal transition and in cancer progression, but no publication are published on muscle cells (Díaz & de Herreros,

2016; Fang et al., 2016; Viñas-Castells et al., 2010). Since that lack of information, before discussion on its role in heart, further research needs to be performed.

Ddb1 could be associated with hypertension phenotype in a certain population with a polymorphism that impairs the function of G $\beta$ 3 to target GRK2 ubiquitination (Zha et al., 2016). Ddb1 assembles in an E3 ubiquitin ligase that targets GRK2. The polymorphism disrupts the binding of Ddb1 to G $\beta$ 3 leading to increased protein levels of GRK2 in patient blood samples. The knockout of Cul4a, which is part of the DDB1-CUL4A-ROC1 E3 ubiquitin ligase resulted in increased blood pressure and diminished heart function.

As Roc1 and Cul1 provide essential subunits of the SCF, they are necessary for the proper functioning of the UPS. However, their knockdown, therefore, interferes with the role of all the E3-ligases containing F-box proteins. Interestingly both showed after the siRNA-mediated knockdown an increase in cell size and  $^3\text{H}$ -isoleucine incorporation, what could be explained, that the function of the SCF is rather the degradation of growth signals. There is no knockout data available on Roc1 or Cul1 mice, what would provide deeper insight into this matter.

Due to the lack of information on these new findings in literature aside from the role of Atrogin-1 as a pivotal player in hypertrophy and atrophy, these results are the first of their kind and future experiments will be needed to determine their significance.

## **7.2 Validation experiments for screening hits**

For further validation of the effect of the knockdown in vitro, we first checked for a sufficient knockdown of the target mRNA in qRT-PCR. According to the publication of Claudia Jentsch, we ensured that the changes in cell size are concomitant by the modification of  $^3\text{H}$ -isoleucine incorporation into cardiomyocytes. Also, we checked the viability of the cell after the treatment of siRNA transfection by using an MTT assay and in cell count analysis.

The knockdown of each mRNA target was an essential experiment for all the in vitro experiments performed. A sufficient knockdown is needed to unravel the possible effect and counteract a general wide security range, such as twenty or less percent of the amount of the protein is sufficient to maintain its function in the cells.

Also, we performed MTT assays and cell count on each target to ensure that the transfection did not damage the cells, which could alter their physiological function.

We could not detect any statistically significant decrease in the MTT turnover in any of our identified targets, which underlines that toxic effect by using the siRNA are not present. Moreover, this could be excluded as a potential bias in our experimental setting. Nevertheless is the decrease after transfection of siRNA against Fbxo45 mRNA remarkable. Thus Peschiaroli et

al. published that the CRL containing Fbxo45 targets p73 and promotes its degradation by the proteasome (Peschiaroli et al., 2009). The siRNA-mediated depletion of Fbxo45 would stabilize p73 and induce cell death in a p53 dependent manner. Their results could explain the decreased viability seen in the MTT assay for Fbxo45.

The significant reduction in the cell count of Fbxo45 experiments would strengthen the hypothesis, that p73 could be responsible for this result.

Interestingly, we see an increase in the cell count for Fbxw5, which is known to play a role in many cancer studies (Z. Wang et al., 2014). However, there are no results available in the context of cardiac diseases. The review of Wang published in Nature, mentions Fbxw5 being identified as a negative regulator of TGF $\beta$ -activated kinase in the Interleukin-1 $\beta$  signaling pathway, suggesting a tumor suppressive potential. Fbxw5 furthermore promotes the degradation of the MYB oncoprotein. These results could explain the increase in the cell count in NRCMs. The same issue remains for DDB1 and Roc1. There are publications in the context of cancer but not for the heart. The publication of Hu et al. shows that Fbxw5 binds to the TSC2 protein (Hu et al., 2008). Overexpression of the F-box protein promotes the degradation of TSC2, a tumor suppressor. Thus a depletion of Fbxw5 could lead to a free action of TSC2 resulting in cell growth. Minoda et al. could show that Fbxw5 negatively regulates the MAP3K pathway. In their experiments, overexpression of Fbxw5 inhibits the activation of JNK/p38 MAPKs and NF- $\kappa$ B (Minoda et al., 2009). The knockdown of Fbxw5 strengthened the activation of these pathways. That could explain the pro-hypertrophic phenotype after the siRNA-mediated knockdown in our assays. For this issue, further experiments need to be conducted.

In analogy to the publication of Claudia Jentsch (Jentsch et al., 2012), we used the  $^3$ H-isoleucin incorporation to confirm the siRNA-mediated hypertrophy. The  $^3$ H-isoleucine is a radioactive labeled essential amino acid that is incorporated into the cells and used to build natural proteins thereby monitoring the anabolic effect. We used this assay in the basal without PE and the phenylephrine-induced hypertrophy settings.

We could confirm under the basal condition that after siRNA-mediated depletion of the respective targets (Fbxo9, Fbxo25, Fbxo30, Fbxo32 (Atrogin-1), Fbxo33, Fbxw4, Fbxw5, DDB1, and Roc1), the  $^3$ H-isoleucine incorporation was increased.

Furthermore, it remains unclear why the targets Fbxo6, Fbxl14, and Cul1 did not show any significant effect in this assay, whereas a significant change was observed in the hypertrophy assay determining their cell size. The reason for this controversial finding could be metabolic changes that are yet to unravel.

Despite the pivotal role of Atrogin-1, the published literature does not provide well-studied information in the literature on the other F-box proteins we found in the context of hypertrophy signaling pathways, thus limiting their discussion in the context of signaling pathways and their underlying molecular function.

## 8 Outlook

13 CRL components (seven Fbxo-, two Fbxw-, one Fbxl- family members and several CRL subunits) were identified that significantly affected NRCM cell size. Of these Fbxo33 and Fbxo25, the substrate receptor of the Cullin1-assembled SCF Fbxo33 ubiquitin ligase and the Fbxo25 ubiquitin ligase were identified as the most potent novel regulators of cardiac hypertrophy. This study identified several CRLs that might play a yet unrecognized role in the regulation of cardiac hypertrophy.

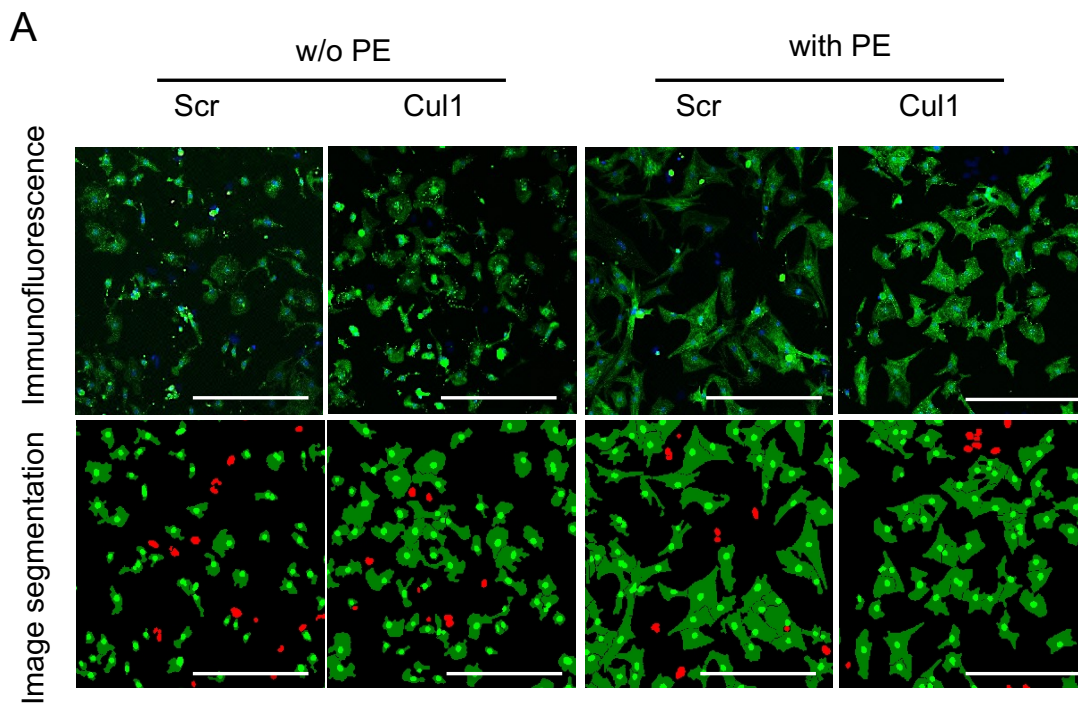
In the next step, the function of the most potent ubiquitin ligases in the heart for physiological and pathophysiological hypertrophy will be assessed *in vivo*.

The role of the ubiquitin-ligases *in vitro* could offer new therapeutic opportunities for cardiac diseases such as heart failure, by directly targeting dysregulated proteins that are involved in critical molecular pathways. While other methodical approaches aim to modulate the mRNA level or gene editing, the regulation of proteins abundance directly by enhancing or inhibition of a target proteins, could offer new perspectives.

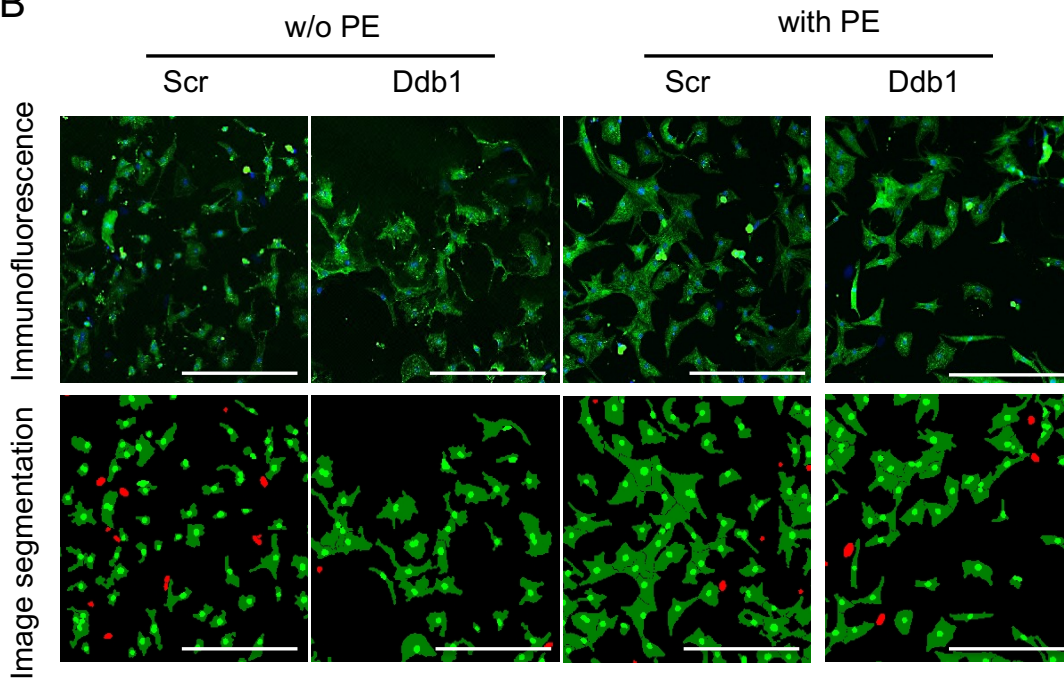
For instance, the protein chimeric molecule 1 (Protac-1) mediates the ubiquitination and degradation of target proteins. That could provide a new approach for the inactivation of disease-causing proteins.

## 9 Supplement

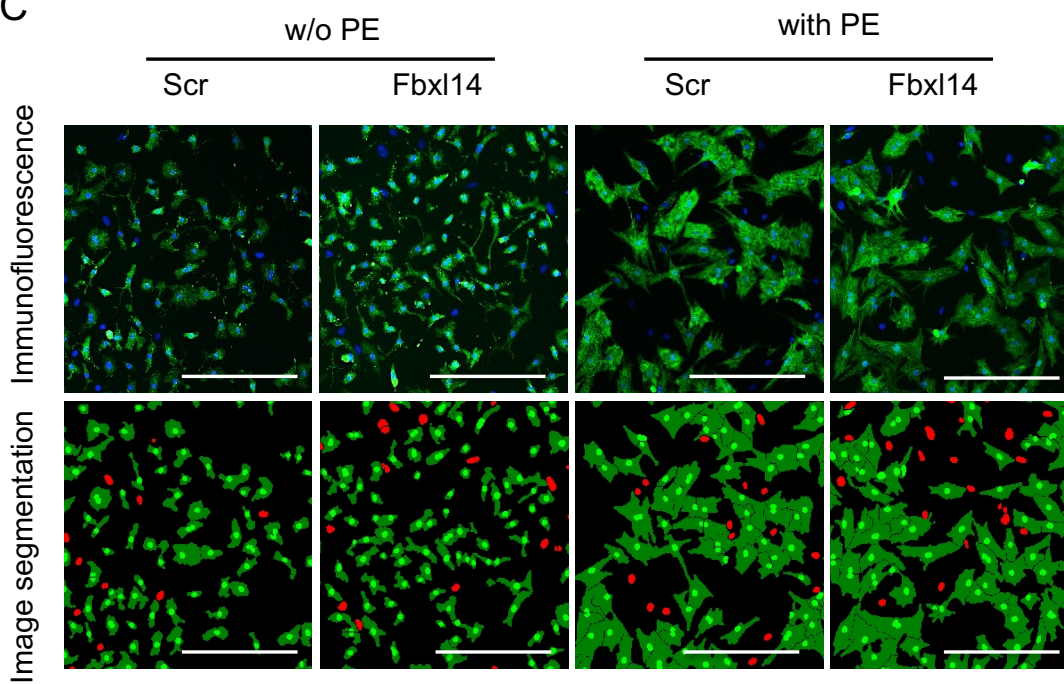
Immunofluorescence and image segmentation pictures of the main target proteins in NRCM culture after staining without and with PE stimulation for induction of hypertrophy. PE concentration 50  $\mu\text{m}$ . White line equals 250  $\mu\text{m}$ . Upper panel immunofluorescence: DAPI stained nuclei in blue,  $\alpha$ -actinin for sarcomeres in green. Lower panel image segmentation: cardiomyocytes in green, non-cardiomyocytes in red. Cul1 (A), Ddb1 (B), Fbxl14 (C), Fbxo6 (D), Fbxo9 (E), Fbxo25 (F), Fbxo30 (G), Fbxo32 (H), Fbxo33 (I), Fbxo45 (J), Fbxw4 (K), Fbxw5 (L), Roc1 (M).



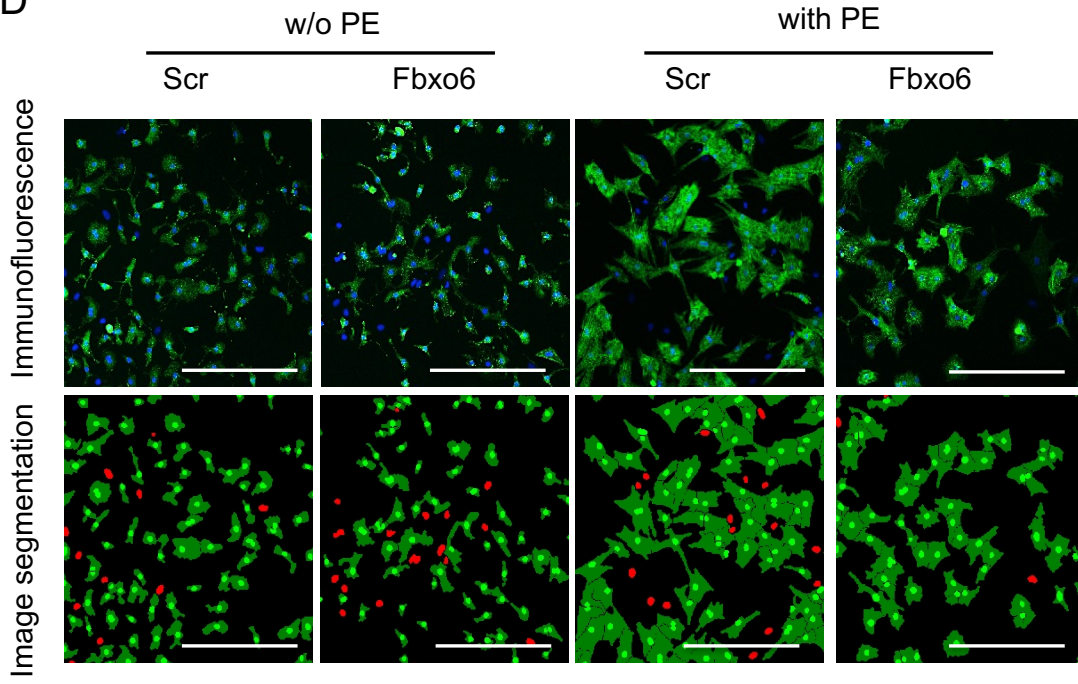
**B**



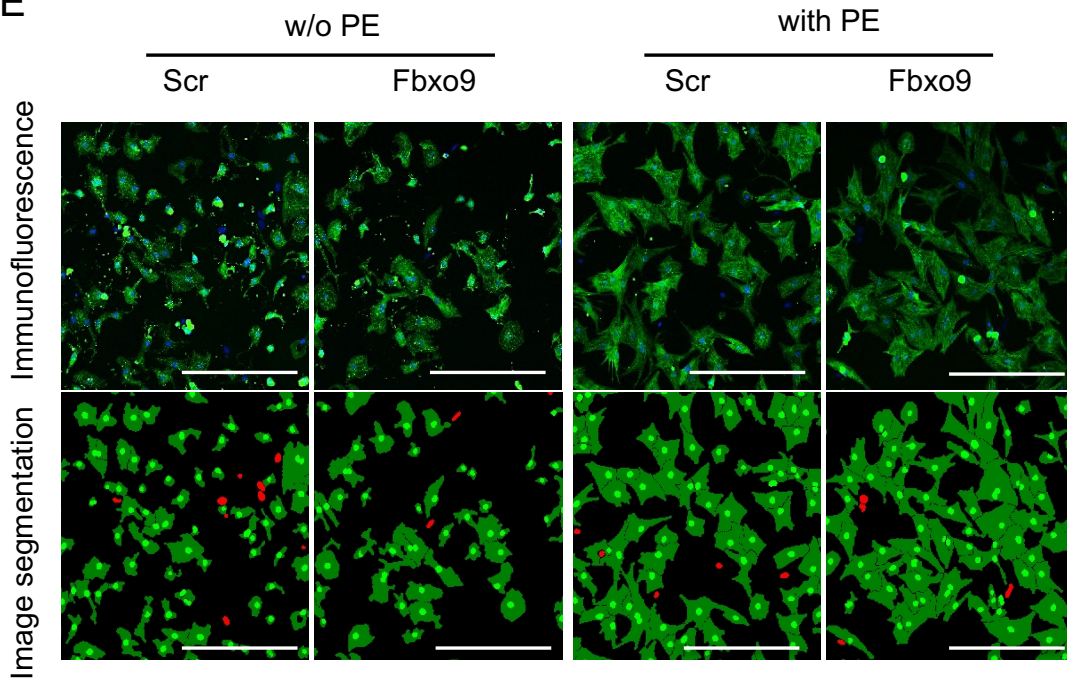
**C**



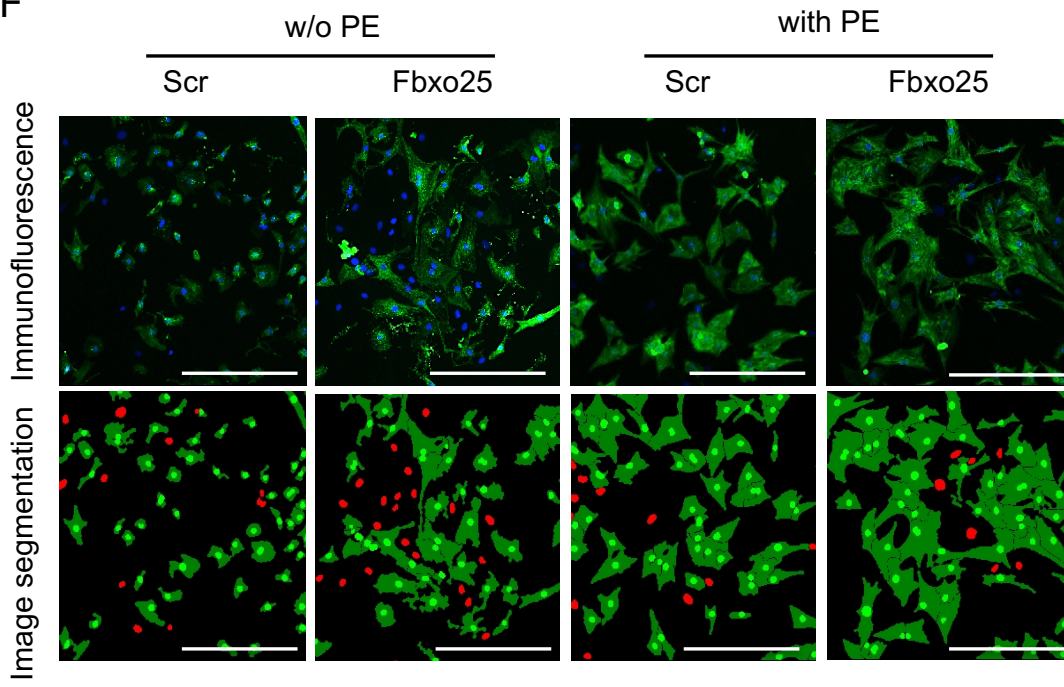
D



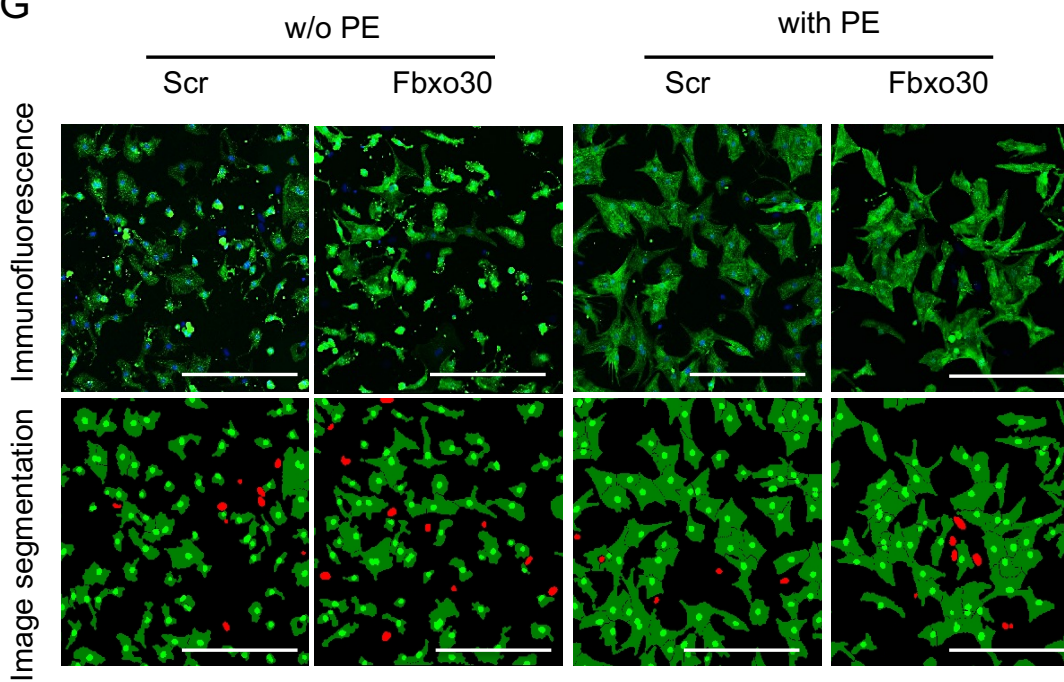
E



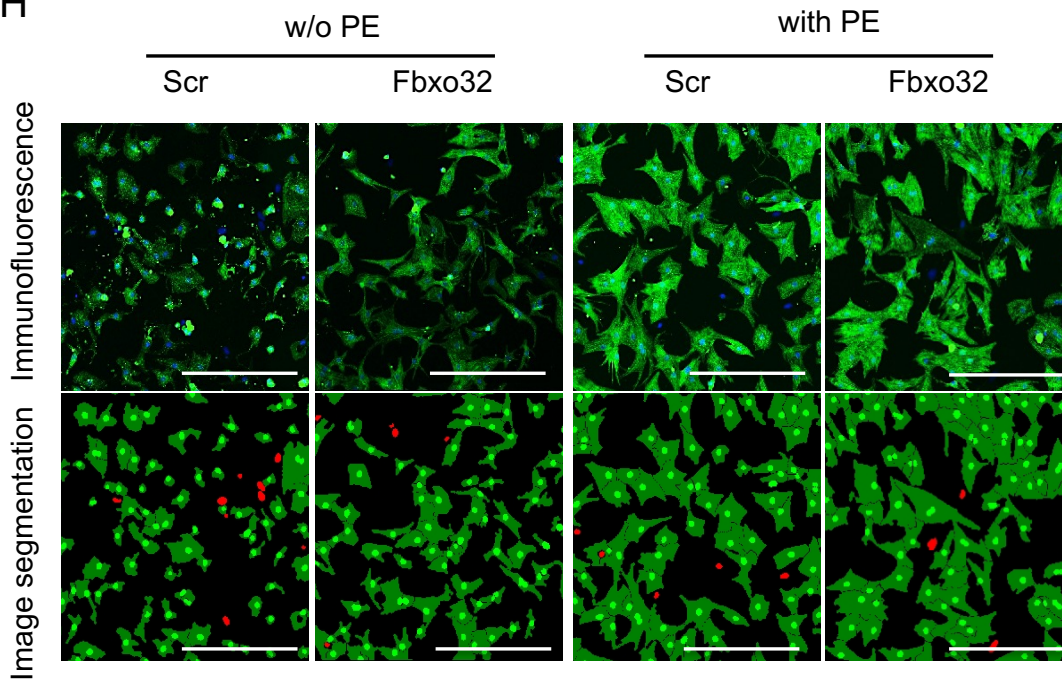
F



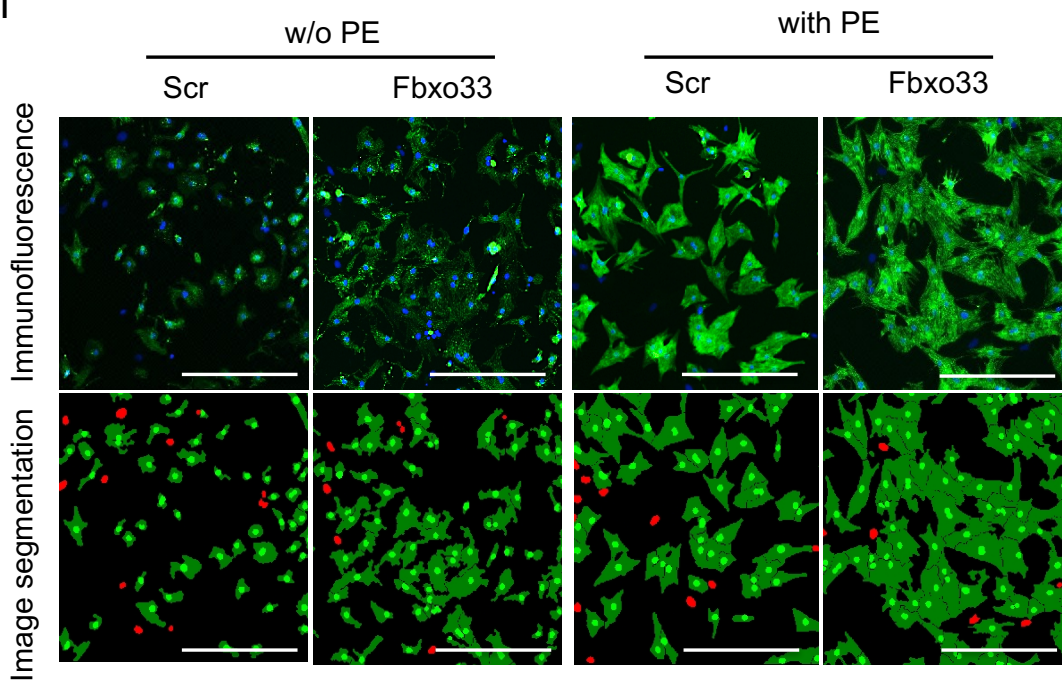
G



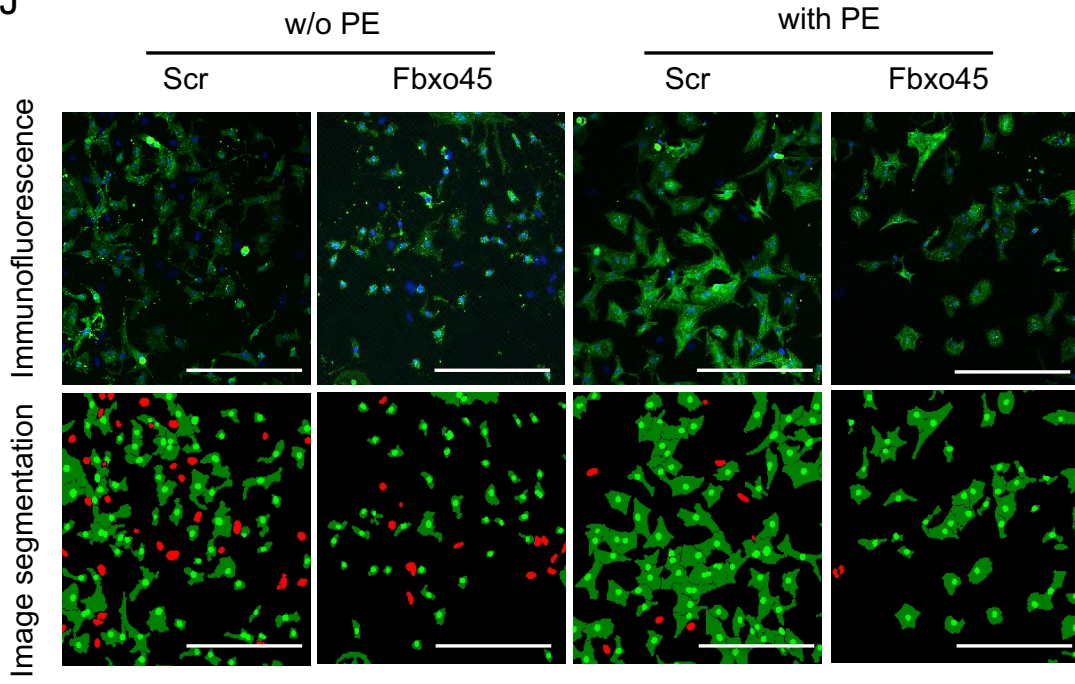
H



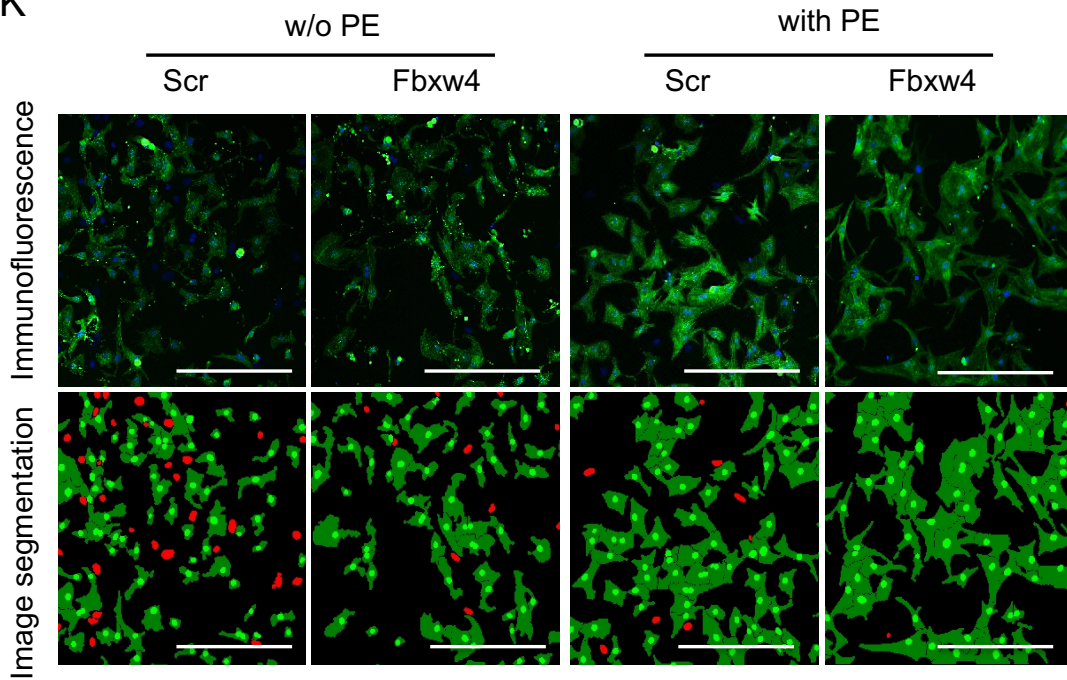
I



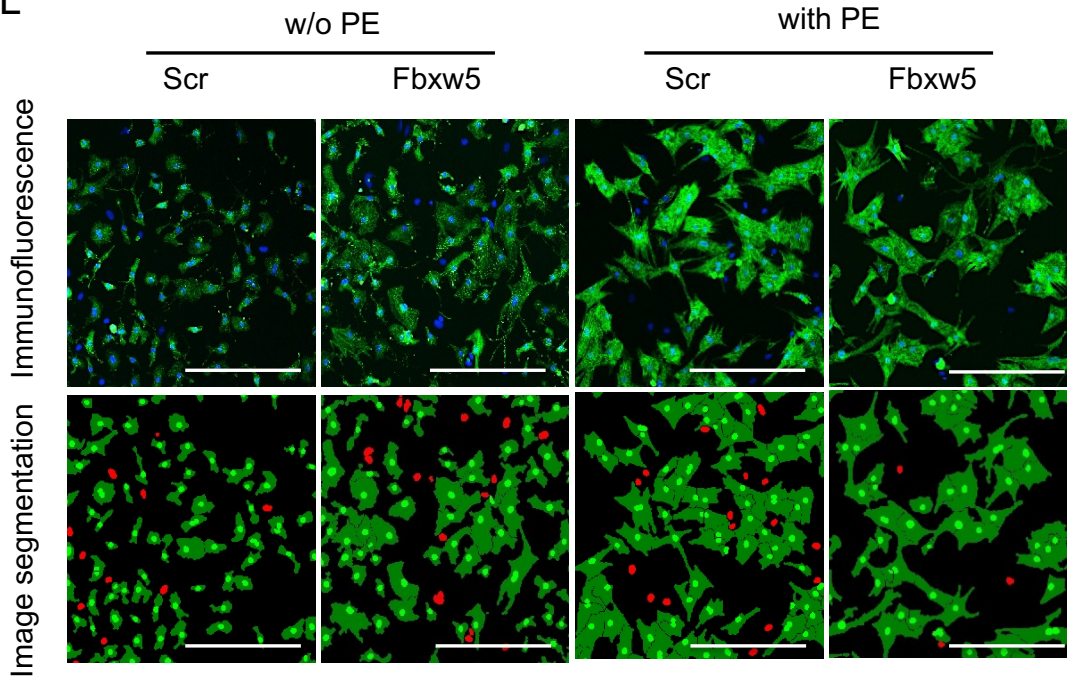
J



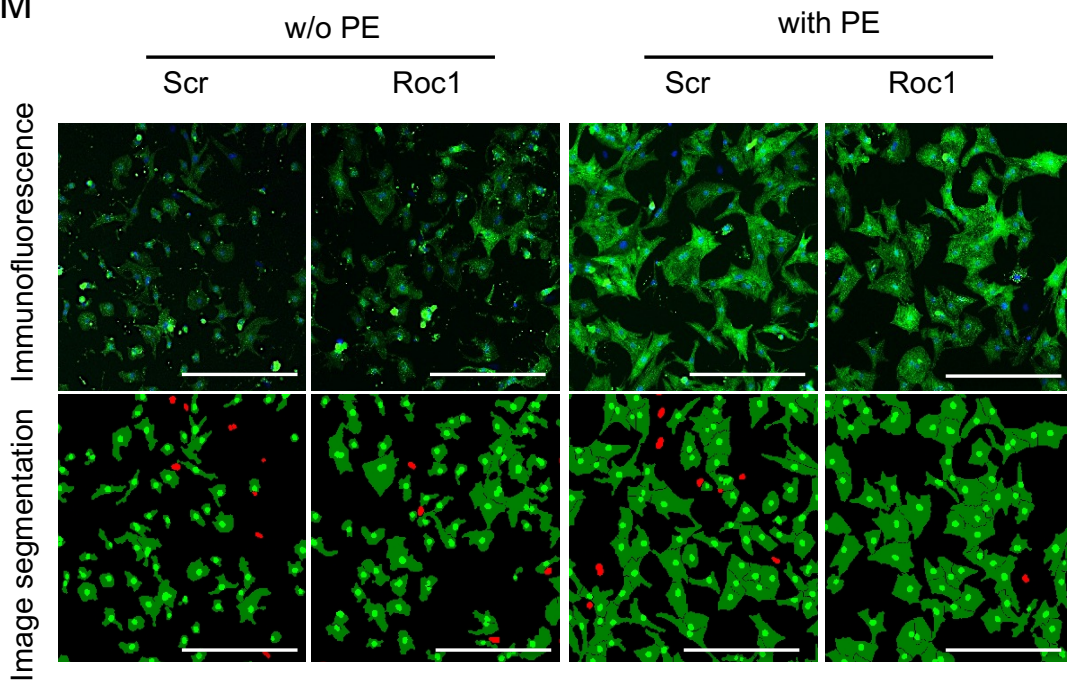
K



L



M



## 10 References

- Ahles, A., & Engelhardt, S. (2014). Polymorphic Variants of Adrenoceptors: Pharmacology, Physiology, and Role in Disease. *Pharmacological Reviews*, 66(3), 598–637. <https://doi.org/10.1124/pr.113.008219>
- Akari, H., Bour, S., Kao, S., Adachi, A., & Strebel, K. (2001). The human immunodeficiency virus type 1 accessory protein Vpu induces apoptosis by suppressing the nuclear factor kappaB-dependent expression of antiapoptotic factors. *The Journal of Experimental Medicine*, 194(9), 1299–311. <https://doi.org/10.1084/jem.194.9.1299>
- Al-Yacoub, N., Shaheen, R., Awad, S. M., Kunhi, M., Dzimiri, N., Nguyen, H. C., Xiong, Y., Al-Buraiki, J., Al-Habeeb, W., Alkuraya, F. S., & Poizat, C. (2016). FBXO32, encoding a member of the SCF complex, is mutated in dilated cardiomyopathy. *Genome Biology*, 17(1), 2. <https://doi.org/10.1186/s13059-015-0861-4>
- Arya, R., Kedar, V., Hwang, J. R., McDonough, H., Li, H.-H., Taylor, J., & Patterson, C. (2004). Muscle ring finger protein-1 inhibits PKC{epsilon} activation and prevents cardiomyocyte hypertrophy. *The Journal of Cell Biology*, 167(6), 1147–59. <https://doi.org/10.1083/jcb.200402033>
- Baskin, K. K., Rodriguez, M. R., Kansara, S., Chen, W., Carranza, S., Frazier, O. H., Glass, D. J., & Taegtmeyer, H. (2014). MAFbx/Atrogin-1 is required for atrophic remodeling of the unloaded heart. *Journal of Molecular and Cellular Cardiology*, 72, 168–176. <https://doi.org/10.1016/j.yjmcc.2014.03.006>
- Baumann, U., Fernández-Sáiz, V., Rudelius, M., Lemeer, S., Rad, R., Knorn, A.-M., Slawska, J., Engel, K., Jeremias, I., Li, Z., Tomiatti, V., Illert, A.-L., Targosz, B.-S., Braun, M., Perner, S., Leitges, M., Klapper, W., Dreyling, M., Miething, C., Lenz, G., Rosenwald, A., Peschel, C., Keller, U., Kuster, B., Bassermann, F. (2014). Disruption of the PRKCD–FBXO25–HAX-1 axis attenuates the apoptotic response and drives lymphomagenesis. *Nature Medicine*, 20(October 2013), 1401–1409. <https://doi.org/10.1038/nm.3740>
- Belke, D. D., Betuing, S., Tuttle, M. J., Graveleau, C., Young, M. E., Pham, M., Zhang, D., Cooksey, R. C., McClain, D. A., Litwin, S. E., Taegtmeyer, H., Severson, D., Ronald Kahn, C., & Dale Abel, E. (2002). Insulin signaling coordinately regulates cardiac size, metabolism, and contractile protein isoform expression. *Journal of Clinical Investigation*, 109(5), 629–639. <https://doi.org/10.1172/JCI200213946>
- Birks, E. J., Latif, N., Enesa, K., Folkvang, T., Luong, L. A., Sarathchandra, P., Khan, M., Ovaa, H., Terracciano, C. M., Barton, P. J. R., Yacoub, M. H., & Evans, P. C. (2008). Elevated p53 expression is associated with dysregulation of the ubiquitin-proteasome system in

- dilated cardiomyopathy. *Cardiovascular Research*, 79(3), 472–480. <https://doi.org/10.1093/cvr/cvn083>
- Bodine, S. C., Latres, E., Baumhueter, S., Lai, V. K., Nunez, L., Clarke, B. A., Poueymirou, W. T., Panaro, F. J., Na, E., Dharmarajan, K., Pan, Z. Q., Valenzuela, D. M., DeChiara, T. M., Stitt, T. N., Yancopoulos, G. D., & Glass, D. J. (2001). Identification of ubiquitin ligases required for skeletal muscle atrophy. *Science (New York, N.Y.)*, 294(5547), 1704–8. <https://doi.org/10.1126/science.1065874>
- Bornstein, G., Ganoth, D., & Hershko, A. (2006). Regulation of neddylation and deneddylation of cullin1 in SCFSkp2 ubiquitin ligase by F-box protein and substrate. *Proceedings of the National Academy of Sciences of the United States of America*, 103(31), 11515–11520. <https://doi.org/10.1073/pnas.0603921103>
- Bour, S., Perrin, C., Akari, H., & Strebel, K. (2001). The Human Immunodeficiency Virus Type 1 Vpu Protein Inhibits NF- $\kappa$ B Activation by Interfering with  $\beta$ TrCP-mediated Degradation of I $\kappa$ B. *Journal of Biological Chemistry*, 276(19), 15920–15928. <https://doi.org/10.1074/jbc.M010533200>
- Carrier, L., Schlossarek, S., Willis, M. S., & Eschenhagen, T. (2010). The ubiquitin-proteasome system and nonsense-mediated mRNA decay in hypertrophic cardiomyopathy. *Cardiovascular Research*, 85(2), 330–338. <https://doi.org/10.1093/cvr/cvp247>
- Castillero, E., Alamdari, N., Lecker, S. H., & Hasselgren, P.-O. (2013). Suppression of atrogin-1 and MuRF1 prevents dexamethasone-induced atrophy of cultured myotubes. *Metabolism: Clinical and Experimental*, 62(10), 1495–502. <https://doi.org/10.1016/j.metabol.2013.05.018>
- Chung, F.-Z., Sahasrabudhe, A. a, Ma, K., Chen, X., Basrur, V., Lim, M. S., & Elenitoba-Johnson, K. S. J. (2014). Fbxo45 Inhibits Calcium-sensitive Proteolysis of N-cadherin and Promotes Neuronal Differentiation. *The Journal of Biological Chemistry*, 289(41), 28448–59. <https://doi.org/10.1074/jbc.M114.561241>
- Cordero-Espinoza, L., & Hagen, T. (2013). Regulation of Cullin-RING ubiquitin ligase 1 by Spliceosome-associated protein 130 (SAP130). *Biology Open*, 2(8), 838–844. <https://doi.org/10.1242/bio.20134374>
- Craig, K. L., & Tyers, M. (1999). The F-box: a new motif for ubiquitin dependent proteolysis in cell cycle regulation and signal transduction. *Progress in Biophysics and Molecular Biology*, 72(3), 299–328. [https://doi.org/10.1016/S0079-6107\(99\)00010-3](https://doi.org/10.1016/S0079-6107(99)00010-3)
- Day, S. M. (2013). The ubiquitin proteasome system in human cardiomyopathies and heart failure. *American Journal of Physiology. Heart and Circulatory Physiology*, 304(10),

H1283-93. <https://doi.org/10.1152/ajpheart.00249.2012>

- Díaz, V. M., & de Herreros, A. G. (2016). F-box proteins: Keeping the epithelial-to-mesenchymal transition (EMT) in check. *Seminars in Cancer Biology*, 36, 71–79. <https://doi.org/10.1016/j.semcancer.2015.10.003>
- Du, K., Takahashi, T., Kuge, S., Naganuma, A., & Hwang, G.-W. (2014). FBXO6 attenuates cadmium toxicity in HEK293 cells by inhibiting ER stress and JNK activation. *The Journal of Toxicological Sciences*, 39(6), 861–6. <https://doi.org/10.2131/jts.39.861>
- Dupuis, J., Langenberg, C., Prokopenko, I., Saxena, R., Soranzo, N., Jackson, A. U., Wheeler, E., Glazer, N. L., Bouatia-Naji, N., Gloyn, A. L., Lindgren, C. M., Mägi, R., Morris, A. P., Randall, J., Johnson, T., Elliott, P., Rybin, D., Barroso, I. (2010). New genetic loci implicated in fasting glucose homeostasis and their impact on type 2 diabetes risk. *Nature Genetics*, 42(2), 105–116. <https://doi.org/10.1038/ng.520>
- Eletr, Z. M., & Wilkinson, K. D. (2014). Regulation of proteolysis by human deubiquitinating enzymes. *Biochimica et Biophysica Acta - Molecular Cell Research*. <https://doi.org/10.1016/j.bbamcr.2013.06.027>
- Fan, C. D., Lum, M. A., Xu, C., Black, J. D., & Wang, X. (2013). Ubiquitin-dependent regulation of phospho-AKT Dynamics by the ubiquitin E3 LIGASE, NEDD4-1, in the insulin-like growth factor-1 response. *Journal of Biological Chemistry*, 288(3), 1674–1684. <https://doi.org/10.1074/jbc.M112.416339>
- Fang, X., Zhou, W., Wu, Q., Huang, Z., Shi, Y., Yang, K., Chen, C., Xie, Q., Mack, S. C., Wang, X., Carcaboso, A. M., Sloan, A. E., Ouyang, G., McLendon, R. E., Bian, X., Rich, J. N., & Bao, S. (2016). Deubiquitinase USP13 maintains glioblastoma stem cells by antagonizing FBXL14-mediated Myc ubiquitination. *Journal of Experimental Medicine*, 245–267. <https://doi.org/10.1084/jem.20151673>
- Fernández-Sáiz, V., Targosz, B., Lemeer, S., Eichner, R., Langer, C., Bullinger, L., Reiter, C., Slotta-Huspenina, J., Schroeder, S., Knorn, A., Kurutz, J., Peschel, C., Pagano, M., Kuster, B., & Bassermann, F. (2013). SCFFbxo9 and CK2 direct the cellular response to growth factor withdrawal via Tel2/Tti1 degradation and promote survival in multiple myeloma. *Nature Cell Biology*, 15(1), 72–81. <https://doi.org/10.1038/ncb2651>
- Filho, A. B., Souza, J., Faucz, F. R., Sotomaior, V. S., Dupont, B., Bartel, F., Rodriguez, R., Schwartz, C. E., Skinner, C., Alliman, S., & Raskin, S. (2011). Somatic/gonadal mosaicism in a syndromic form of ectrodactyly, including eye abnormalities, documented through array-based comparative genomic hybridization. *American Journal of Medical Genetics, Part A*, 155(5), 1152–1156. <https://doi.org/10.1002/ajmg.a.33942>

- Fonzo, a Di, & Dekker, M. C. J. (2009). FBXO7 mutations cause autosomal pyramidal syndrome. *Erasmus*. <https://doi.org/10.1212/01.wnl.0000338144.10967.2b>
- Galan, J. M., & Peter, M. (1999). Ubiquitin-dependent degradation of multiple F-box proteins by an autocatalytic mechanism. *Proceedings of the National Academy of Sciences of the United States of America*, *96*(16), 9124–9. <https://doi.org/10.1073/pnas.96.16.9124>
- Galasso, G., De Rosa, R., Piscione, F., Iaccarino, G., Vosa, C., Sorriento, D., Piccolo, R., Rapacciuolo, A., Walsh, K., & Chiariello, M. (2010). Myocardial expression of FOXO3a-Atrogin-1 pathway in human heart failure. *European Journal of Heart Failure*, *12*(12), 1290–1296. <https://doi.org/10.1093/eurjhf/hfq102>
- Goldenberg, S. J., Cascio, T. C., Shumway, S. D., Garbutt, K. C., Liu, J., Xiong, Y., & Zheng, N. (2004). Structure of the Cand1-Cul1-Roc1 complex reveals regulatory mechanisms for the assembly of the multisubunit cullin-dependent ubiquitin ligases. *Cell*, *119*(4), 517–28. <https://doi.org/10.1016/j.cell.2004.10.019>
- Gomes, M. D., Lecker, S. H., Jagoe, R. T., Navon, A., & Goldberg, A. L. (2001). Atrogin-1, a muscle-specific F-box protein highly expressed during muscle atrophy. *Proceedings of the National Academy of Sciences*, *98*(25), 14440–14445. <https://doi.org/10.1073/pnas.251541198>
- Gutkind, J. S., & Offermanns, S. (2009). A New Gq-Initiated MAPK Signaling Pathway in the Heart. *Developmental Cell*, *16*(2), 163–164. <https://doi.org/10.1016/j.devcel.2009.01.021>
- Han, S., Kim, S., Bahl, S., Li, L., Burande, C. F., Smith, N., James, M., Beauchamp, R. L., Bhide, P., DiAntonio, A., & Ramesh, V. (2012). The E3 ubiquitin ligase protein associated with Myc (Pam) regulates mammalian/mechanistic target of rapamycin complex 1 (mTORC1) signaling in vivo through N- and C-terminal domains. *The Journal of Biological Chemistry*, *287*(36), 30063–72. <https://doi.org/10.1074/jbc.M112.353987>
- Haq, S., Choukroun, G., Lim, H., Tymitz, K. M., Monte, F., Gwathmey, J., Grazette, L., Michael, A., Hajjar, R., Force, T., & Molkentin, J. D. (2015). Human Hearts With Hypertrophy Versus Advanced.
- Hein, S., Arnon, E., Kostin, S., Schönburg, M., Elsässer, A., Polyakova, V., Bauer, E. P., Klövekorn, W. P., & Schaper, J. (2003). Progression from compensated hypertrophy to failure in the pressure-overloaded human: Heart structural deterioration and compensatory mechanisms. *Circulation*, *107*(7), 984–991. <https://doi.org/10.1161/01.CIR.0000051865.66123.B7>
- Heineke, J., & Molkentin, J. D. (2006). Regulation of cardiac hypertrophy by intracellular signalling pathways. *Nature Reviews Molecular Cell Biology*, *7*(8), 589–600.

<https://doi.org/10.1038/nrm1983>

- Hicke, L., & Dunn, R. (2003). Regulation of Membrane Protein Transport by Ubiquitin and Ubiquitin-Binding Proteins. *Annual Review of Cell and Developmental Biology*, 19(1), 141–172. <https://doi.org/10.1146/annurev.cellbio.19.110701.154617>
- Hsu, J. M., Lee, Y. C. G., Yu, C. T. M., & Huang, C. Y. F. (2004). Fbx7 functions in the SCF complex regulating Cdk1-cyclin B-phosphorylated hepatoma up-regulated protein (HURP) proteolysis by a proline-rich region. *Journal of Biological Chemistry*, 279(31), 32592–32602. <https://doi.org/10.1074/jbc.M404950200>
- Hu, J., Zacharek, S., He, Y. J., Lee, H., Shumway, S., Duronio, R. J., & Xiong, Y. (2008). WD40 protein FBW5 promotes ubiquitination of tumor suppressor TSC2 by DDB1 – CUL4 – ROC1 ligase service WD40 protein FBW5 promotes ubiquitination of tumor suppressor TSC2 by DDB1 – CUL4 – ROC1 ligase, (919), 866–871. <https://doi.org/10.1101/gad.1624008>
- Huber, C., Dias-Santagata, D., Glaser, A., O’Sullivan, J., Brauner, R., Wu, K., Xu, X., Pearce, K., Wang, R., Uzielli, M. L. G., Dagoneau, N., Chemaitilly, W., Superti-Furga, A., Dos Santos, H., Mégarbané, A., Morin, G., Gillissen-Kaesbach, G., Hennekam, R., Van der Burgt, I., Black, GC., Clayton, PE., Read, A., Le Merrer, M., Scambler, PJ., Munnich, A., Pan, ZQ., Winter, R., Cormier-Daire, V. (2005). Identification of mutations in CUL7 in 3-M syndrome. *Nature Genetics*, 37(10), 1119–24. <https://doi.org/10.1038/ng1628>
- Jang, J.-W., Lee, W.-Y., Lee, J.-H., Moon, S.-H., Kim, C.-H., & Chung, H.-M. (2011). A novel Fbxo25 acts as an E3 ligase for destructing cardiac specific transcription factors. *Biochemical and Biophysical Research Communications*, 410(2), 183–8. <https://doi.org/10.1016/j.bbrc.2011.05.011>
- Jentzsch, C., Leierseder, S., Loyer, X., Floherschütz, I., Sassi, Y., Hartmann, D., Thum, T., Lagerbauer, B., & Engelhardt, S. (2012). A phenotypic screen to identify hypertrophy-modulating microRNAs in primary cardiomyocytes. *Journal of Molecular and Cellular Cardiology*, 52(1), 13–20. <https://doi.org/10.1016/j.yjmcc.2011.07.010>
- Jin, J. (2004). Systematic analysis and nomenclature of mammalian F-box proteins. *Genes & Development*, 18(21), 2573–2580. <https://doi.org/10.1101/gad.1255304>
- Katzmann, D. J., Babst, M., & Emr, S. D. (2001). Ubiquitin-dependent sorting into the multivesicular body pathway requires the function of a conserved endosomal protein sorting complex, ESCRT-I. *Cell*, 106(2), 145–155. [https://doi.org/10.1016/S0092-8674\(01\)00434-2](https://doi.org/10.1016/S0092-8674(01)00434-2)
- Kipreos, E. T., & Pagano, M. (2000). The F-box protein family. *Genome Biology*, 1(5),

REVIEWS3002. <https://doi.org/10.1186/gb-2000-1-5-reviews3002>

- Kuiken, H. J., Egan, D. A., Laman, H., Bernards, R., Beijersbergen, R. L., & Dirac, A. M. (2012). Identification of F-box only protein 7 as a negative regulator of NF-kappaB signalling. *Journal of Cellular and Molecular Medicine*, 16(9), 2140–2149. <https://doi.org/10.1111/j.1582-4934.2012.01524.x>
- Kunkel, G. H., Chaturvedi, P., & Tyagi, S. C. (2015). Resuscitation of a dead cardiomyocyte. *Heart Failure Reviews*, 20(6), 709–719. <https://doi.org/10.1007/s10741-015-9501-z>
- Lecker, S. H., Jagoe, R. T., Gilbert, A., Gomes, M., Baracos, V., Bailey, J., Price, S. R., Mitch, W. E., & Goldberg, A. L. (2004). Multiple types of skeletal muscle atrophy involve a common program of changes in gene expression. *The FASEB Journal: Official Publication of the Federation of American Societies for Experimental Biology*, 18(1), 39–51. <https://doi.org/10.1096/fj.03-0610com>
- Lee, K. W., Kwak, S. H., Ahn, B. Y., Lee, H. M., Jung, H. S., Cho, Y. M., Park, Y. J., Chung, S. S., & Park, K. S. (2013). F-box only protein 9 is required for adipocyte differentiation. *Biochemical and Biophysical Research Communications*, 435(2), 239–43. <https://doi.org/10.1016/j.bbrc.2013.04.072>
- Levkowitz, G., Waterman, H., Zamir, E., Kam, Z., Oved, S., Langdon, W. Y., Beguinot, L., Geiger, B., & Yarden, Y. (1998). c-Cbl/Sli-1 regulates endocytic sorting and ubiquitination of the epidermal growth factor receptor. *Genes and Development*, 12, 3663–3674. <https://doi.org/10.1101/gad.12.23.3663>
- Li, C., Angione, K., & Milunsky, J. (2015). Identification of Critical Region Responsible for Split Hand/Foot Malformation Type 3 (SHFM3) Phenotype through Systematic Review of Literature and Mapping of Breakpoints Using Microarray Data. *Microarrays*, 5(1), 2. <https://doi.org/10.3390/microarrays5010002>
- Li, F., Buck, D., De Winter, J., Kolb, J., Meng, H., Birch, C., Slater, R., Escobar, Y. N., Smith, J. E., Yang, L., Konhilas, J., Lawlor, M. W., Ottenheijm, C., & Granzier, H. L. (2015). Nebulin deficiency in adult muscle causes sarcomere defects and muscle-type-dependent changes in trophicity: Novel insights in nemaline myopathy. *Human Molecular Genetics*, 24(18), 5219–5233. <https://doi.org/10.1093/hmg/ddv243>
- Li, H.-H., Du, J., Fan, Y.-N., Zhang, M.-L., Liu, D.-P., Li, L., Lockyer, P., Kang, E. Y., Patterson, C., & Willis, M. S. (2011). The ubiquitin ligase MuRF1 protects against cardiac ischemia/reperfusion injury by its proteasome-dependent degradation of phospho-c-Jun. *The American Journal of Pathology*, 178(3), 1043–58. <https://doi.org/10.1016/j.ajpath.2010.11.049>

- Li, H. H., Willis, M. M. S., Lockyer, P., Miller, N., McDonough, H., Glass, D. J., & Patterson, C. (2007). Atrogin-1 inhibits Akt-dependent cardiac hypertrophy in mice via ubiquitin-dependent coactivation of Forkhead proteins. *Journal of Clinical Investigation*, *117*(11), 3211–3223. <https://doi.org/10.1172/JCI31757>.and
- Li, H., Kedar, V., Zhang, C., McDonough, H., Arya, R., Wang, D., & Patterson, C. (2004). Atrogin-1 / muscle atrophy F-box inhibits calcineurin-dependent cardiac hypertrophy by participating in an SCF ubiquitin ligase complex, *114*(October). <https://doi.org/10.1172/JCI200422220>.1058
- Li, J., Horak, K. M., Su, H., Sanbe, A., Robbins, J., & Wang, X. (2011). Enhancement of proteasomal function protects against cardiac proteinopathy and ischemia/reperfusion injury in mice. *Journal of Clinical Investigation*, *121*(9), 3689–3700. <https://doi.org/10.1172/JCI45709>
- Li, J., Powell, S. R., & Wang, X. (2011). Enhancement of proteasome function by PA28alpha overexpression protects against oxidative stress. *Faseb J*, *25*(3), 883–893. <https://doi.org/10.1096/fj.10-160895>
- Li, J., Zhang, T., Meng, Y., Du, J., & Li, H. (2011). Cellular Physiology and Biochemistry Stability of F-box Protein Atrogin-1 is Regulated by p38 Mitogen-activated Protein Kinase Pathway in Cardiac H9c2 Cells.
- Li, N., Wang, H.-X., Han, Q.-Y., Li, W.-J., Zhang, Y.-L., Du, J., Xia, Y.-L., & Li, H.-H. (2015). Activation of the cardiac proteasome promotes angiotension II-induced hypertrophy by down-regulation of ATRAP. *Journal of Molecular and Cellular Cardiology*, *79*(2015), 303–314. <https://doi.org/10.1016/j.yjmcc.2014.12.007>
- Li, W., Bengtson, M. H., Ulbrich, A., Matsuda, A., Reddy, V. A., Orth, A., Chanda, S. K., Batalov, S., & Joazeiro, C. A. P. (2008). Genome-wide and functional annotation of human E3 ubiquitin ligases identifies MULAN, a mitochondrial E3 that regulates the organelle's dynamics and signaling. *PLoS ONE*, *3*(1). <https://doi.org/10.1371/journal.pone.0001487>
- Liu, B., Zheng, Y., Wang, T., Xu, H., Xia, L., Zhang, J., Wu, Y., Chen, G., & Wang, L. (2012). Proteomic Identification of Common SCF Ubiquitin Ligase FBXO6-Interacting Glycoproteins in Three kinds of Cells.
- Liu, Y., Wang, Y., Du, Z., Yan, X., Zheng, P., & Liu, Y. (2016). Fbxo30 Regulates Mammopoiesis by Targeting the Bipolar Mitotic Kinesin Eg5. *Cell Reports*, *15*(5), 1111–1122. <https://doi.org/10.1016/j.celrep.2016.03.083>
- Lockwood, W. W., Chandel, S. K., Stewart, G. L., Erdjument-Bromage, H., & Beverly, L. J.

- (2013). The novel ubiquitin ligase complex, SCF(Fbxw4), interacts with the COP9 signalosome in an F-box dependent manner, is mutated, lost and under-expressed in human cancers. *PLoS One*, 8(5), e63610. <https://doi.org/10.1371/journal.pone.0063610>
- Lutz, M., Wempe, F., Bahr, I., Zopf, D., & von Melchner, H. (2006). Proteasomal degradation of the multifunctional regulator YB-1 is mediated by an F-Box protein induced during programmed cell death. *FEBS Letters*, 580(16), 3921–30. <https://doi.org/10.1016/j.febslet.2006.06.023>
- Lyabin, D. N., Eliseeva, I. A., & Ovchinnikov, L. P. (2014). YB-1 protein: Functions and regulation. *Wiley Interdisciplinary Reviews: RNA*. <https://doi.org/10.1002/wrna.1200>
- Maillet, M., van Berlo, J. H., & Molkentin, J. D. (2013). Molecular basis of physiological heart growth: fundamental concepts and new players. *Nat Rev Mol Cell Biol*, 14(1), 38–48. <https://doi.org/10.1038/nrm3495>
- Margottin, F., Bour, S. P., Durand, H., Selig, L., Benichou, S., Richard, V., Thomas, D., Strebler, K., & Benarous, R. (1998). A Novel Human WD Protein, h- $\beta$ TrCP, that Interacts with HIV-1 Vpu Connects CD4 to the ER Degradation Pathway through an F-Box Motif. *Molecular Cell*, 1(4), 565–574. [https://doi.org/10.1016/S1097-2765\(00\)80056-8](https://doi.org/10.1016/S1097-2765(00)80056-8)
- McDowell, G. S., & Philpott, A. (2013). Non-canonical ubiquitylation: mechanisms and consequences. *The International Journal of Biochemistry & Cell Biology*, 45(8), 1833–42. <https://doi.org/10.1016/j.biocel.2013.05.026>
- Mearini, G., Gedicke, C., Schlossarek, S., Witt, C. C., Krämer, E., Cao, P., Gomes, M. D., Lecker, S. H., Labeit, S., Willis, M. S., Eschenhagen, T., & Carrier, L. (2010). Atrogin-1 and MuRF1 regulate cardiac MyBP-C levels via different mechanisms. *Cardiovascular Research*, 85(2), 357–366. <https://doi.org/10.1093/cvr/cvp348>
- Meiners, S., Dreger, H., Fechner, M., Bieler, S., Rother, W., Günther, C., Baumann, G., Stangl, V., & Stangl, K. (2008). Suppression of cardiomyocyte hypertrophy by inhibition of the ubiquitin-proteasome system. *Hypertension*, 51(2), 302–8. <https://doi.org/10.1161/HYPERTENSIONAHA.107.097816>
- Minoda, Y., Sakurai, H., Kobayashi, T., Yoshimura, A., & Takaesu, G. (2009). An F-box protein, FBXW5, negatively regulates TAK1 MAP3K in the IL-1 $\beta$  signaling pathway. *Biochemical and Biophysical Research Communications*, 381(3), 412–417. <https://doi.org/10.1016/j.bbrc.2009.02.052>
- Molkentin, J. D., Lu, J. R., Antos, C. L., Markham, B., Richardson, J., Robbins, J., Grant, S. R., & Olson, E. N. (1998). A calcineurin-dependent transcriptional pathway for cardiac hypertrophy. *Cell*, 93(2), 215–228. [https://doi.org/10.1016/S0092-8674\(00\)81573-1](https://doi.org/10.1016/S0092-8674(00)81573-1)

- Nash, P., Tang, X., Orlicky, S., Chen, Q., Gertler, F. B., Mendenhall, M. D., Sicheri, F., Pawson, T., & Tyers, M. (2001). Multisite phosphorylation of a CDK inhibitor sets a threshold for the onset of DNA replication. *Nature*, *414*(6863), 514–521. <https://doi.org/10.1038/35107009>
- Ohh, M., Kim, W. Y., Moslehi, J. J., Chen, Y., Chau, V., Read, M. A., & Kaelin, W. G. (2002). An intact NEDD8 pathway is required for Cullin-dependent ubiquitylation in mammalian cells. *EMBO Reports*, *3*(2), 177–182. <https://doi.org/10.1093/embo-reports/kvf028>
- Patterson, C., Willis, M. S., & Portbury, A. (2011). Rise Above: Muscle Ring-Finger-1 (MURF1) Regulation of Cardiomyocyte Size and Energy Metabolism. *Transactions of the American Clinical and Climatological Association*, *122*(919), 70–81. Retrieved from <http://www.pubmedcentral.nih.gov/articlerender.fcgi?artid=3116371&tool=pmcentrez&rendertype=abstract>
- Patton, E. E., Peyraud, C., Rouillon, a, Surdin-Kerjan, Y., Tyers, M., & Thomas, D. (2000). SCF(Met30)-mediated control of the transcriptional activator Met4 is required for the G(1)-S transition. *The EMBO Journal*, *19*(7), 1613–24. <https://doi.org/10.1093/emboj/19.7.1613>
- Peschiaroli, A., Scialpi, F., Bernassola, F., Pagano, M., & Melino, G. (2009). The F-box protein FBXO45 promotes the proteasome-dependent degradation of p73. *Oncogene*, *28*(35), 3157–66. <https://doi.org/10.1038/onc.2009.177>
- Petroski, M. D., & Deshaies, R. J. (2005). Function and regulation of cullin-RING ubiquitin ligases. *Nature Reviews. Molecular Cell Biology*, *6*(1), 9–20. <https://doi.org/10.1038/nrm1547>
- Pickart, C. M. (2001). Mechanisms Underlying Ubiquitination. *Annual Review of Biochemistry*, *70*(1), 503–533. <https://doi.org/10.1146/annurev.biochem.70.1.503>
- Pierce, N. W., Lee, J. E., Liu, X., Sweredoski, M. J., Graham, R. L. J., Larimore, E. A., Rome, M., Zheng, N., Clurman, B. E., Hess, S., Shan, S., & Deshaies, R. J. (2013). Cand1 promotes assembly of new SCF complexes through dynamic exchange of F box proteins. *Cell*, *153*(1), 206–15. <https://doi.org/10.1016/j.cell.2013.02.024>
- Predmore, J. M., Wang, P., Davis, F., Bartolone, S., Westfall, M. V., Dyke, D. B., Pagani, F., Powell, S. R., & Day, S. M. (2010). Ubiquitin proteasome dysfunction in human hypertrophic and dilated cardiomyopathies. *Circulation*, *121*(8), 997–1004. <https://doi.org/10.1161/CIRCULATIONAHA.109.904557>
- Price, C. T., Al-Khodor, S., Al-Quadani, T., Santic, M., Habyarimana, F., Kalia, A., & Kwaik, Y. A. (2009). Molecular mimicry by an F-box effector of *Legionella pneumophila* hijacks a

- conserved polyubiquitination machinery within macrophages and protozoa. *PLoS Pathogens*, 5(12). <https://doi.org/10.1371/journal.ppat.1000704>
- Ravid, T., & Hochstrasser, M. (2008). Diversity of degradation signals in the ubiquitin–proteasome system. *Nature Reviews Molecular Cell Biology*, 9(9), 679–689. <https://doi.org/10.1038/nrm2468>
- Razeghi, P., Baskin, K. K., Sharma, S., Young, M. E., Stepkowski, S., Essop, M. F., & Taegtmeyer, H. (2006). Atrophy, hypertrophy, and hypoxemia induce transcriptional regulators of the ubiquitin proteasome system in the rat heart. *Biochemical and Biophysical Research Communications*, 342(2), 361–4. <https://doi.org/10.1016/j.bbrc.2006.01.163>
- Reiss, K., Cheng, W., Ferber, A., Kajstura, J., Li, P., Li, B., Olivetti, G., Homcy, C. J., Baserga, R., & Anversa, P. (1996). Overexpression of insulin-like growth factor-1 in the heart is coupled with myocyte proliferation in transgenic mice. *Proceedings of the National Academy of Sciences of the United States of America*, 93(16), 8630–5. <https://doi.org/10.1073/pnas.93.16.8630>
- Saiga, T., Fukuda, T., Matsumoto, M., Tada, H., Okano, H. J., Okano, H., & Nakayama, K. I. (2009). Fbxo45 forms a novel ubiquitin ligase complex and is required for neuronal development. *Molecular and Cellular Biology*, 29(13), 3529–43. <https://doi.org/10.1128/MCB.00364-09>
- Sakamoto, K. M., Kim, K. B., Kumagai, a, Mercurio, F., Crews, C. M., & Deshaies, R. J. (2001). Protacs: chimeric molecules that target proteins to the Skp1-Cullin-F box complex for ubiquitination and degradation. *Proceedings of the National Academy of Sciences of the United States of America*, 98(15), 8554–8559. <https://doi.org/10.1073/pnas.141230798>
- Samuelsson, A.-M., Bollano, E., Mobini, R., Larsson, B.-M., Omerovic, E., Fu, M., Waagstein, F., & Holmäng, A. (2006). Hyperinsulinemia: effect on cardiac mass/function, angiotensin II receptor expression, and insulin signaling pathways. *American Journal of Physiology. Heart and Circulatory Physiology*, 291(2), H787-96. <https://doi.org/10.1152/ajpheart.00974.2005>
- Sandberg, J. K., Andersson, S. K., Bachle, S. M., Nixon, D. F., & Moll, M. (2012). HIV-1 Vpu interference with innate cell-mediated immune mechanisms. *Curr HIV Res*, 10(4), 327–333. <https://doi.org/10.2174/157016212800792513>
- Sarikas, A., Carrier, L., Schenke, C., Doll, D., Flavigny, J., Lindenberg, K. S., Eschenhagen, T., & Zolk, O. (2005). Impairment of the ubiquitin–proteasome system by truncated cardiac myosin binding protein C mutants. *Cardiovascular Research*, 66(1), 33–44. <https://doi.org/10.1016/j.cardiores.2005.01.004>

- Sarikas, A., Hartmann, T., & Pan, Z.-Q. (2011). The cullin protein family. *Genome Biology*, 12(4), 220. <https://doi.org/10.1186/gb-2011-12-4-220>
- Sarikas, A., Xu, X., Field, L. J., & Pan, Z. (2008). The Cullin7 E3 ubiquitin ligase: A novel player in growth control. *Cell Cycle*, 7(20), 3154–3161. <https://doi.org/10.4161/cc.7.20.6922>
- Sartori, R., Schirwis, E., Blaauw, B., Bortolanza, S., Zhao, J., Enzo, E., Stantzou, A., Mouisel, E., Toniolo, L., Ferry, A., Stricker, S., Goldberg, A. L., Dupont, S., Piccolo, S., Amthor, H., & Sandri, M. (2013). BMP signaling controls muscle mass. *Nature Genetics*, 45(11), 1309–18. <https://doi.org/10.1038/ng.2772>
- Scheffner, M., Huibregtse, J. M., Vierstra, R. D., & Howley, P. M. (1993). The HPV-16 E6 and E6-AP complex functions as a ubiquitin-protein ligase in the ubiquitination of p53. *Cell*, 75(3), 495–505. [https://doi.org/10.1016/0092-8674\(93\)90384-3](https://doi.org/10.1016/0092-8674(93)90384-3)
- Schlossarek, S., Englmann, D. R., Sultan, K. R., Sauer, M., Eschenhagen, T., & Carrier, L. (2012). Defective proteolytic systems in Mybpc3-targeted mice with cardiac hypertrophy. *Basic Research in Cardiology*, 107(1). <https://doi.org/10.1007/s00395-011-0235-3>
- Schlossarek, S., Frey, N., & Carrier, L. (2014). Ubiquitin-proteasome system and hereditary cardiomyopathies. *Journal of Molecular and Cellular Cardiology*, 71, 25–31. <https://doi.org/10.1016/j.yjmcc.2013.12.016>
- Shimizu, Ippei, Komuro, I. (2010). Excessive cardiac insulin signaling exacerbates systolic dysfunction induced by pressure overload in rodents. *Journal of Clinical Investigation*, 120(5), 1506. <https://doi.org/10.1172/JCI40096DS1>
- Shimizu, I., & Minamino, T. (2016). Physiological and pathological cardiac hypertrophy. *Journal of Molecular and Cellular Cardiology*, 97, 245–262. <https://doi.org/10.1016/j.yjmcc.2016.06.001>
- Shioi, T. (2000). The conserved phosphoinositide 3-kinase pathway determines heart size in mice. *The EMBO Journal*, 19(11), 2537–2548. <https://doi.org/10.1093/emboj/19.11.2537>
- Skaar, J. R., Pagan, J. K., & Pagano, M. (2013). Mechanisms and function of substrate recruitment by F-box proteins. *Nature Reviews Molecular Cell Biology*, 14(6), 369–381. <https://doi.org/10.1038/nrm3582>
- Skurk, C., Izumiya, Y., Maatz, H., Razeghi, P., Shiojima, I., Sandri, M., Sato, K., Zeng, L., Schiekhofer, S., Pimentel, D., Lecker, S., Taegtmeyer, H., Goldberg, A. L., & Walsh, K. (2005). The FOXO3a transcription factor regulates cardiac myocyte size downstream of AKT signaling. *Journal of Biological Chemistry*, 280(21), 20814–20823. <https://doi.org/10.1074/jbc.M500528200>
- Spaich, S., Will, R. D., Just, S., Spaich, S., Kuhn, C., Frank, D., Berger, I. M., Wiemann, S.,

- Korn, B., Koegl, M., Backs, J., Katus, H. a, Rottbauer, W., & Frey, N. (2012). F-box and leucine-rich repeat protein 22 is a cardiac-enriched F-box protein that regulates sarcomeric protein turnover and is essential for maintenance of contractile function in vivo. *Circulation Research*, *111*(12), 1504–16. <https://doi.org/10.1161/CIRCRESAHA.112.271007>
- Takeishi, Y., Ping, P., Bolli, R., Kirkpatrick, D. L., Hoit, B. D., & Walsh, R. A. (2000). Transgenic overexpression of constitutively active protein kinase C epsilon causes concentric cardiac hypertrophy. *Circulation Research*, *86*(12), 1218–1223. <https://doi.org/10.1161/01.RES.86.12.1218>
- Takimoto, E., Champion, H. C., Li, M., Belardi, D., Ren, S., Rodriguez, E. R., Bedja, D., Gabrielson, K. L., Wang, Y., & Kass, D. a. (2005). Chronic inhibition of cyclic GMP phosphodiesterase 5A prevents and reverses cardiac hypertrophy. *Nat Med*, *11*(2), 214–22. <https://doi.org/10.1038/nm1175>
- Teixeira, F. R., Manfiolli, A. O., Soares, C. S., Baqui, M. M. a, Koide, T., & Gomes, M. D. (2013). The F-box protein FBXO25 promotes the proteasome-dependent degradation of ELK-1 protein. *The Journal of Biological Chemistry*, *288*(39), 28152–62. <https://doi.org/10.1074/jbc.M113.504308>
- Toh, K. L., Jones, C. R., He, Y., Eide, E. J., Hinz, W. a, Virshup, D. M., Ptáček, L. J., & Fu, Y. H. (2001). An hPer2 phosphorylation site mutation in familial advanced sleep phase syndrome. *Science (New York, N.Y.)*, *291*(5506), 1040–1043. <https://doi.org/10.1126/science.1057499>
- Toischer, K., Rokita, A. G., Unsöld, B., Zhu, W., Kararigas, G., Sossalla, S., Reuter, S. P., Becker, A., Teucher, N., Seidler, T., Grebe, C., Preu, L., Gupta, S. N., Schmidt, K., Lehnart, S. E., Krüger, M., Linke, W. A., Backs, J., Regitz-Zagrosek, V., Schäfer, K., Field L. J., Maier, L. S., Hasenfuss, G. (2010). Differential cardiac remodeling in preload versus afterload. *Circulation*, *122*(10), 993–1003. <https://doi.org/10.1161/CIRCULATIONAHA.110.943431>
- Tsukamoto, O., Minamino, T., Okada, K. I., Shintani, Y., Takashima, S., Kato, H., Liao, Y., Okazaki, H., Asai, M., Hirata, A., Fujita, M., Asano, Y., Yamazaki, S., Asanuma, H., Hori, M., & Kitakaze, M. (2006). Depression of proteasome activities during the progression of cardiac dysfunction in pressure-overloaded heart of mice. *Biochemical and Biophysical Research Communications*, *340*(4), 1125–1133. <https://doi.org/10.1016/j.bbrc.2005.12.120>
- Usui, S., Maejima, Y., Pain, J., Hong, C., Cho, J., Park, J. Y., Zablocki, D., Tian, B., Glass, D. J., & Sadoshima, J. (2011). Endogenous muscle atrophy F-box mediates pressure

- overload-induced cardiac hypertrophy through regulation of nuclear factor-kappaB. *Circulation Research*, 109(2), 161–71. <https://doi.org/10.1161/CIRCRESAHA.110.238717>
- Van Berlo, J. H., Maillet, M., & Molkentin, J. D. (2013). Signaling effectors underlying pathologic growth and remodeling of the heart. *Journal of Clinical Investigation*, 123(1), 37–45. <https://doi.org/10.1172/JCI62839>
- Viñas-Castells, R., Beltran, M., Valls, G., Gómez, I., García, J. M., Montserrat-Sentís, B., Baulida, J., Bonilla, F., De Herreros, A. G., & Díaz, V. M. (2010). The hypoxia-controlled FBXL14 ubiquitin ligase targets SNAIL1 for proteasome degradation. *Journal of Biological Chemistry*, 285(6), 3794–3805. <https://doi.org/10.1074/jbc.M109.065995>
- Wang, C., Gale, M., Keller, B. C., Huang, H., Brown, M. S., Goldstein, J. L., & Ye, J. (2005). Identification of FBL2 as a geranylgeranylated cellular protein required for hepatitis C virus RNA replication. *Molecular Cell*, 18(4), 425–434. <https://doi.org/10.1016/j.molcel.2005.04.004>
- Wang, Z., Liu, P., Inuzuka, H., & Wei, W. (2014). Roles of F-box proteins in cancer. *Nature Reviews. Cancer*, 14(4), 233–47. <https://doi.org/10.1038/nrc3700>
- Weeks, K. L., & McMullen, J. R. (2011). The athlete's heart vs. the failing heart: can signaling explain the two distinct outcomes? *Physiology (Bethesda, Md.)*, 26(2), 97–105. <https://doi.org/10.1152/physiol.00043.2010>
- Wilkins, B. J., Dai, Y. S., Bueno, O. F., Parsons, S. A., Xu, J., Plank, D. M., Jones, F., Kimball, T. R., & Molkentin, J. D. (2004). Calcineurin/NFAT Coupling Participates in Pathological, but not Physiological, Cardiac Hypertrophy. *Circulation Research*, 94(1), 110–118. <https://doi.org/10.1161/01.RES.0000109415.17511.18>
- Willis, M. M. S., Rojas, M., Li, L., Selzman, C. H., Tang, R., Stansfield, W. E., Rodriguez, J. E., Glass, D. J., Patterson, C., Ms, W., Rojas, M., Li, L., Ch, S., Tang, R., Je, R., Dj, G., & Muscle, P. C. (2009). Muscle ring finger 1 mediates cardiac atrophy in vivo. *American Journal of Physiology- Heart and Circulatory Physiology*, 7525, 997–1006. <https://doi.org/10.1152/ajpheart.00660.2008>.
- Willis, M. S., Schisler, J. C., Li, L., Rodriguez, J. E., Hilliard, E. G., Charles, P. C., & Patterson, C. (2009). Cardiac muscle ring finger-1 Increases susceptibility to heart failure in Vivo. *Circulation Research*, 105(1), 80–88. <https://doi.org/10.1161/CIRCRESAHA.109.194928>
- Winston, J. T., Koepp, D. M., Zhu, C., Elledge, S. J., & Harper, J. W. (1999). A family of mammalian F-box proteins. *Current Biology*, 9(20), 1180-S3. [https://doi.org/10.1016/S0960-9822\(00\)80021-4](https://doi.org/10.1016/S0960-9822(00)80021-4)

- Wohlschlaeger, J., Sixt, S. U., Stoeppler, T., Schmitz, K. J., Levkau, B., Tsagakis, K., Vahlhaus, C., Schmid, C., Peters, J., Schmid, K. W., Milting, H., & Baba, H. A. (2010). Ventricular unloading is associated with increased 20s proteasome protein expression in the myocardium. *Journal of Heart and Lung Transplantation*, *29*(1), 125–132. <https://doi.org/10.1016/j.healun.2009.07.022>
- Wu, C. L., Kandarian, S. C., & Jackman, R. W. (2011). Identification of genes that elicit disuse muscle atrophy via the transcription factors p50 and Bcl-3. *PLoS ONE*, *6*(1). <https://doi.org/10.1371/journal.pone.0016171>
- Xu, X., Sarikas, A., Dias-Santagata, D. C., Dolios, G., Lafontant, P. J., Tsai, S.-C., Zhu, W., Nakajima, H., Nakajima, H. O., Field, L. J., Wang, R., & Pan, Z.-Q. (2008). The CUL7 E3 ubiquitin ligase targets insulin receptor substrate 1 for ubiquitin-dependent degradation. *Molecular Cell*, *30*(4), 403–14. <https://doi.org/10.1016/j.molcel.2008.03.009>
- Zeng, Y., Wang, H.-X., Guo, S.-B., Yang, H., Zeng, X.-J., Fang, Q., Tang, C.-S., Du, J., & Li, H.-H. (2013). Transcriptional effects of E3 ligase atrogin-1/MAFbx on apoptosis, hypertrophy and inflammation in neonatal rat cardiomyocytes. *PLoS One*, *8*(1), e53831. <https://doi.org/10.1371/journal.pone.0053831>
- Zha, Z., Han, X.-R., Smith, M. D., Lei, Q.-Y., Guan, K.-L., & Xiong, Y. (2016). Hypertension-associated C825T polymorphism impairs the function of Gβ3 to target GRK2 ubiquitination. *Cell Discovery*, *2*, 16005. <https://doi.org/10.1038/celldisc.2016.5>
- Zhang, E. E., Liu, Y., Dentin, R., Pongsawakul, P. Y., Liu, A. C., Hirota, T., Nusinow, D. A., Sun, X., Landais, S., Kodama, Y., Brenner, D. A., Montminy, M., & Kay, S. A. (2010). Cryptochrome mediates circadian regulation of cAMP signaling and hepatic gluconeogenesis. *Nature Medicine*, *16*(10), 1152–6. <https://doi.org/10.1038/nm.2214>
- Zhang, L., Villa, N. Y., & McFadden, G. (2009). Interplay between poxviruses and the cellular ubiquitin/ubiquitin-like pathways. *FEBS Letters*, *583*(4), 607–614. <https://doi.org/10.1016/j.febslet.2009.01.023>
- Zhang, Y. W., Brognard, J., Coughlin, C., You, Z., Dolled-Filhart, M., Aslanian, A., Manning, G., Abraham, R. T., & Hunter, T. (2009). The F Box Protein Fbx6 Regulates Chk1 Stability and Cellular Sensitivity to Replication Stress. *Molecular Cell*, *35*(4), 442–453. <https://doi.org/10.1016/j.molcel.2009.06.030>
- Zhao, W., Waggoner, J. R., Zhang, Z. G., Lam, C. K., Han, P., Qian, J., Schroder, P. M., Mitton, B., Kontogianni-Konstantopoulos, A., Robia, S. L., & Kranias, E. G. (2009). The anti-apoptotic protein HAX-1 is a regulator of cardiac function. *Proceedings of the National Academy of Sciences of the United States of America*, *106*(49), 20776–20781. <https://doi.org/10.1073/pnas.0906998106>

- Zheng, J., Yang, X., Harrell, J. M., Ryzhikov, S., Shim, E.-H., Lykke-Andersen, K., Wei, N., Sun, H., Kobayashi, R., & Zhang, H. (2002). CAND1 Binds to Unneddylated CUL1 and Regulates the Formation of SCF Ubiquitin E3 Ligase Complex. *Molecular Cell*, *10*(6), 1519–1526. [https://doi.org/10.1016/S1097-2765\(02\)00784-0](https://doi.org/10.1016/S1097-2765(02)00784-0)
- Zhou, P., & Howley, P. M. (1998). Ubiquitination and Degradation of the Substrate Recognition Subunits of SCF Ubiquitin–Protein Ligases. *Molecular Cell*, *2*(5), 571–580. [https://doi.org/10.1016/S1097-2765\(00\)80156-2](https://doi.org/10.1016/S1097-2765(00)80156-2)
- Zolk, O., Schenke, C., & Sarikas, A. (2006). The ubiquitin-proteasome system: focus on the heart. *Cardiovascular Research*, *70*, 410–421. <https://doi.org/10.1016/j.cardiores.2005.12.021>

## 11 Acknowledgement

First I want to thank Prof. Dr. Dr. Stefan Engelhardt, chairman of the Institute of Pharmacology of the TU Munich, for all the advise, thoughts and feedback he provided each time, I presented my work in the institute seminar. His experience and mindfull annotations for each result and enthusiasm were inspiring.

I am grateful to PD Dr. Antonio Sarikas for giving me the opportunity to work on this project in his group. He had always time for discussion, an open door and a good advise, when facing problems. The weekly Tuesday Seminar helped me to gain a critical thinking about published literature and improved my presentation skills. The progress seminar on each Friday made it possible to immediately to discuss the result with the whole research group and kept me pushing forward with new annotations and ideas emerging.

Furthermore I want to thank Thomas Hartmann, Kathleen Mayer and Florian Scheufele for the great first month of research training, giving me real insight and teaching on different assays and experiments performed in the Institute of the Technical University of Munich. Especially Kathleen Mayer provided always good advise during my two years time in the lab.

This work would not been possible without all the other institute members of the IPT. Sorry for not mentioning all of you in this page of my work. I especially appreciate the advise of Michael Regn and Deepak Ramanujan for always being helpfull when I was confronted with difficulties and problems. Without you two, I wouldn't be able to submit this work. Your explanations and experience in the lab and great skills of how to perform experiments widened my mind.

I am gratefull to my parents and my sister for all their support during my study time and the work on my MD thesis. I love you.

Last but not least, I want to thank you, Katja, for all your love and understanding, providing me always support no matter what.

**Affidavit**

I hereby confirm that my thesis entitled "Identification of hypertrophy-modulating Cullin-RING E3 ubiquitin ligases in primary cardiomyocytes" is the result of my own work. I did not receive any help or support from commercial consultants. All sources and / or materials applied are listed and specified in the thesis.

Furthermore, I confirm that this thesis has not yet been submitted as part of another examination process neither in identical nor in similar form.